 doi:10.20944/preprints202006.0206.v1

Proteomic profiling of protease-primed virus-permissive Caco-2 cells display abortive-interferon pathway and deregulated thromboinflammatory SERPINS

Maryada Sharma* and Naresh K. Panda

Department of Otolaryngology and Head & Neck Surgery
Postgraduate Institute of Medical Education and Research, Chandigarh, 160012

Abstract: Emerging paradigms in interferon (IFN) biology suggest a dynamic INF induced interactome that extends through broader Interferon Stimulated Gene (ISG)- induction, which implicates interferon- ISG coordinated cross-talk with mRNA processing, post-translational modification and metabolic processes that underlie pathological (viral, autoimmune and tumor biology) and physiological (stem cell regenerative pathways) processes. INF immune responses can also be triggered by endogenous host-derived molecules that are generated in response to cellular stress or hemostasis imbalance to establish tissue repair and regeneration in first place, however, overactivation or lack of countermeasures can result in host tissue damage. The proteases are integral to viral and tumor pathology, and importantly serine proteases TMPRSS2 and trypsin have been identified as important molecular determinants underlying COVID-19 pathology, and emergence of coronaviruses cultured *in vitro*, respectively. We propose that pathogen associated proteases can act as novel stress-inducers to facilitate viral- competent immunomodulation. We term it as Protease Induced Transcriptomic/ epi-Transcriptomic Reshaping (PITTR) of host cells to counter cellular stress. We present a novel experimental model and our preliminary findings of trypsin- primed Caco-2 cells (CPT) that result in translational halt comparable to cells grown under serum-starvation conditions (CSS). CPT at escalating trypsin concentration (CPT- EC) induce upregulation of selective proteins that majorly map to ribosomal, RNA transport, and spliceosome ribonucleoproteins (RNPs). The inclusion of proinflammatory IL1-β to CPT (CPT- IL) resulted in global overexpression of proteins comparable to Caco-2 cells cultured in growth-factor rich serum conditions (CFBS), indicating a likely de-repression of trypsin- induced translational halt. Caco-2 cells display abortive interferon proteome under differential trypsin conditions (CPT, CPT-EC and CPT-IL), which is marked by complete lack of INF generation despite induction of intermediate ISGs, suggestive of protease (trypsin)- dependent regulation of INF response.

Viruses regulate the proteome of stress granules (SGs) that are induced to cope transient translational halt as a central adaptive response to pathogen induced cellular stress. The integral components of SGs include non-translating mRNA, ribonucleoproteins (RNPs) and RNA binding proteins (RBPs), which together form biological condensates through a biophysical process involving weak electrostatic interactions through intrinsically disordered regions in RBPs resulting in liquid-liquid phase separation. We compared the CPT- EC proteome to the Mammalian Stress Granules Proteome (MSGP) database to explore potential RBPs that could possibly regulate INF response (and could act as potential anti-viral targets). Notably, differentially upregulated RNPs and potential RBPs from ISG family including ADAR and PRKRA, and RNA helicases implicated in viral pathogenesis were found to be upregulated in the CPT- EC proteome further strengthening the role of proteases (trypsin) in regulating INF pathways independent of the pathogen. We propose that the supplementation of viable SARS-CoV-2 viral loads to trypsin- primed host cells could recapitulate an infectious disease model, which may closely phenocopy pathogen- driven inflammation and signaling events. Based on the global downregulation of seven SERPINS (serine protease inhibitors) linked to thromboinflammation in our LCMS profiling data, we support the candidature of serine protease inhibitors for protease mediated viral pathologies. COVID-19 is increasingly linked to coagulopathy and resemblance to Neutrophil Extracellular Trap (NET) related thromboinflammatory features; SERPIN A1AT (alpha 1 antitrypsin) being a potent neutrophil- elastase inhibitor and a negative regulator of coagulation complement pathway may be a promising candidate for establishing hemostasis rebalancing in COVID-19 pathology.

 doi:10.20944/preprints202006.0206.v1

Key words- serine protease, interferon, ribonucleoproteins, RNA binding proteins, SERPIN, A1AT, hemostasis rebalancing

To whom correspondence should be addressed: Maryada Sharma, Department of Department of Otolaryngology and Head & Neck Surgery, Nehru Extension Block, Postgraduate Institute of Medical Education and Research, Sector 12, Chandigarh, 160012.
Email: maryada24@yahoo.com, sharma.maryada@pgimer.edu.in
Phone: 91-9872429552; 91-0172-2754903

Preprints (www.preprints.org) | NOT PEER-REVIEWED | Posted: 17 June 2020 doi:10.20944/preprints202006.0206.v1

Introduction

A novel betacoronavirus, severe acute respiratory syndrome coronavirus 2 (SARS-CoV-2) is currently spreading across many countries globally (**Zhou et al., 2020**; **Sun et al., 2020**; **Li et al. 2020**; **Lai et al., 2020**). Coronavirus disease 2019 (COVID-19) is a pandemic with no specific therapeutic agents and hence substantial mortality. The potential drugs in preclinical and clinical studies include viral protease targeting inhibitors-Lopinavir- Ritonavir (**Cao et al., 2020**), lysmotrophic molecule hydroxychloroquine (**Gautret et al., 2020**), ribosome and RNA metabolism modulators -remdesivir and ribavirin (**Beigel et al., 2020**; **Kmietowicz, 2020; Alexander et al., 2020; Khalili et al., 2020**), anticoagulant heparin (**Negri et al., 2020),** IL-6 neutralizing antibody (**Xu et al., 2020**), triple combination of interferon-1β, lopinavir- ritonavir, and ribavirin (**Hung et al., 2020**), and ribavirin in combination with anti-viral interferons α/β (**Khalili et al., 2020**). Other suggested therapeutic strategies are directed toward the viral entry pathway that involves host cell receptors ACE2 and serine protease TMPRSS2. TMPRSS2 serine protease inhibitors Camostat and Nafamostat have been implicated in COVID-19 treatment (**Bittmann et al., 2020**). ACE2 (virus-binding receptor) blockers, antimalarials; antivirals; immunoenhancers, monoclonal antibodies, and vaccines (**Zhang et al., 2020**) are proposed for COVID-19 treatment. In silico approaches (**Mercurio et al., 2020)** driven potential drug candidates (**Balkrishna, 2020),** non-human primate model for COVID-19 pathogenesis (**Lu et al., 2020**), and nutritional supplements (lactoferrin) (**Chang et al., 2020**), are other research guided strategies that are being actively investigated. However, exploring COVID-19 treatment still remains a global challenge (**Mohta et al., 2020**), and accelerating drug development through repurposed FDA approved drugs is encouraged for COVID-19 treatment, which involves employing pathogen- or host-directed approaches that may potentiate anti-viral immune response by interfering with host cell factors or dampening pro-inflammatory cytokine storm (**Gordy et al, 2020**). Enhanced type I interferon (IFN) susceptibility (**Loukugamage et al., 2020**), yet induction of low type I interferon anti-viral responses in SARS-CoV-2 infection as compared to SARS-CoV strongly encourages clinical trials of interferon lambda to treat early COVID-19 (**O'Brien et al., 2020**).

Further, the emerging studies indicate that COVID-19 is commonly complicated with coagulopathy (**Gris J-Christophe et al., 2020; Connors and Levy, 2020**), marked by higher platelet count, and elevated D-dimer (**Yin et al., 2020; Zhou et al., 2020)**. Continuous efforts to find potential treatments and understand the molecular determinants of disease mechanism are underway (**Wang et. al., 2020**; **Shen et al., 2020; Liu et al., 2020; Yang and Chen et al., 2020; Xia et al., 2020, Dong et al., 2020**), primary efforts are geared toward understanding the host immune responses to the viral infection (**Fung et al., 2020; Merad and Martin, 2020; Bojkova et al., 2020; Blanco-Melo et al., 2020; Kadkhoda, 2020; Lamers et al., 2020; Ortea and Bock, 2020; Tay et al., 2020**). An excessive inflammatory response to SARS-CoV-2 (**Mehta et al., 2020**), elevated inflammatory markers in blood (including C-reactive protein, ferritin, and D-dimers), raised neutrophil-to-lymphocyte ratio (**Wu et al., 2020; Chen et al., 2020; Zhou et al., 2020, Wang et al., 2020**, **Liu et al., 2020, Mo et al., 2020; Qin et al., 2020, Li et al., 2020**), heightened serum levels of proinflammatory cytokines and chemokines (**Chen et al., 2020; Yang et al., 2020**; **Gong et al., 2020; Qin et al., 2020**), and significant T cell depletion from the secondary lymphoid organs of patients infected with SARS-CoV-2 (**Chen et al., 2020**) have been reported in COVID-19 disease. Further studies are needed to understand the ambiguous role of

Preprints (www.preprints.org) | NOT PEER-REVIEWED | Posted: 17 June 2020 doi:10.20944/preprints202006.0206.v1

innate T cells in COVID-19 (**van der Heide, 2020).** Neutrophil infiltration has also been reported in pathological findings from autopsied COVID-19 patients (**Fox et al., 2020; Yao et al., 2020**) implicating neutrophilia as a potential source of excess Neutrophil Extracellular Traps (NETs) in case of COVID-19 (**Barnes et al., 2020; Mozzini and Girelli, 2020; Zuo et al., 2020, Bonow et al., 2020; Thierry and Roch, 2020**). The clinical presentations of severe COVID-19 patients (including ARDS and microthrombosis) strikingly overlap with the established NETopathies (**Barnes et al., 2020)**. Most notably, COVID-19 is characterized by a unique immunological profile marked by a profoundly impaired IFN type I response, which features a low interferon production and downregulation of interferon-stimulated genes (ISGs). Improved identification of therapeutic targets requires better understanding of the differential immunological responses underlying SARS-CoV-2 pathogenicity in COVID-19 disease. Intriguingly, sustained refractory interferon response (resulting in reduced viral clearance) in parallel to massive proinflammatory responses (leading to host-tissue destruction) in COVID-19 disease (**Hadjadj et al., 2020**), suggests existence of yet unexplored pathways supportive of persistent low level of type I interferon induction. Identification of the precise mechanisms that contribute to reduced type I interferon activity are proposed to be critical in the development of targeted immunomodulatory strategies in patients with COVID-19 (**Merad and Martin, 2020**).

Several coronavirus proteins including MERS-CoV encoded ORF 8b (**Lee et al., 2019**), SARS-CoV proteins 8b and 8ab (**Wong et al., 2018**), and NS7b and NS8, in 2019-nCoV (**Fahmi et al., 2020**), are implicated in immune modulation. The coronavirus S glycoprotein binds host cell receptors and promotes fusion of the viral and cellular membranes (**Walls et al., 2016; 2017**). The extensively N-glycosylated S protein trimers are the main target of neutralizing antibodies and the focus of therapeutic and vaccine design efforts (**Tortorici and Veesler, 2019**), the recent comprehensive structural and functional insights into the SARS-CoV-2 spike S protein and its interaction with host protein ACE2 and TMPRSS2 (**Walls et al., 2020; Wrapp et al., 2020, Hofmann et al., 2020; Letko et al., 2020; Yan et al., 2020; Shang et al., 2020; Lan et al., 2020**) have generated a blueprint for the design of vaccines and inhibitors of viral entry. A recent study repots cross-neutralization of SARS-CoV-2 by a human monoclonal SARS-CoV antibody S309 (**Pinto et al., 2020**). Interestingly, coronavirus (CoV) proteases are also reported to have host immunomodulatory properties, (**Zhu et al., 2017; Wang et al., 2015**, **Mielech et al., 2014**; **Yuan et al., 2015; Ma-lauer et al., 2016**). Herpes Simplex Virus (HSV-1) serine protease UL24 is known to impair NF-κB activation and modulate host antiviral immune pathways (**Xu et al., 2017**). Emerging studies indicate that the viral proteases possess side-functions extending beyond the polyprotein clipping, which are linked to host immune evasion by these viruses (**Kikkert, 2020).**

SARS-CoV-2 enters the host cells by using its spike protein receptor binding domain, which binds to the host cell receptor ACE2 (carboxypeptidase) (**Walls et al., 2020; Letko et al., 2020**), and a nearby serine protease TMPRSS2 later cleaves it off to permit the cell-cell fusion and viral entry (**Hoffmann et al., 2020**). TMPRSS2 is also likely key protease for SARS-CoV-2 replication (**Matsuyama et al., 2020**). Expression of two mucosa-specific serine proteases, TMPRSS2 and TMPRSS4 have recently been shown to facilitate SARS-CoV-2 spike fusogenic activity highlighting the intestine as a potential site of SARS-CoV-2 replication (**Zang et al., 2020**). Importantly, serine proteases TMPRSS2 and trypsin have been identified as important molecular players

Preprints (www.preprints.org) | NOT PEER-REVIEWED | Posted: 17 June 2020 doi:10.20944/preprints202006.0206.v1

underlying pathology and emergence of coronaviruses, respectively. Particularly trypsin-treatment (proteolytic processing) of viral spike protein has come up as potential species barrier for emergence of zoonotic coronaviruses, hence posing a potential threat for future outbreaks driven by cross-species transmission of coronaviruses (**Walls et al., 2020; Hoffmann et al., 2020; Matsuyama et al., 2020 Menachery et al., 2020; Letko et al., 2020**). It was recently proposed that the small intestine additional proteases such as trypsin might enhance SARS-CoV-2 viral infection and pathogenesis by triggering more robust cell fusion (**Zang et al., 2020**).

Gene expression is a tightly regulated process and integrally linked to regulation of RNA homeostasis. Cellular mRNA transcription, decay, transport, localization, translation and degradation is further regulated by specific proteins, which majorly belong to the family of ribonucleoproteins (RNPs) or RNA binding proteins (RBPs). Currently, these RNA-protein complexes are called membraneless organelles (MOs), and are focus of intensive research to understand precise regulation of gene expression under physiological and pathological conditions. RNAs and RBPs enriched MOs can form and localize to nucleus as speckles, paraspeckles or Cajal bodies, and in the cytoplasm as P-bodies and stress granules (**FU, 2020**). MOs are preferred targets of invading viruses as they exploit them for faithful replication (hiding from host immune sentinels), and in case MOs are associated with gene repression, viruses tend to evolve mechanisms to counteract their assembly and formation (**Gaete-Argel et al., 2019**) Different types of MO ribonucleoprotein granules (speckles, paraspeckles, SGs or P-bodies) have overlapping constituents however they involve distinct RBPs scaffolds to form. Interestingly recent studies report the G3BP protein homologues (G3BP1 and G3BP2) and other intrinsically disordered region (IDR) containing proteins as integral to MLO biogenesis via liquid–liquid phase separation (LLPS) process (**Deniz, 2020, Yang et al., 2020**, **Tauber et al., 2020**; **Guillen-Boixet**, **2020**), which is an adaptive response to environmental stresses required for cellular function (reviewed in **Fay and Anderson, 2018**). Viral infections are a major trigger of cellular stress and many classes of viruses are known to interact with host ribonucleoproteins, RNA transport, and RNA binding proteins (**Brandt et al., 2020, Wendt et al., 2020**) with implication in MO formation, regulation or counter formation.

Based on authors' previous findings (**Sharma et al., 2013; Sharma et al., 2017; Sharma et al., 2019**) and recent emerging studies, we envisaged a novel role for proteases in viral pathogenesis, which suggests Pathogen (protease) Induced Transcriptomic/ epiTranscriptomic Reshaping (PITTR) of host cells for pathogen-competent immunomodulation. We tested the following reasonable hypothesis – "Trypsin-priming of virus-permissive host cells reshapes host metabolic circuitry, which drives transcriptional and epitranscriptomic remodeling conducive to viral-competent immunomodulation. We present our preliminary findings that offer a new framework of protease induced interferon deregulation of host cells and implicate SERPINS as potential therapeutic molecules that may help trigger anti-viral immune response. Our high-throughput proteomics data links partial loss of A1AT in protease- primed host cells (SARS-CoV-2 permissive Caco-2) to induction of viral-competent immunomodulatory pathways.

Materials and Methodology:

Culture of human intestinal cells derived from Caco-2 cells: Caco-2 cell line was obtained from National Repository for cell lines at National Centre for Cell Science

(NCCS), Pune, India. The cells were maintained in Dulbecco's Modified Eagle Medium with 10% fetal bovine serum and grown to confluency before using them for the desired treatments for proteomic studies. The study was approved by the Institute Ethics Committee of Postgraduate Institute of Medical Education and Research, (PGIMER) Chandigarh, India.

LC-MS and protein data analysis: For LC-MS studies, total cellular proteins were extracted from Caco-2 cells grown under 5 different conditions (**Fig.1**)- i) DMEM serum free medium- Control 1, ii) DMEM medium and 10% FBS, iii) DMEM serum free medium supplemented with varying doses of trypsin (Catalog #: 17-161E, Lonza). T1 is the maximum concentration (500μg /ml) and T2 is 1:10 of T1 (50 μg /ml). T3 is a unique treatment, which includes the well characterized conditioned media of ARPE19 (adult retinal pigment epithelial) cell line cultured in presence of residual trypsin (50 μg /ml). Briefly, confluent Caco-2 cells were trypsinized using 500μg /ml of trypsin solution, the trypsinized cells were spun and 1/10th of residual trypsin was retained, diluted 10 times in serum free media and replated at a high cell density of 1 million cells/ml for 24-48h. This conditioned media is marked by secretion of biologically active bFGF (basic fibroblast growth factor) and interleukin IL-1β as determined by using multiplex assays previously reported by the author (**Sharma et al., 2013; Sharma et al., 2017; Sharma et al., 2019**). Therefore, T3 is ARPE19 conditioned media containing bFGF, IL-1β and active trypsin (as qualitatively determined by gelatin zymography- data not shown), however, absolute concentrations of trypsin were not determined using a commercial trypsin substrate. The Caco-2 cells cultured under different conditions as aforementioned, were incubated for 48 h in standard CO_2 incubator at 37°C and 5% CO_2.

Sample preparation for LCMS proteomic profiling- at the end of experiment, the cells were washed in 1X TBS to remove media or any other residual buffer. 90 µl of hot 6M Guanidine Hydrochloride (GnHCl)/ 0.1M Tris (pH 8.5) was added. The mixture was thoroughly mixed and vortexed and immediately kept at 90°C for 10 minutes to achieve lysis of the cells. Brief sonication (5-10 second single pulse) of the samples was carried out followed by returning the samples to 90°C for further 5 minutes. The cell lysates were spun at maximum speed (14000rpm/20 minutes at room temperature) to allow the debris to settle completely. The clear supernatants were secured sparing the residual dirty glue of the pellet to prevent any contaminating artifact (lysis buffer 6M GnHCl). 25 µg of each sample was taken and subjected to reduction and alkylation as follows- 10 mM DTT (2 µl of 200mM stock) was added to each tube containing 20 µl protein sample. Tubes were incubated for 45 minutes in dark at 37°C, this was followed by addition of IAA (Idoacetamide) to each tube to achieve final concentration of 50mM (2 µl of 500mM stock was added to each tube) and incubated for 45 minutes in dark at 37°C.

Trypsinization- after reduction and alkylation, the protein samples were diluted 10X (180 µl of LCMS grade H2O was added to 20 µl of protein sample) to bring down the GnHCl concentration from 6M to 0.6M. The pH for trypsin activity is crucial, therefore, pH for all tubes was checked using precise pH strips. If it was not found to be in range of 8.0 -8.5, it was reset with 0.1M tris (pH 8.0). Trypsin (2 µl) was added to each tube at the concentration of 0.5 µg/ µl, making final amount to 1 µg. The tubes were incubated overnight (16h) at 37 °C.

 doi:10.20944/preprints202006.0206.v1

Sample Clean up- following trypsinization, the pH was readjusted to around 2.0 using 2-3 µl of 10% TFA. The C18 clean-up columns were washed with 400 µl of methanol, spun at 2000 rpm for 1 minute (this step was repeated 2 times). It was followed by washing with 400 µl of Solution A. Composition of Solution A was as follows 80% ACN, 20% H20, 0.1% formic acid. The column was the equilibrated with 400 µl of Solution B-2% ACN, 98% H20, 0.1% formic acid. This step was repeated twice. The samples were now loaded onto the respective columns, which were spun at 1500rpm for 1 minute (the flow through was made to pass the columns thrice). The columns were washed with Solution B five times. The bound proteins were eluted with 150 µl Solution C- 50% ACN, 50% H20, 0.1% formic acid. Bound proteins were twice more eluted using Solution A (150 µl and 100 µl). At this step the total volume of eluted protein was 400 µl.

Protein identification and data analyses- the samples were concentrated by speed vacuuming that was kept on heater-off mode to prevent sample evaporation. After drying up, the samples were resuspended in 30-50ul of 0.1% formic acid and mixed well. The protein concentrations were measured using nanodrop (ThermoFisher Scientific). The samples were then bath sonicated briefly (1 minute) to break down the air bubbles if any and transferred to auto sampler vials to be loaded onto the LC-MS machine (Thermo Scientific™ Orbitrap Fusion™ Tribrid™ Mass Spectrometer, ThermoFischer Scientific) at the Central Sophisticated Instrument Cell (CSIC) at Postgraduate Institute of Medical Education and Research, Chandigarh, India.

The experiment was performed using EASY-nLC 1000 system (Thermo Fisher Scientific, Waltham, MA, USA) coupled to Thermo Fisher-Orbitrap Fusion Trybrid mass spectrometer equipped with nano-electrospray ion source. 1.0 µg of the peptide mixture was separated using a 25 cm thermos Easy-spray PepMap C18 column. Elution buffer was a 0–40% gradient of (95% acetonitrile, 0.1% formic acid) buffer at a flow rate of 300 nl/ min for 180 min. Mass Spectrometric (MS) data was acquired using a data-dependent top10 method dynamically choosing the most abundant precursor ions from the survey scan. The data was further processed for protein database search.

The system recommends loading protein samples with 1-2 µg /µl concentration, the injection volume was adjusted accordingly. The run time for sample was 180 minutes, following which the raw files were generated and were analysed in Proteome Discoverer 2.2 analysis software. Identification and quantification of proteins in complex biological samples was carried out using Thermo Scientific™ Proteome Discoverer™ software. This software simplifies a wide range of proteomics workflows, from protein and peptide identification to posttranslational modification analysis in label-free quantitation. The analyses were carried out against a standard homo sapiens database from UniprotKB. The samples were divided into desired groups/conditions/replicates and compared on intra and inter basis (to evaluate replicability and assess differentially expressed proteins, respectively). The results thus obtained reflected the PEP scores, unique peptides and more importantly the abundances of detected proteins in each sample.

The RAW files generated were analysed with Proteome Discoverer (v2.2) against the Uniprot HUMAN reference proteome database. For Sequest search, the precursor and fragment mass tolerances were set at 10 ppm and 0.5 Dalton, respectively. The protease used to generate peptides, i.e. enzyme specificity was set for trypsin/P

Preprints (www.preprints.org) | NOT PEER-REVIEWED | Posted: 17 June 2020 doi:10.20944/preprints202006.0206.v1

(cleavage at the C terminus of "K/R: unless followed by "P") along with maximum missed cleavages value of 2. Carbamidomethyl on cysteine amino acid was considered as fixed modification and oxidation of methionine & N-terminal acetylation were considered as variable modifications for database search. Both peptide spectrum match and protein false discovery rate (FDR) were set to 0.01.

Results

Model of inducing protease-mediated cellular stress in Caco-2 cells:

We hypothesized that the COVID-19 associated serine proteases could act as stress-inducers and display stress- granule (SG)- like proteome, marked by compromised translational output with suppressed anti-viral interferon pathway. However, the protease- primed cellular proteome would retain the translational expression of proteins involved in the formation of biological substructures like SGs and negative regulation of interferon pathway. We established a novel experimental model of inducing cellular stress using serine protease trypsin as a stress-inducer. Caco-2 cell cells were maintained in Dulbecco's Modified Eagle Medium with 10% fetal bovine serum and grown to confluency before using them for the desired treatments for proteomic studies. The different treatments and the cellular morphology under respective treatment has been shown by bright field microscopy (**Fig. 1A**)

Bioinformatics analysis of identified proteins

Differential analysis- Abundance values of Treated (T) and Control (C) samples were taken and differential analysis was performed to see the degree of fold change among the conditions. Abundance values were Log2 transformed and then filtered protein wise for whole samples on the basis of valid values by taking at least present in all conditions. Total 3088 proteins were filtered out from 4860 proteins. These values were then Z-score standardized. Categorical grouping was also for both the conditions: Control and Treatment- Control: (Control1:F2, Control2:F4), Treatment: (Treatment 1: F1, Treatment 2: F3, Treatment 3: F5), as detailed (**Fig S1 A-F**). Student t-test was used as the numbers of groups needed to be compared were 2 and statistical significance was considered for P value < = 0.05 and fold change > = 2.

Plots and histograms

Correlation Plot- The correlation plot shows the spearman correlation coefficient value that lies between -1 (negative correlation) to +1 (positive correlation). The colour code follows the indicated values of correlation coefficient. PCA- PCA is a widely used mathematical technique designed to extract, display and rank the variance within a data set. The overall goal of PCA is to reduce the dimensionality of a data set, simultaneously retaining the information present in the data. The PCA- biplot contains a lot of information and can be helpful in interpreting relationships between experimental samples. In this biplot, we can see that runs from each sample as representing different experimental conditions are far from each other. Screeplot: The contribution of all ten principal components to the profiling classification in plot of percentage explained variance of PC (**Figs. 2 A-C, Fig. S2 A-F**). Heatmaps- Clustering was performed on the LFQ abundance of total 23 statistically Significant proteins (**Fig. 2D**) and on all the 3088 proteins (**Fig. 1B**) that were filtered as identified in all samples. Red and Blue colours, respectively, represent low and high expression of proteins. whereas yellow (median) blocks indicate no difference in expression. Heatmap plot of the samples produced after abundance values were log2 transformed

Preprints (www.preprints.org) | NOT PEER-REVIEWED | Posted: 17 June 2020 doi:10.20944/preprints202006.0206.v1

and z-normalized. Hierarchical clustering was performed using Euclidian distance and average linkage using In-House R script (Package: ComplexHeatmap).

Pathway Enrichment analysis was performed on both group of Proteins filtered (3088 and 23). 3,077 out of 3,088 Proteins were successfully mapped to 3,123 Entrez Gene ID and used for pathway analysis. Out of 202 KEGG pathways gene sets were statistical significantly enriched over following pathways and highlighted in "Red" colour as identified in the KEGG pathway diagram- hsa03010 Ribosome, hsa03040 Spliceosome, hsa03013 RNA transport (**Figure 5**), hsa03050 proteosome and hsa04141 protein processing in endoplasmic reticulum (data not shown). 23 Proteins were found to be T-test statistically significant. These 3088 Proteins and 23 statistically significant proteins values were then visualized using In-house R Programming Scripts. 23 out of 23 proteins were successfully mapped to 23 Entrez Gene IDs. Out of 202 KEGG pathways gene sets were statistical significantly enriched over 1 pathway and genes were highlighted in "Red" colour as Identified in the KEGG pathway diagram- hsa00190 oxidative phosphorylation (**Figure 3 A and B**).

Mitochondrial proteins in trypsin-treated Caco-2 cells and implication in viral pathogenesis- We compared the upregulated proteins in oxidative phosphorylation pathway (**Figure 3**) under various trypsin treatments (T1>T2>T3) compared to control 2. Interestingly, 5 out of 6 significant proteins were upregulated in T1 and T2, however these proteins were either down regulated or modestly upregulated in T3 (**Fig. 3B,** logarithmic fold changes). The upregulated proteins (NDUFB1, UQCRB, COX5A, ATP5O and ATP5J) are associated with assembly of the five oxidative phosphorylation system complexes (OXPHOS) in the inner mitochondrial membrane.

KEGG pathway analyses for biological pathways implicated in viral pathogenesis by employing colour coded expression tags

For the current set of LCMS experiments, the triplicates for each condition were pooled and processed prior to LCMS profiling, therefore, we could not apply ANOVA statistical significance between the groups since we had only one representative treatment (intra group- containing 3 pooled independent replicates) in each group. We, therefore, tried to leverage the 3 independent escalating trypsin concentration (T3<T2<T1) data (inter-group) for some meaningful interpretations. We attempted to carry out a trypsin dose response pathway analyses using simple colour coded expression tags for 26 pathways that are implicated in viral pathogenesis using unique expression tags (**Figures 5, 11, 12, 14**). Following modifications were made for further analysis - for KEGG pathway analysis and mappings, all the identified proteins were included in the analysis as there are many possibilities of missed identification mainly due to uncharged peptides; masking by other peptides etc. (these are being overcome by using multiple biological replicates in our in-process experiments). For this study, missing abundance values were imputed on the basis of normal distribution and used for the pathway analysis. Protein abundances (Log2 transformed and z-score standardized values) for Treatment 1, Treatment 2 and Treatment 3 with respect to Control 2 were shown by using in-house R scripts for pathway based data integration and visualization (Package: "Pathview"). Red and green colours were used to show the up-regulation and down-regulation respectively. The pathways were slightly modified for comparative analyses of trypsin concentrations with copyright permission (**Luo et al., 2013; Kanehisa and Goto, 2000; Kanehisa et al., 2019; Kanehisa, 2019**).

Preprints (www.preprints.org) | NOT PEER-REVIEWED | Posted: 17 June 2020 doi:10.20944/preprints202006.0206.v1

We comprehensively analysed 26 biological pathways (**Figure 4A**), which are linked to viral pathogenesis and generated modified respective KEGG pathways highlighting the expression of a particular pathway intermediate protein/gene using color-coded gradations (log2FC -1 to +1, green to red colour gradients), for the most relevant pathways (**Figures 5B, 11, 12, 14**). This helped us to assess the dose dependent expression (3 independent concentrations of trypsin) of the "concerned" pathway protein in color-coded read outs. However, owing to the limitation of missing independent replicates and inclusion of all the proteins for pathway analyses (as discussed above), a fraction of proteins did not accurately map to the color coding on the pathways (the missing upregulated proteins in T1 group are highlighted in blue arrows). Therefore, to get an accurate quantitative fold change value for the identified proteins we tabulated all the pathway proteins (above and below 1, on Log2 scale) including upregulated (+1 to +7) and downregulated (-1 to -6) proteins on log2 FC scale (**supplementary files 1 and 2**). Interestingly, there were many proteins present (up or own regulated) in trypsin treated Caco-2 cells as can been seen from colored boxes in the respective pathways (**Figures 5, 11, 12, 14**). Further, we observed a consistent trend in protein upregulation (red color) that was negatively correlated with trypsin concentration (T) for most of the pathway proteins. Major fraction of mapped proteins was upregulated (red color) in T3 (lowest concentration of trypsin used) and hence most of the "red-color" is restricted to right 1/3rd of each box (for most of the pathways), which is the position assigned to T3. The mid part of each box is T2 and left 1/3rd is T1 (maximum concentration of trypsin) (expression tags, **Figure 4B**).

Modulation of ribosome and RNA pathways in trypsin-treated Caco-2 cells

The ribosome, spliceosome and RNA transport pathways emerged as most significantly abundant pathways in our data set (**Figure 5 A-C, upper panel**). To explore their relative abundance in T1, T2 and T3 over control 2, we did the KEGG pathways analysis employing colour coded expression tags as described above (**Figure 5 A-C, bottom panel**). We hypothesized that serine- proteases linked to COVID-19 pathology might act as stress-inducers to trigger biological condensate associated translational halt, involving global proteome suppression that compromises induction of anti-viral proteins, primarily the interferon pathway. We asked if trypsin treatment of Caco-2 cells was associated with the integral components of stress associated biological condensates, which include i) non-translating mRNA pool, ii) ribonucleoproteins, and iii) RNA binding proteins. In support of our hypothesis, we found the ribosome, spliceosome and RNA pathways had 68 proteins upregulated in their T1 group (**Figure 6A),** implicated in RNA transport, metabolism, transcription and translation. We also analysed the other (non-protease) stress control (control1), where we grew Caco-2 cells in presence of DMEM under serum starvation (SS) for extended 48h. We did not observe obvious differences at the level of ribosomal proteins across T1 and T5 (SS) (**Figure 6B**). However, interestingly we observed appreciable heterogenous and small ribonucleoproteins **(Figure 7 A and B**) upregulated in the trypsin treatment groups (T1 and T3) compared to stress control C1 (SS), indicating limiting ribonucleoprotein availability in SS conditions, which may discourage faithful RNP-concentration dependent formation of biological condensates. We further explored the potential of RNA binding proteins present in our dataset, which could offer potential anti-viral therapeutic value. We took leverage of the open access electronic resource The Mammalian Stress Granule Proteome (MSGP) containing all known SG recruited proteins reported to date (**Nunes et al., 2019**) available at

Preprints (www.preprints.org) | NOT PEER-REVIEWED | Posted: 17 June 2020 doi:10.20944/preprints202006.0206.v1

https://msgp.pt/. We particularly compared the reported RBPs in MSGP database to our proteomic data set, and it was found that nearly three-fourth (171) of the total RBPs were present in our database out of which nearly one-third were upregulated (~ 1.4-fold, 0.5 log2) in T1 (**Figure 8A and B**). Most notably, we identified 2 interferon stimulatory genes ADAR and PRKRA that were upregulated in T1 and in T1/T5 respectively (**Figure 9A and B**). We observed appreciable number of RNA- binding RNA helicase proteins, which are implicated in viral pathogenesis. It is noteworthy that we identified several helicases in our dataset (**Figure 10 A and B**) that could be potential G4 interactors.

We found modest downregulation of Ras GTPase-activating protein-binding protein 2 (G3BP2) in all treated groups (T1, T2 and T3), however, G3BP2 was appreciably downregulated in T1 and T2 (log2 -1.0), indicating suppressed anti-viral response. We further searched for de-capping enzymes in our data set and found appreciable downregulation of mRNA- decapping enzyme 1A (DCP1A) in T1 (log2 -2.5) and T2 (log2 -1.0) and modest downregulation in T3. Among other cap related proteins, m7GpppX diphosphatase (log2 -2.7), mRNA cap guanine-N7 methyltransferase (log2 -0.8), cap-specific mRNA (nucleoside-2'-O-)-methyltransferase (CMTR1) (log2 -1.5) were downregulated in T1 (**supplementary file 2**). There was downregulation (log2 -1.5) of CPSF3 and CPSF6 in T1 treated Caco-2 cells (**supplementary file 2**), and although we could not detect CSPF30 in our total proteins, however, very interestingly, the highest upregulated protein was found to be polyadenylation pre-mRNA 3' end processing protein WDR33 in T1 (log2 7.3) and T3 (Log2 6.5), with appreciable upregulation in T2 (Log2 3.2) as well (**supplementary file 1).** We also observed upregulation of YTHDC1 protein (log2 3.2) in T1, which is implicated in m6A recognition by YTH domain. The m6A effectors include the writer protein (m6A methyltransferase complex including METTL3–METTL14), eraser proteins (RNA demethylases; FTO and ALKBH5), and reader proteins (YTHDC1, YTHDC2, YTHDF1, YTHDF2). Alpha-ketoglutarate-dependent dioxygenase FTO and RNA demethylase ALKBH5 were found to be downregulated by (log2 -1.7), and (log2 -1.5) respectively, indicating complex regulation of RNA N^6methyl adenosine recognition and regulation. Pseudouridylate synthase 7 (PUS7) and HIV Tat-specific factor 1 (HTATSF1) were upregulated in T1 by (Log2 1 and Log2 1.5) respectively. The other highly expressed splicing factor that was upregulated in all 3 groups included Putative pre-mRNA-splicing factor ATP-dependent RNA helicase DHX16, with log fold changes of 4.9, 3.2 and 4.2 in T1, T2 and T3 respectively (**supplementary file 1)**.

Host cell immunomodulation in trypsin-treated Caco-2 cells

We mapped the total proteins to the known viral pathways in the KEGG data base including- 05168-Herpes simplex virus 1 infection, 05203- viral carcinogenesis, 05416- viral myocarditis and 04061-Viral protein interaction with cytokine and cytokine receptor (**Figure 11 A-D**). With most proteins downregulated in these pathways under T1 conditions (green color restricted to left), it was intriguing to observe upregulation of few proteins in T1 (red -shit toward left side of box) including the host factors Oct-1 and HCF (in 05168-Herpes simplex virus 1 infection pathway), which are known to promote viral infection in host cells (detailed in discussion). The T1 treatment appeared to be conducive to productive viral replication/ infection and, therefore, we focused on upregulated proteins in T1 in remaining pathways (**Figures 12,13**) to establish a correlation (if any) between pro-viral activity in T1 (indicated by Oct-1 overexpression and interferon-downregulation) (**Figure 11A**) with other potential host

Preprints (www.preprints.org) | NOT PEER-REVIEWED | Posted: 17 June 2020 doi:10.20944/preprints202006.0206.v1

cell determinants as indicated in our data set to speculate a possible hypothesis underlying protease-mediated downmodulation of immune cell pathways, and identify potential host target proteins for viral drug development. Further, the viral nucleotide sensing cytosolic proteins (RIG-1 and cGAS, see discussion for details) eventually converge at generating antiviral interferon response (INF-α and INF-β) and pro-inflammatory cytokines. INF-γ induced activation of INFGR (interferon gamma receptor) (upregulated in T3), which results in transcription of antiviral proteins showed upregulation of OAS interferon-stimulatory gene (ISGs) in T3, however, no IFN gene transcription was seen for any of the antiviral pathways at any of the trypsin concentration tested (**Figures 11A, 12**).

Induction of abortive-interferon anti-viral immune pathways in trypsin-treated Caco-2 cells

As shown (**Figure 12 A-D)** the major innate immune (TLR, RIG-I, cGAS, NF-κB) pathway proteins were downregulated in T1 (green color restriction to left part of the box) as opposed to T3 (red color restriction to right part of the same box). Notably, the central (RIG-I RNA sensing pathway) protein ISG- ISG15 was appreciably downregulated in T1, modestly upregulated in T2 and over 2 fold upregulated in T3, thereby, indicating a likely "trypsin-dependent" suppression of interferon pathway intermediate/ISG15, which however fail to trigger the production of terminal effector antiviral interferons (at all the trypsin concentrations- T1, T2, T3), thereby resulting in an "abortive-interferon" pathway (**Figure 12 and 13**). This is in contrast to cyclic GAMP-AMP synthase (cGAS), which was downregulated in all the treatments (T1, T2, T3) (**Figure 13**). Intriguingly, we found upregulation of interferon protein ADAR (adenosine deaminase acting on RNA), RNA-editing enzyme in T1 (**Figure 12C, 13C**).

ISGs execute their inhibitory function by degrading viral RNA and/or blocking translation of viral mRNAs including 2′,5′-oligoadenylate synthetase (OAS) and latent ribonuclease L (RNase L), protein kinase R (PKR), Moloney leukemia virus 10 homolog (MOV10), and zinc-finger antiviral protein (ZAP), many of which were downregulated in our data set (**figure 13**). ISG15 is the most highly induced interferon stimulated gene, which can inhibit viral translation, replication, or egress. It is a ubiquitin-like protein with an ability to covalently attach to target proteins (ISGylation). Plethora of proteins are involved in ISGylation and deISGylation including UBE2L6, HERC5, HERC6, UBE1LA, TRIM25, and USP18. TRIM25 was downregulated in T1, T2, and T3 (**Figure 13**), and HERC4 was highly downregulated in T1 (log2 -4.0) (**supplementary file 2**). Since ubiquitination and phosphorylation are key regulatory post translation modification in innate immune RIG-I -ISG15-dependent signaling pathway, we tabulated all the proteins with keyword "ubiquitin" and "phosphatase" (**Figure S3 and B**), respectively. To our surprise we found many ubiquitinating/deubiquitinating proteins that may have potential implication in interferon response pathway including Lys-63-specific deubiquitinase BRCC36 (downregulated in T1- log2 -4.9), which is known to have role in interferon signaling by deubiquitination of the type 1 interferon receptor alpha (IFNAR1), resulting in stabilization and cell surface expression of INFRA1 (**Figure 13B**).

We further did a "theme" based search with key word "Interferon" and tabulated 11 entries that were present in at least 2 groups (**Figure 13B**). 7/11 proteins were down regulated in T1, and 2 proteins were not found. The 3 most downregulated proteins included Interferon-induced, double-stranded RNA-activated protein kinase

Preprints (www.preprints.org) | NOT PEER-REVIEWED | Posted: 17 June 2020 doi:10.20944/preprints202006.0206.v1

(EIF2AK2), Interferon gamma receptor 1 (IFNGR1) and Interferon-induced 35 kDa protein (IFI35) that showed highest downregulation (log2 -4.0). The study by Kerr et al., observed an increase in ribosome RPL28, which was selectively incorporated into ribosomes/polysomes during the IFN response, they further reported an increase in ISG abundance upon RPL28 knockdown (siRPL28) in cells, indicating it as a negative regulator of ISG synthesis. We tabulated the proteins present in the heatmap (**Kerr et al., 2020; Fig. 6H**) showing abundance of select well-studied ISGs in siRPL28-treated and IFN-stimulated cells compared to controls. To our surprise, out of 12 proteins in their heatmap, we were able to find 10 proteins in our proteomics data including RPL28, which was over 2 fold upregulated in T1 (log2, 1.2), unchanged in T2 and modestly upregulated in T3. Further, we could correlate the downregulation of ISGs to the expression levels of RPL28 and interestingly, increased levels of RPL28 appreciably correlated with more downregulation of ISGs in T1 compared to T2 and T3 wrt Control 2 (**Figure 13D**). The most highly downregulated ISG was CD55, a complement decay-accelerating factor that showed a remarkable downregulation (logF2 -4.9), other ISGs that were highly downregulated included anti-viral SAMHD1 (logF2 -2.49), proteasome subunit PSDM1(logF2 -1.9) and ISG15 (logF2 -1.8) in T1.

Trim21, a E3 ubiquitin ligase was reported as a negative regulator of anti-viral Nmi-IFI35 complex with implications for various autoimmune diseases associated uncontrolled antiviral signaling (**Das et al., 2015**). We did not find Trim21 in our data, however, Trim21 regulated ISG protein- Sterile alpha motif and histidine–aspartic acid domain-containing protein 1 (SAMHD1) was downregulated in T1 (log2 -2.5) (**Figure 13D**). Further, we also tabulated the INF responsive proteins as reported in the mRNA expression profiles of proteins that were significantly upregulated at the proteomic level at 24 h of IFN stimulation (**Kerr et al., 2019**). We could find 17 proteins in our data set that were present in at least 2 conditions out of 3 (T1, T2, T3), with top downregulated proteins being IFI35 (logF2 -4.0), STAT2 (logF2 -3.09), E3 ubiquitin-protein ligase RNF213 (logF2 -3.02), and E3 ubiquitin/ISG15 ligase TRIM25, which ubiquitinates RIG-I and activates it (**Figure 13E**).

We further explored the spectra of ISGs present in our proteomic profiling data set by tabulating shared ISGs (**Figure 13C**) as reported in (**Lamers et al., 2020**). Interestingly, we could find total of 15 proteins that were present in at least 2 treatments out of 3 (T1, T2, T3 wrt control2) and 1 protein (TRIM56) was present only in T3. Most of the proteins were downregulated in T1 as (as opposed Lamers et al., results) and interestingly, modestly upregulated in T3. We observed another interesting shared result with Lamers et al., as the expression of 3 genes (downregulated in the expansion organoids/ intestinal progenitor populations) compared to more differentiated organoids (**Lamers et al., 2020**) were found to be downregulated in our cell culture model of trypsin treated Caco-2 cells. These included Transthyretin/TTR (logF2 -2.92), Apolipoprotein A-1/ APOA1 (logF2 -4.3) and Galectin-2/ LGALS2 (logF2 -2.76). The level of downregulation for APOA-1 and LGALS2 was higher in T1, however, interestingly, TTR was more downregulated in T3 (log2 -4.30) (**supplementary file 2**).

Extending the Interferon-Ribosomal-RNA pathway axis to Coagulation-Complement Networking via thromboinflammatory SERPINS

We observed downregulation of a coagulation-complement pathway intermediate serine protease inhibitor A1AT (alpha-1 antitrypsin)/ SERPINA1 in all three trypsin

Preprints (www.preprints.org) | NOT PEER-REVIEWED | Posted: 17 June 2020 doi:10.20944/preprints202006.0206.v1

treatments (T1, T2, and T3) (**Figure 14A-C**). Encouraged by the presence of SERPIN (serine protease inhibitor) A1AT in our system, we explored other potential SERPINS (if any) present in our data set (that may have potential thromboinflammatory regulating functions) using a keyword "serine protease inhibitor and/or SERPIN". We could find 7 serine protease inhibitors with implications in thromboinflammatory diseases. 7/7 serine protease inhibitors were downregulated in T1, and interestingly, 6/7 serine protease inhibitors except SPINT2 were downregulated in T2 and T3 (**Figure 14B**). SERPINS downregulation at all trypsin concentrations indicated a likely similar pattern of downmodulation as seen for abortive- interferon response in T1, T2, and T3. We further searched for serine proteases present in our data set to assess their expression pattern and draw a correlation (if any) with protease/antiprotease balance and interferon response. Total of 3 serine proteases were identified in our dataset as opposed to 7 SERPINs (**Figure 14C**). The serine proteases present in the data set included Prostasin (PRSS8), Suppressor of tumorigenicity 14 protein (ST14) encoding Matriptase, and Serine protease HTRA2, mitochondrial (HTRA2), which showed the following expression levels in T1 (log2 -4.25, log2 -0.79 and log2 1.46) respectively, indicating a more complex regulation of proteases compared to serine protease inhibitors, which were all downregulated in T1. Prostasin was recently shown to have an anti-inflammatory effect via downregulation of TLR4 expression in colonic epithelial cells (**Sugitani et al., 2020**). SPINT1 was the most downregulated serine protease inhibitor in T1 (log2 -4.0), SERPINB6 in T2 (log2 -4.0), and SERPINA1 or A1AT in T3 (log2 -2.76). Interestingly, SERPINB6 and A1AT were appreciably downregulated in all 3 treatments of trypsin (T1, T2, and T3) (**Figure 14C)**

Discussion and Future Perspective

Proteases TMPRSS2 and trypsin have been identified as indispensable molecular players underlying COVID-19 disease, particularly trypsin-treatment (proteolytic processing) of viral spike protein has come up as potential species barrier for emergence of zoonotic coronaviruses, hence posing a potential threat for future outbreaks driven by cross-species transmission of coronaviruses (**Walls et al., 2020; Hoffmann et al., 2020; Matsuyama et al., 2020, Menachery et al., 2020; Letko et al., 2020).** TMPRSS2 was shown to be inhibited by protease inhibitor A1AT (Alpha-1 antitrypsin), ACE2 carboxypeptidase (SARS-CoV-2 receptor on human cells) was recently proposed to regulate inflammation by regulating neutrophil influx through IL-17-STAT3 pathway (**Sodhi et al., 2019**), further emphasising the role of proteases as mechanistic determinants of viral entry, replication and modulation of inflammatory pathways driven by neutrophils. Recent studies implicate coagulation pathways, neutrophils and NETs (Neutrophil Extracellular Traps) as clinical correlates of COVID-19 disease (**Zuo et al., 2020, Negri et al., 2020; Wang et al. 2020; Fox et al., 2020; Yao et al., 2020; Barnes et al., 2020; Liu et al., 2020, Gris J-Christophe et al., 2020, Mozzini and Girelli, 2020; Connors, 2020; Thierry and Roch, 2020**). Importantly, neutrophils and NET components are increasingly linked to thrombotic diseases (**Stakos et al., 2020**), and NET components including (primarily) neutrophil elastase (NE) and DNA are linked to impairment of fibrinolytic pathways resulting in stabilization of thrombosis (**Varju and Kolev, 2019; Barbosa da Cruz, 2019; Tan et al., 2019**, **Ducroux et al., 2018**). The current NE and /or NET targeting drugs (**Crocetti et al. 2019**) do not hold much promise for COVID-19 treatment (**Barnes et al., 2020**). These insights have encouraged targeting alternate coagulation pathway proteins as potential anticoagulants for treating COVID-19 disease (**Lemke and Silverman, 2020;**

Preprints (www.preprints.org) | NOT PEER-REVIEWED | Posted: 17 June 2020 doi:10.20944/preprints202006.0206.v1

Levi et al., 2020; Paranjpe et al, 2020). Dissecting pathophysiology of COVID-19 in terms of interplaying mechanisms that underlie SARS-CoV-2 virulence, human immune response, overactive inflammatory reactions and majorly the coagulation pathways (**Kowalik et al., 2020**) is urgently required. Identifying and targeting possible molecular determinants driving coagulation-thromboinflammation axis/ loop in COVID-19 to achieve hemostasis rebalancing, is a potential novel area to design better therapeutic options for COVID19 treatment.

The current study correlates the partial loss of A1AT, a coagulation-complement pathway protein (potent neutrophil elastase inhibitor) to immunomodulation of protease-treated Caco-2 cells. Based on our preliminary findings (discussed below), we propose the following hypothesis- "down-regulation of A1AT enhances protease - mediated (virus-competent) immunometabolic reprograming of Caco-2 cells, rescuing this loss by exogenous A1AT may be a promising candidate in treating viral pathologies like COVID-19. The unique immunological profile marked by a profoundly impaired interferon (IFN) type I response in parallel to massive proinflammatory responses (host-tissue destruction) in COVID-19 disease (**Hadjadj et al., 2020**; **O'Brien et al., 2020**), despite higher susceptibility to type I interferons (**Loukugamage et al., 2020**) suggests existence of yet unexplored pathways supportive of persistent low interferon induction. Several studies are underway to clarify the role of antiviral and immunomodulating drugs in changing morbidity and mortality in severely ill COVID-19 patients (**Lega et al., 2020**), which are aimed at targeting viral protease (**Vatansever et. al., 2020**), and host serine protease TMPRSS2 (**Nguyen, 2020, Azouz et al., 2020**). Few drugs for COVID-19 treatment are already in preclinical or clinical platforms including combination of interferon-1β, lopinavir- ritonavir, and ribavirin (**Hung et al., 2020**), lopinavir- ritonavir (**Cao et al., 2020**), ribavirin in combination with interferons α/ β (**Khalili et al., 2020**), ribosome/ RNA pathway targeting drugs Remdesivir and ribavirin (**Beigel et al., 2020**; **Kmietowicz, 2020; Alexander et al., 2020; Khalili et al., 2020**), anticoagulant heparin (**Negri et al., 2020),** and IL-6 neutralizing antibody (**Xu et al., 2020**). However, exploring COVID-19 treatment still remains a global challenge (**Mohta et al., 2020**), and accelerating drug development through repurposed FDA approved drugs is highly encouraged for COVID-19 (**Gordy et al, 2020**). Transcriptomic, proteomic and bioinformatic approaches are providing insights to identify potential themes underlying the disease pathways (**Grifoni et al., 2020; Xiong et al., 2020; Bojkova et al., 2020; Ortea and Bock, 2020**), to guide better therapeutics.

Based on the emerging studies and other drug candidates implicated in COVID-19; it emerges that the potential targets for COVID-19 treatment include- 1) viral proteases, 2) host serine protease TMPRSS2, 3) ribosomal/ RNA pathways, 4) host proinflammatory cytokines, 5) anti-viral interferon pathways, and 6) coagulation pathways. We had a "virus-free" cell culture model with complete absence of proinflammatory cytokines (as opposed to cytokine storm seen in COVID-19). Therefore, we excluded 2 druggable targets (viral proteases and proinflammatory cytokines) owing to their absence in our *in vitro* culture system that lacks infective viral loads. We tried to gather insights from our high throughput proteomics data and recent literature on COVID-19 pathology, to establish a functional/mechanistic network with an effort to understand the cross-talk between innate immune interferon response and ribosomal/ RNA pathways, which may help to develop improved strategies/ repurpose drugs to treat COVID-19 disease.

Preprints (www.preprints.org) | NOT PEER-REVIEWED | Posted: 17 June 2020 doi:10.20944/preprints202006.0206.v1

The proteases are integral to viral and tumor pathology and emerging studies are establishing parallels in metabolic reprogramming between oncogenesis and human oncogenic viruses, which hijack host metabolite and lipid machinery to leverage progeny virus formation (**Purdy and Luftig, 2019**). Further, the interplay of cellular metabolism (immunometabolism) with innate immune response has been linked to respiratory viral infections (**Zhang et al., 2018; Cheng et al., 2014**), pointing to a (possible) viral infection- associated metabolic remodeling for achieving host immunomodulation. Interferon signalling induced alterations in ribosome composition that selectively downregulated ISG synthesis associated with IFN response modulation, offers a differential network map of the IFN-induced interactome to interpret IFN response in the context of viral infection and autoimmune diseases (**Kerr et al., 2019**). Notably, the IFN stimulation response extends beyond antiviral program and can facilitate ISG induction more broadly by activating mTOR-AKT-S6K signalling pathways of the MAPK signaling cascade (**Ivashkiv and Donlin, 2012**). The evolving interferon biology landscape implicates interferon/ISG signaling in regulation of mRNA processing, post-translational modification, metabolism, cellular trafficking, chromatin organization, and the cytoskeleton pathways (**Schneider et al., 2014**), which underlie pathological (viral, autoimmune and tumor biology) and physiological (stem cell regenerative pathways) processes.

Recent emerging paradigms point towards an increased trend towards “trypsin-reliance” for zoonotic coronavirus emergence that might predict cross-species transmission of coronaviruses possibly employing alternative route(s) like digestive tract/gut, which is proposed to be a potential site for future coronavirus emergence events in humans and perhaps alternative yet unidentified ACE2-independent host-cell receptors (**Shulla et al., 2011**; **Menachery et al., 2020; Letko et al., 2020; Yang et al., 2020)**. Further, the *in vitro* cell culture models demonstrated positive correlation between SARS-CoV-2 permissiveness with ACE2 and TMPRSS2 expression in Caco-2 and Calu-3 cell lines (**Bojkova et al., 2020; Hoffmann et al., 2020**), and hence decreased infection in low ACE2 expressing A549 cells (**Harcourt et al, 2020; Hoffman et al. 2020; Blanco-melo et al., 2020**). However, emerging studies are strongly linking infection of SARS-CoV-2 cells into enterocyte progenitors that are low in ACE2 expression (**Lamers et al., 2020**), indicating lower ACE2 thresholds for successful infection in some tissues or presence of alternative receptors for viral entry. Similarly, SARS-CoV-2 infected trachea transcriptomic signatures paralleled hematopoietic lineage progenitor cells indicating a possibility of hematopoiesis induction by SARS-CoV-2 (**Blanco-Melo et al., 2020).** These paradigms encouraged us to explore the potential mechanisms that might be active at the trypsin (protease)-host interface, which may extend beyond the layer of “viral- spike processing” and could possibly be linked to “host-receptor alterations” (**Letko et al., 2020**).

Based on these observations, insights and our previous findings (**Sharma et al., 2013, Sharma et al., 2017; Sharma et al., 2019**), we speculated that the pathogen/protease induced (metabolic) reprogramming events may underlie SARS-CoV-2 mediated infection of host cells to trigger viral-competent immunomodulatory pathways. We were interested to investigate the proposed hypothesis based on the recent findings from diverse groups reporting the “co- emergence/ -existence of SARS-CoV-2 and reprogramming events” indicating extended SARS-CoV-2 associated reprogramming trajectories including the possible haematopoiesis, (**Blanco-melo et al., 2020)** ,

preferred enterocyte progenitor (ACE2 low) permissive replication (**Lamers et al., 2020**), and transit-amplifying cells or intestinal stem cells supporting SARS-CoV-2 infections (**Zhang et al., 2020**). We were intrigued to explore if CoV associated serine protease(s) facilitated host/Caco-2 cell remodeling to usurp its cellular machinery resulting in dampened immune response.

Our preliminary proteomics data with trypsin-treated Caco-2 (SARS-CoV-2 permissive gut/intestinal) cells suggests that the enhanced bioenergetics in trypsin treated Caco-2 cells might drive metabolic resetting, which can facilitate viral competent immunomodulation. Assembly of the OXPHOS system (upregulated in trypsin treatment, **Fig 3**) is an intricate and vaguely defined process (**Signes and Fernandez-Vizarra, 2018**), however, the mitochondrial F type -ATP synthase, is established to be critical for mitochondrial functions. The deregulation of this enzyme was recently shown to be associated with dampened mitochondrial oxidative phosphorylation (OXPHOS) and activated mitochondrial permeability transition via OSCP (ATP5O) (**Beck et al., 2016**). Moreover, defects in COX5A overexpression were reported to attenuate mitochondrial respiratory dysfunction (**Zhang et al., 2020**). PB1-52, a mitochondrial inner membrane interacting viral protein has emerged as an innate immune modulator and virulence factor that regulated Type 1 interferon response (**Cheung et al., 2020**), thereby reflecting a possible host cell- metabolism rewiring that may regulate interferon responses for pathogen benefitting.

Cellular stress- stimuli including endogenous molecules result in phosphorylation of eIF2a mediated translational halt as a consequence of integrated stress response (**Aulas et al., 2017; Tauber and Parker, 2019**) leading to formation of stress granules (SGs). However, SGs can also form independently of eIF2a phosphorylation through inhibition of the eIF4F complex or osmotic stress (**Aulas et al., 2017**). SGs contain pools of non-translating mRNAs, which interact with RNA binding proteins and ribonucleoproteins to form biological condensates (**Ivanov et al., 2019**) known as membraneless organelles (MO) or non-membrane organelles through weak molecular interactions involving low complexity or intrinsically disordered regions (IDRs) in RNA binding proteins like G3PBs in a biophysical process called liquid-liquid phase separation (**Guillen-Boixet et al., 2020, Deniz, 2020, Yang et al., 2020**). The stress granules may trigger innate immune responses by activating cellular nucleic acid sensors (**Kim et al., 2019; McCormick and Khaperskyy, 2017**), and therefore, CoVs and other respiratory viruses manipulate stress granule formation tailored to their requirements (**Rabouw et al., 2016**; **Slaine et al., 2017; Khpaerskyy et al., 2014**, **Gaete-Argel et al., 2019**). Coronaviruses like SARS-CoV and MERS-CoV trigger host shut-off at the transcriptional and the translational levels, preventing translation of host mRNAs (**Tanaka et al., 2012; Lokugamage et al., 2012; Huang et al., 2011; Kamitani et al., 2009; Lokugamage et al., 2015**). Most viruses including MERS-CoV target stress SG ribonucleoprotein complexes triggered by cellular stress, however, no such association has been reported for SARS-CoV (**Gaete Aragel, 2019**). Emerging studies are increasingly implicating RNA metabolism to viral immune evasion (**Oyarzun-Arrau et al., 2020**), and SARS-CoV-2 is also proposed to camouflage its RNA from innate immune recognition by modifying RNA capping machinery (**Encinar and Menendez, 2020**). Importantly, certain interferon-stimulated genes (ISGs) including PKR, ADAR1, RIG-I, RNase L, and OAS also belong to the family of RNA binding proteins, therefore, anti-viral interferon response is interlinked with regulation of MO biogenesis/disassembly. SARS-CoV-2 transmits rapidly and its

Preprints (www.preprints.org) | NOT PEER-REVIEWED | Posted: 17 June 2020 doi:10.20944/preprints202006.0206.v1

infection has been associated with poor anti-viral interferon response. Therefore, we further investigated if SARS-CoV-2 associated protease trypsin can induce stress-granule like proteome marked by suppressed interferon response. Interestingly, we observed that trypsin- primed Caco-2 cells displayed abortive- interferon proteome under differential stress conditions that was marked by complete lack of INF generation despite induction of intermediate ISGs under certain treatments. We asked if the lack of interferon response was a generalizable phenomenon related to the translational halt triggered by cellular stress, or if we had some success in simulating the SG-like proteome phenotype, which is linked to regulation of interferon pathway as many interferon proteins like ADAR and PRKRA (RNA binding proteins) can interact with the SG components. We briefly discuss our findings in the subsequent section.

We included protease- primed stress conditions in our experimental set up with a goal to develop protease- mediated induction of host -dependent (viral regulatory) biological substructures that may offer investigation of interferon- regulatory networks with implications in viral pathology. The cellular- stress inducers included- a) Caco-2 cells grown under serum- free conditions in DMEM medium with no added growth supplement (SS/ C1)-T5; b) Caco-2 cells grown under trypsin (50 μg /ml) conditions-T2 (CPT); c) Caco-2 cells grown under ARPE19 conditioned media as established by the author (**Sharma et al., 2013; Sharma et al., 2017; Sharma et al., 2019**). This conditioned media is marked by presence of activated trypsin (50 μg /ml), IL-1β, and biologically active bFGF (basic fibroblast growth factor). IL-1β is strongly implicated in COVID-19 pathology, therefore, we asked if we could more closely approximate the cellular stress underlying SARS-CoV-2 infection by combining trypsin and pro-inflammatory IL-1β (CPT-IL). We envisaged it to be a more potent stress inducer than CPT, and d) Caco-2 cells grown under escalating trypsin dose (500 μg /ml)- T1 (CPT-EC). Notably, trypsin (Catalog # 17-161E, Lonza) used in this study was procured from Lonza, which comes at a working concentration of 500 μg /ml with 5mM dextrose, and physiologic ionic concentration of 5mM KCl and 137mM NaCl. However, the concentration of sodium bicarbonate is around 7mM in trypsin solution as opposed to around 44mM bicarbonate in DMEM media. Since bicarbonate exists as a conjugate base (the dissolved bicarbonate ions in the medium) to control a stable physiological pH through the bicarbonate buffering system under artificial cell culture conditions *in vitro*, we consistently observed a slight drop in pH (it was around 6.9) over 48h priming of Caco-2 cells in trypsin T1 conditions. Further, cell culture media of a standard composition contains source of energy and compounds which regulate the cell cycle and supplementation with amino acids, vitamins, inorganic salts, glucose, and serum as a source of growth factors, hormones, and attachment factors. In addition to nutrients, the medium also helps maintain pH and osmolality. The T1 condition with no added amino acids, vitamins or growth factors could support the survival of cells (**Figure 1 A**) until 48h post trypsin- inclusion. Apparently dextrose (1000mg/ml or 5mM) was sufficient to keep cells viable under stress. We believe that the trypsin activation of its receptor PAR-2 on Caco-2 cells resulted in upregulation of various ion channels and transporters (**Figure S3 C**) to further regulate the osmolality of the system. Glutamine and pyruvate have also been excluded from T1 condition (as there is no basal media), yet the cells could cope up with stress and survived for 48h indicating yet unidentified pathways to be driving survival under stress. Importantly, recent studies implicate glutamine independence as a selectable feature of pluripotent stem cells (**Vardhana et al., 2019**). Presence of anaplerotic molecules, pentose

Preprints (www.preprints.org) | NOT PEER-REVIEWED | Posted: 17 June 2020 doi:10.20944/preprints202006.0206.v1

phosphate pathway intermediates and purine- pyrimidine pathway intermediates are also indicated in our data, however, detailed investigation would provide better insights to the metabolic pathways governing T1 cell survival under extreme stress. We attempted to test this culture condition as we were aiming to establish protease-mediated LLPS (liquid-liquid phase separation) driven stress granule formation *in vitro*. It is reported that LLPS formation is facilitated by temperature, pH, salt, and crowding agent dependent manner (**Fu, 2020**), therefore, we hypothesized that physiological salts and slight pH alterations (and perhaps perturbed osmolality) might promote SG-like features *in vitro* under CPT-EC conditions.

Our preliminary findings show near-global downregulated protein expression with lower trypsin concentrations (T2/CPT) closer to the proteome patterns of stressed, nutrient-deprived serum starved (T5/ SS) cells (**Figure 1B**), indicating low translational activity. Surprisingly, distinct and moderately stretched tracts of overexpressed proteins appeared in proteome of Caco-2 cells primed with trypsin at escalating concentrations, (CPT-EC), which could be majorly mapped to ribosomal, RNA transport, and spliceosome ribonucleoproteins (**Figures 5-10**). Intriguingly, the proteome of T1 and T3 contained upregulated SG- forming components, including ribonucleoproteins and RNA- binding proteins (**Figures 7-10**) that were absent or downregulated in T2 and T5 , indicating propensity of T1 and T3 towards formation of SGs. However, T3 exhibited overwhelming expression of protein tracts as seen for Caco-2 cells cultured under growth-factor rich serum conditions (C2) indicating a likely de-repression of trypsin- induced translational halt, and diminishing possibility of formation of SGs owing to global translation upregulation as seen for serum treated Caco-2 cells (**Figure 1B**). It appears that the inclusion of growth factor bFGF in the T3 conditions released the apparent translational halt in T3 treated cells. Intriguingly, the inclusion of proinflammatory IL-1β to trypsin treated Caco-2 cells (CPT- IL) failed to trigger INF and proinflammatory cytokines, despite the presence of IL-1β in the cell culture milieu suggestive of protease/ trypsin- dependent regulation of INF response, this has a close resemblance to refractory interferon response amidst proinflammatory cytokine storm as seen in COVID-19 disease, suggesting a yet underappreciated role of serine proteases in regulating anti-viral interferon response. We further investigated if interferon stimulated genes were a part of the SG-like proteome in T1 conditions. It is established that following viral infection the cells happen to sense dsRNA (viral) detection, and alternate between periods of translation inhibition and process of active protein synthesis. The cytokines mRNA translation is hampered by translation inhibition (as appear under T1 conditions), which is mediated by dsRNA-induced PKR activation and consecutive translation initiation factor eIF2a phosphorylation indicating translational halt. PKR-dependent eIF2a phosphorylation is key for translation shut-off and stress granules formation **(Dalet et al., 2015)**. Interferon induced proteins like ADAR and PRKRA are RNA binding proteins that can interact with the SG components and are negative regulators of interferon response. ADAR deficiency is shown to cause chronic type I interferon production and inflammatory pathology in humans and mice (**Hartner et al., 2009; Rice et al., 2012).** A recent study linked the loss of ADAR1 in tumours to MDA5-dependent IFN-I production and inflammation (**Ishizuka et al., 2019**).

The proposed mechanisms that cells may utilize to restrict the formation or disassembly SGs/ MOs involve regulation of RNA synthesis rates and RNA modifications underlying RNA-RNA interactions, ribosome association and regulation

Preprints (www.preprints.org) | NOT PEER-REVIEWED | Posted: 17 June 2020 doi:10.20944/preprints202006.0206.v1

of RNA concentrations through RNA decay pathway (**Burke et al., 2019, Tauber et al., 2020**). RNA sensing is central to viral infections, therefore, RNA unwinding enzymes called RNA helicases (DEAD-box proteins) can perturb RNA- RNA interactions by invoking their inherent ATPase activity. This can block the formation of RNP condensates like stress granule, hence RNA helicases can counteract biological RNA- RNP condensate formation as has been recently shown for RNA helicase eIF4 (**Tauber et al., 2020**). Four-stranded G-quadruplex (G4) secondary structures are key structural features in viral mRNA and they tend to be highly conserved despite the high rate of mutations in viruses, indicating the importance of G4 targeting approach for broader antiviral therapy. Viral G-quadruplexes are new frontiers in virus pathogenesis and antiviral therapy (**Ruggiero and Richter, 2020**). Notably, G4s are enriched in functionally important regions in mRNA including 5′- and 3′-untranslated regions (UTRs), and recognition of mRNA secondary structures by RNA binding proteins (RBPs) is essential for post-transcriptional modifications. Therefore, recognition and unwinding of G4s are thought to be important for post-transcriptional processes such as mRNA translation, transport or stability. Interestingly, the major group of G4 interacting proteins consist of proteins involved in RNA splicing and processing, followed by proteins involved in translation. A dynamic balance between formation and resolution of G4 structures in host cells and presence of conserved G4 structures in viruses, offer a promising window of opportunity for targeting viral pathologies. Our data presents appreciable expression of RNA helicases in T1 and T3 (**Figure 10 A-B**) indicating ensuing secondary structural alterations in mRNA, which may underlie the formation of SG-like condensates under T1 conditions.

Other candidates that can regulate translational outputs under T1 primed conditions include PUS7 and HTATSF1. It was recently reported that PUS7 bound to distinct tRNAs to control biogenesis of tRNA derived fragments and hence regulated translation in stem cells (**Guzzi et al., 2018).** HTATSF1 was recently shown to regulate ribosomal RNA transcription and processing and subsequent efficient protein synthesis by specifically controlling splicing and intron retention (**Corsini et al., 2018).** Nuclear retention of incompletely spliced or mature mRNAs is emerging as a novel layer of gene regulation, which sensitizes the cell to instantly respond to stress, viral infection, differentiation cues or changing environmental conditions (**Wegener et al., 2017**). Notably, the host RNA modification inventory is dynamic, and emerging modulators of RNA virus gene expression have been proposed (**Netzband and Pager, 2019**). These RNA regulatory events can significantly impact virus gene expression, regulation, cytopathology and pathogenesis. Therefore, RNA viruses use, usurp and/or avoid the associated RNA machinery to impact the outcome of infection (**Cross et al., 2019**). RNA splicing is a new paradigm in host-pathogen interactions (**Chuahan et al., 2019),** and it was recently proposed that the alternative splicing landscape of host-cells determined the outcome of infection (productive vs abortive) **(Boudreault et al., 2019).** Recent studies report exciting convergence of the epitranscriptomic and virology research areas involving the N7-methylguanosine, ribose 2' -O-methylation, pseudouridine, inosine, N6-methyladenosine, and 5-methylcytosine epitranscriptomic marks on gene expression of RNA viruses. Interestingly, viral interaction and subversion of host cellular RNA transcription, splicing, translation, storage, and decay pathways underlie faithful viral infection cycles (**Cross, Michalski, Miller, & Wilusz, 2019; Kouba, et al, 2019**; **Velthuis, 2019**) and spatiotemporal viral gene expression (**Gonzales-van Horn & Sarnow, 2017**). We believe that our data set might offer novel host cell candidates/determinants

Preprints (www.preprints.org) | NOT PEER-REVIEWED | Posted: 17 June 2020 doi:10.20944/preprints202006.0206.v1

that may be potential targets for viral drug discovery. The functional characterization of such candidates will provide viable drug discovery platforms. The predominant candidates in our data that support the display of SG-like proteome signatures belong to the family of snRNPs, and many splicing factors, including the hnRNP proteins and the serine/arginine (SR)-rich protein family, which are reported to identify primary cis elements in the pre-mRNA (**Sebbag-Sznajder et al., 2020**). Interestingly, recent data implicate LLPS as a pre-requisite for transcription activation (**Kantidze and Razin, 2020**). Nuclear speckles (subnuclear compartments) are hubs of active genes/ pre-mRNA metabolism and are driven by ribonucleoproteins dependent large-scale condensates (**Smith et al., 2020**), reinforcing the emerging role of pre-mRNA in mediating euchromatin regulation (**Li and Fu, 2019**).

The POU transcription factor Oct-1 is known to represses virus-induced interferon gene expression (**Mesplede et al., 2005**), and promote disruption of viral latency (**Robinson et al., 2011**). The mammalian transcriptional coactivator host cell factor-1 (HCF-1) is known to function in concert with Oct-1 and VP16 to assemble the HSV immediate early (IE) transcription enhancer core complexes, which mediated the enhanced transcription of these genes upon infection (**Narayanan et al., 2005**), and triggered herpesvirus reactivation (**Carroll et al., 2007**). Both Oct-1 and HCF were upregulated in T1 conditions in our data (**Figure 11A, supplementary file 1**). Further, type I interferons can act in an autocrine/ paracrine manner by binding to their receptor (interferon-α/β receptor- IFNAR), which activates the Janus kinases (JAKs). JAKs subsequently activate the transcription factors signal transducer and activator of transcription 1 (STAT1) and STAT2, resulting in expression of major anti-viral interferon-stimulated genes (ISGs) (reviewed in **Rehwinkel and Gack, 2020** and cited references). Multiple signaling pathways that are targeted by viruses tend to converge on preventing the phosphorylation, dimerization, and nuclear translocation of the transcription factors IRF-3/7 **(Soham et al., 2020).** The coordinated ISG–ISGylation network has been recently shown to play a central role in providing anti-tumor immunity (**Fan et al., 2020**). IFNs activate the JAK-STAT pathway, which triggers induction of many IFN-stimulated genes (ISGs), and not all of these have been completely characterized (**Stark et al., 2012; Borden et al., 2019**). Since ISG inventory is dynamic and many ISGs are yet to be reported/ characterized, we consulted recent rigorous papers (**Kerr et al., 2019; Lamers et al., 2020**) and tabulated shared ISGs and Interferon Response Genes (IRGs) from these studies (comparing them to our data proteins) to extract meaningful ISGs/ IRGs (**Figure 13 C-E**), which may have a potential role in viral pathogenesis.

IFI35 and CD55 emerged as the highest downregulated (log2Fc -4.0) ISGs in our data set (see results section). IPF35/ IFI35 was reported as a potential cellular factor that attenuated the IFN response by negatively regulating RIG-I antiviral signaling leading to vesicular stomatitis virus replication (**Das et al., 2014**), increasing susceptibility to highly pathogenic H5N1- and pandemic H1N1-influenza A infection (**Gounder et al., 2018; 2019**), and promoting sustained virological response to pegylated-interferon plus ribavirin treatment in chronic HCV infection (**Estrabaud et al., 2015).** Interestingly, intracellular IFP/ IFI35 and its partner NMI (N-myc interacting protein) are reported to act as negative regulators of innate immune signaling pathways, targeting RIG-I, nuclear factor IFN regulatory factor 7 and NF-κB (**Wang et al., 2013; Hou et al., 2016**). However, recent reports assign them exciting (extracellular) role as proinflammatory DAMPs (danger associated molecular patterns), which activate the

Preprints (www.preprints.org) | NOT PEER-REVIEWED | Posted: 17 June 2020 doi:10.20944/preprints202006.0206.v1

NF-κB signaling pathway through TLR4 and facilitate the release of TNF (**Xiahou et al., 2017**). Therefore, IFI35 appears to have a context dependent role during inflammatory pathologies. A reduced intracellular IFI35 in the our study is suggestive of a suppressive interferon response, however, our study "did not evaluate the secreted extracellular proteome signatures". Therefore, it would be interesting to assess the extracellular levels of the IFI35 as enhanced trypsin concentrations might induce certain forms of cell death/ cell debris, we expect (some extent) of collateral detrimental effects to contribute to likely generation of DAMPs in our cell culture model.

DAMPs can be produced or released by damaged and dying cells facilitating sterile inflammation, which underlies tissue repair and regeneration, however, overactivation of DAMP signaling or lack of counter measures can result in development of numerous inflammatory diseases including metabolic disorders, autoimmune diseases, and tumours. Emerging studies clearly demonstrate that PAMPs and DAMPs can initiate immune responses by activating PRRs- including TLRs, RIG-I-like receptors (RLRs), C-type lectin receptors (CLRs) and multiple intracellular DNA sensors. Alternatively, DAMPs can also be sensed by non-PRRs that include receptor for advanced glycation end products (RAGE), triggering receptors expressed on myeloid cells (TREMs), G-protein-coupled receptors (GPCRs) and ion channels (**Gong et al.,2020**). The predominant DAMP present in our data set include Histone deacetylase complex subunit SAP130 (log2 3.4) and expression (up/down) of other histones (**Figure S4**). A future work up to identify and annotate functional roles to the possible DAMPs in our current experimental model, and upgrading the cell-culture model (by adding viable SARS-CoV-2 viral load) to recapitulate infectious disease would phenocopy PAMP-driven 'pathogenic inflammation' and signaling events, as opposed to likely DAMP-driven 'sterile -inflammation' in the current model.

Interestingly, SAMHD1 (other potential ISG downregulated in our dataset) was initially identified as an interferon-γ-induced gene, and an anti-HIV-1 restriction factor (**Hrecka et al., 2011; Laguette et al., 2011**). Its anti-viral activity is attributed to depletion of the intracellular pool of deoxynucleotide triphosphates (SAMHD1 is a deoxynucleoside triphosphate triphosphohydrolase) thereby limiting viral DNA synthesis. HIV-2 and SIV evolved the Vpx protein to degrade SAMHD1 via the proteasome pathway by hijacking the Cul4A/DDB1/DCAF1 E3 ligase, and a recent study demonstrates Trim21 dependent degradation of SAMHD1 in modulation of its anti-viral activity (**Li et al., 2020; Coggins et al., 2020).** DDB1- and CUL4-associated factor 7 (DCAF7) (log2Fc -1.7), Cullin-4A (CUL4A) (log2 Fc -2.3) and DNA damage-binding protein 1 (DDB1) (log2Fc -2.4) were downregulated in T1 (**supplementary file 2**). Another recent study implicated O-GlcNAcylation of SAMHD1 in promoting anti-HBV immunity as opposed to its anti-viral activity towards HIV (**Hu et al., 2020**), indicating another complex and crucial role of metabolic reprogramming underlying viral pathogenesis. The ubiquitin deconjugases encoded in the N-terminal domain of Epstein-Barr virus (EBV), Kaposi Sarcoma herpesvirus (KSHV) and human cytomegalovirus (HCMV) proteins were reported to target an early step of the IFN signaling cascade characterized by trimolecular complex formation with the ubiquitin ligase TRIM25 and the 14-3-3 molecular scaffold (**Gupta et al., 2020**). TRIM25 is suppressed in our study upon trypsin treatment of Caco-2 cells. These studies again support the absence activated interferon immune pathways in trypsin-treated Caco-2 cells.

Preprints (www.preprints.org) | NOT PEER-REVIEWED | Posted: 17 June 2020 doi:10.20944/preprints202006.0206.v1

Further, ISGs upregulated in intestinal organoids upon SARS-CoV-2 infection were recently reported (**Lamers et al., 2020**). Since our source/host cells were Caco-2 derived intestinal epithelial cells, we found it a reasonable reference data set to evaluate if we had any similar ISGs. A comparable data would strengthen our hypothesis that implicates the role of protease treatment of Caco-2 cells in partially recapitulating the viral infection. A unifying observation in Lamers et al., and our study was the lack of robust interferon response. Despite the induction of ISGs, the authors (**Lamers et al., 2020**) did not observe a robust Type I and III interferon response. Therefore, with our current preliminary findings, we propose that our trypsin treated Caco-2 cells proteomics data partially and appreciably recapitulates the features of SARS-CoV-2 infected intestinal organoids. Nevertheless, the lack of appreciable anti-viral interferon response despite the robust (**Lamers et al., 2020**) and modest (in our T3) upregulation of ISGs, point to a yet unidentified layer of complexity that regulates interferon production under *in vitro* conditions. We do not have additional data (at this point) to justify this observation, however, we could speculate a higher propensity of virus infection in Caco-2 cells that are treated with trypsin as opposed to serum (rich in trypsin-inhibitors). The "trypsin-reliance" for enhanced infection under *in vitro* conditions in presence of viable virus loads (missing in our experimental design) would recapitulate the current emerging studies, which demonstrate indispensable trypsin requirement of coronaviruses under *in vitro* conditions for productive infection underlying zoonotic emergence (**Letko et al., 2020, Menachery et al., 2020**). We are currently attempting organoid generation using diverse trypsin formulations employing ARPE19 and Caco-2 cells (Sharma et al. unpublished data) based on our preliminary findings, which resulted in release of bioactive bFGF (stem cell maintenance/ otic-induction factor) in ARPE19 conditioned media (**Sharma et al., 2013; Sharma et al., 2017; Sharma et al 2019**), under influence of proteases indicating yet unexplored potential role of proteases in dedifferentiation of adult cells *in vitro*.

Encouraged by the coagulopathy manifestation in COVID-19 patients, we considered re-analysing the complement- coagulation KEGG pathway to see if we had some potential hit(s) that could help us establish mechanistic networks with interferon and ribosome/RNA pathways. Uncontrolled enzyme activity is known to have pathological consequences as in thrombosis marked by excessive activity of serine proteases of the coagulation system and kallikrein-kinin system. Serine proteases are regulated by SERPINs (serine protease inhibitors), which are widely implicated in regulating thromboinflammatory processes and hemostatic maintenance/ rebalancing (**Crocetti et al., 2019**; **Emmerich, 2009**). We explored the potential serine protease and SERPINS present in our data set with implication in thromboinflammatory disorder like COVID-19. Our data identified seven serine protease inhibitors, which were all downregulated in T1, and interestingly, 6/7 serine protease inhibitors except SPINT2 were downregulated in T2 and T3 (see results for details). We briefly discuss their established roles in inflammatory disorders. The regulation of protease/antiprotease balance during pathologic insults (marked by up or down regulation of serine protease/ SERPIN), is very complex. Type II transmembrane serine proteases such as matriptase and kallikreins, are known to activate protease activated receptor-2 (PAR-2), and regulated by SERPIN SPINT1/ HAI-1 (**Kawaguchi et al., 2020**). Matriptase is regulated by hepatocyte activator inhibitors (HAIs), HAI-1 and HAI-2, encoded by the genes serine peptidase inhibitor Kunitz type -1 and -2 (SPINT1 and SPINT2), and a recent study demonstrated intestinal regulation of suppression of tumorigenicity 14 (ST14 encodes matriptase) and serine peptidase inhibitor SPINT1 by intestinal

Preprints (www.preprints.org) | NOT PEER-REVIEWED | Posted: 17 June 2020 doi:10.20944/preprints202006.0206.v1

transcription factor CDX2 (**Danielsen et al., 2018**); further SPINT2 was found to be an essential cellular inhibitor for maintaining intestinal epithelium architecture (**Kawaguchi et al., 2019**). Overactivation of HGF (hepatocyte growth factor) receptor MET by upregulation of matriptase and hepsin driven by downregulation of SPINT1 was recently reported in urological cancer (**Mukai et al., 2020**), indicating the crucial role of protease/antiprotease balance in inflammation, tumor biology and tissue integrity.

Recent studies implicate coagulation proteases like TF: FVIIa and FXa in activation of PAR-2, which is linked to pro-viral responses via TLR3 (**Antoniak and Mackman, 2014; Nhu et al., 2010; Weithauser et al., 2013; Rallabhandi et al., 2008; Antoniak, 2018; Wojtukiewicz et al., 2015; Kasthuri et al., 2009; Camerer et al., 2000; Posma et al., 2019**). A recent study proposed that targeting FXa and thrombin by using specific anticoagulant drugs can inhibit PARs, which may have beneficial role in human inflammatory diseases (**Posma et al., 2019**). PAR-2 signaling can also be triggered trypsin, tryptase, neutrophil elastase, GPI anchored serine protease (PRSS8) prostasin, and membrane anchored hepsin and TMPRSS2 (a potential COVID-19 associated serine protease). Notably, PRSS8/ prostasin is downregulated in T1, and upregulated in T2 and T3 (**Figure 14C**), and we did not detect PAR-2 and TMPRSS2 expression in our data; however, beta-arrestin (PAR-2 regulator) was found to be modestly downregulated in T1 and T2 and modestly upregulated in T3. A recent study demonstrated increased activation of PAR-2 in beta-arrestin depleted cells (**Thibeault and Ramachandran, 2020**), indicating possibility of functional trypsin- mediated-PAR-2 signalling in PAR-2 replete Caco-2 cells. Nevertheless, a detailed mechanistic insight of PAR-2 signaling outcomes in Caco-2 cells treated with varying concentrations of trypsin will determine its candidature for regulating protease-driven immunomodulatory pathways and evaluate if PAR-2 targeting can have beneficial effects in context of infectious pathology, notably PAR-2 mediated NETosis was recently linked to pathogen benefits (**Bryzek et al., 2019**). We suggest that the activation of PAR-2 by trypsin, coagulation serine proteases and **neutrophil elastase**, makes it a tempting target of **A1AT** (neutrophil elastase inhibitor), which may exert its anticoagulant effects (in part) by inhibiting coagulation serine protease- PAR-2 signaling node, besides its potential role in binding complement C3 component and inhibiting the downstream coagulation- complement pathways as has been recently reported (**O'Brien et al., 2020**).

As discussed before, the interferon treated cells preferably incorporated RPL28 ribosomal subunit to regulate the ISG expression. We found remarkable similarity in the overexpression of expression of RPL28 in T1 and concomitant downregulation of ISG CD55 (**Figure 13C**), which is a complement pathway protein. Decay-accelerating factor (DAF or CD55) is a known inhibitor of the complement system and CD55 deficiency results in complement hyperactivation, and angiopathic thrombosis. In addition, CD55 has been reported to be an essential host receptor for infection by the malaria parasite (**Dho et al., 2018**), however, CD55 was found to be the most potent complement regulatory protein in counteracting complement-mediated virus inactivation (**Rangaswamy et al., 2016**). Parainfluenza virus incorporated CD55 and CD46 to delay complement-mediated neutralization and exhibited an increased potency of inhibiting complement-mediated neutralization with CD55 (**Li and Parks, 2018**). Interestingly, a recent study demonstrated a correlation between complement component 3 (C3) and alpha-1 antitrypsin deficiency (AATD), displaying airways

Preprints (www.preprints.org) | NOT PEER-REVIEWED | Posted: 17 June 2020 doi:10.20944/preprints202006.0206.v1

disease and pulmonary emphysema (**O'Brien et al., 2020**); implicating A1AT in thromboinflammatory diseases.

A1AT is at the intersection node of coagulation and innate immune system. A1AT variants are proposed as potential SERPINs to block contact system–driven thromboinflammation (**de Maat et al., 2019**). Interestingly, a spontaneous mutant of A1AT, A1AT-P (M358R)- acquires antithrombin as opposed anti-neutrophil elastase activity, thereby linking A1AT and its variants to "serine protease/ anti-protease stoichiometric deregulation" underlying coagulopathies (such as COVID-19). Further, A1AT-P scaffold has been adapted to acquire functionality to inhibit furin and complement factor C1s to yield a Serp1 (viral serpin), inhibiting furin pro-convertases mediated viral pathogenicity (**Tardif et al., 2010**). Serpin PC (also called 1 -AT KRK) and 1 -AT-Fc fusion proteins are other designer SERPINs in early clinical trials (NCT04073498; NCT03815396, 2019). The crystallographic datasets for wild type and mutant AAT proteins point to considerable variability in the surface clefts, indicative of AAT protein as a potential target for structure-based drug designing (**Janciauskiene et al., 2018**), to promote homeostasis rebalancing in coagulopathies involving thrombo-inflammation (**de Maat et al., 2019; Schmaier, 2019; Luo et al., 2019; Scott and Sheffield 2019**).

Figure 1. Scheme representing experimental design, Caco-2, (SARS-CoV-2 permissive gut epithelial) cells were treated as shown in the scheme. Microscopy image of Caco-2 cells. Scale bars indicate 200 µm (A). Heatmap clustering was performed on the LFQ abundance of total 3088 proteins that were filtered as identified in all samples. Red and Blue colours, respectively, represent low and high expression of proteins while the yellow (median) blocks indicate no difference in expression. Heatmap plot of the samples were produced after abundance values were log2 transformed and z-normalized. Hierarchical clustering was performed using Euclidian distance and average linkage using In-House R script (Package: ComplexHeatmap) (B).

Figure 2. It shows the normalized sample abundance plot (A), and correlation plots (B and C) for the 23 most abundant proteins. D) Heatmap: Clustering was performed on the LFQ abundance of total 23 statistically Significant

Figure 3. KEGG pathway analysis of 23 most abundant proteins showing hsa00190 Oxidative phosphorylation as the only upregulated significant pathway (p-value cutoff 0.05, calculated by hypergeometric distribution) (A). The abundant proteins that mapped to oxidative phosphorylation pathway, the table shows Log2 fold change in T1, T2, and T3 with respect to control 2 (B).

Figure 4. Total of 26 pathways that are implicated in viral pathogenesis were analyzed using KEGG pathway analysis (A). Expression tag that were used to highlight the protein expression of Treatment1, 2, 3 with respect to Control2. The left one-third of each box is position assigned to T1 and right one-third is position is for T3, mid-part is for T2. The red color denotes upregulation and green color is down regulation on, the colored scale denotes log2 fold change.

Preprints (www.preprints.org) | NOT PEER-REVIEWED | Posted: 17 June 2020 doi:10.20944/preprints202006.0206.v1

Figure 5. KEGG pathway analysis of total 3088 proteins showing significant pathways (p-value cutoff 0.05 calculated by hypergeometric distribution) identified in all treatments (upper panel); the relative abundance in T1, T2 and T3 with respect to control 2 (Caco-2 cells grown in DMEM and 10% serum) (bottom panel). Ribosome Pathway (A), Spliceosome pathway (B), RNA transport pathway (C). The bottom panel could not map a fraction of proteins accurately to the assigned color codes. These proteins are marked by blue arrow for T1 proteins. The link to these pathways is provided in figure 4.

Figure 6. The proteins upregulated in T1 from figure 5 (A, B, and C- bottom panel), were tabulated and compared to relative fold changes in T2 and T3 and T5 (C1, positive stress control- it represents the proteome of serum starved Caco-2 cells) over Caco-2 cells grown in serum (control 2). The red color in table denotes all proteins with log2 fold change of 0.5 (~1.4 fold) and above. Bottom of each box is divided in 4 quadrants (q) (q1-T1, q2-T2, q3-T3, q4-T5, from left to right) and represent log2 FC of T1, T2, T3 and T5 over Control 2 (A). Heat map of the proteins searched with key word “ribosom/al ” proteins depicting the log2 FC of T1, T2, T3 and T5 over C2 (B).

Figure 7. The tabulated proteins represent all the proteins searched with key word “ribo/nucleo/protein” in the total data set and compared to relative fold changes in T1, T2, T3 and T5 (C1, positive stress control- it represents the proteome of serum starved Caco-2 cells) over Caco-2 cells grown in serum (control 2). The red color in table denotes all proteins with log2 fold change of 0.5 (~1.4 fold) and above (A). Heat map of the proteins tabulated in (7A), depicting the relative log2 FC of T1, T2, T3 and T5 over C2 (B).

Figure 8. The tabulated proteins represent (108/171) RNA binding proteins (RBPs) present in our data set as compared (RBPs) with open access electronic resource The Mammalian Stress Granule Protein (MSGP) database reported recently (Nunes et al., 2019), and available at https://msgp.pt/ . The RBPs are tabulated for relative log2 FC in T1, T2, and T3 over Caco-2 cells grown in serum (control 2). The red color denotes all proteins with log2 fold change of 0.5 (~1.4 fold) and above (A). Heat map of the proteins tabulated in (8 A) and T5, depicting the relative log2 FC of T1, T2, T3 and T5 over C2 (B).

Figure 9. Heat Map from 8B blown up to show the RNA binding proteins upregulated in T1 as compared to T5 (A) The red color denotes all proteins with log2 fold change of 0.5 (~1.4 fold) and above (A). The heat map RBPs tabulated to show the relative log2 FC in T1, T2, T3 and T5 over C2 (B).

Figure 10. The tabulated proteins represent all the proteins searched with key word RNA helicase / DDx/ DHx in the total data set and compared to relative fold changes in T1, T2, T3 and T5 (C1, positive stress control- it represents the proteome of serum starved Caco-2 cells) over Caco-2 cells grown in serum (control 2). The red color in table denotes all proteins with log2 fold change of 0.5 (~1.4 fold) and above (A). Heat map of the proteins tabulated in (8 A), depicting the relative log2 FC of T1, T2, T3 and T5 over C2 (B).

Figure 11. KEGG pathway analysis showing relative log2 FC expression of proteins in T1, T2 and T3 with respect to control C2. Blue arrows denote proteins not mapped accurately to color gradations. Herpes Simplex Virus pathway (A), viral carcinogenesis pathway (B), viral myocarditis pathway (C), and viral protein interaction with protein and cytokine receptor (D). The pathway were modified with copyright permission.

Figure 12. KEGG pathway analysis showing relative log2 FC expression of proteins in T1, T2 and T3 with respect to control 2. Viral sensing immune pathways- 04620-Toll-like receptor signaling pathway (A), 04622-RIG-I-like receptor signaling pathway (B), 04623-Cytosolic DNA-sensing pathway (C), and 04064-NF-kappa B signaling pathway (D).

Figure 13. Interferon Stimulated Genes (ISGs) or Interferon Response Genes (IRGs) tabulated with relative log2 FC expression of proteins in T1, T2 and T3 with respect to control 2. The well-known ISGs having antiviral function (A), the proteins searched in our dataset with keyword “interferon” (B), ISGs/ IRGs present in our data set when compared to ISGs induced upon SARS-CoV-2 infection in intestinal organoids as reported in a recent study (**Lamers et al., 2020**), (C), ISGs in our data set when compared to ISGs generated upon Interferon response in - presence and knockdown of ribosomal protein RPL28 (D), proteins upregulated upon interferon response at 24h (E), as reported in a recent study **(Kerr et al., 2019, https://doi.org/10.1101/766808).**

Figure 14. KEGG pathway analysis showing relative log2 FC expression of proteins in T1, T2 and T3 with respect to control 2 (A), the identified proteins as mapped in 13 A, tabulated and the red color depicting all proteins with log2 fold change of 0.5 (~1.4 fold) and above (B). SERPINS and serine proteases identified in our data set, tabulated to show relative log2 FC expression of proteins in T1, T2 and T3 with respect to control 2 (C).

Supplementary Figure 1. Venn diagrams and histogram comparison plots depicting the total proteins (A and D), treatment proteins (B and E) and control proteins (C and F). The unique proteins can be seen for each group in the Venn diagrams and histogram plots.

Supplementary Figure 3. It shows the normalized sample abundance plot (A), correlation plots (B and C), screeplot - PCs vs variance (D), PC-correlation plot (E), and PCA-biplot (F). Abundance values of Treated (T) and Control (C) samples were taken and differential analysis was performed to see the degree of fold change among the conditions. Abundance values were Log2 transformed and then filtered protein wise for whole samples on the basis of valid values by taking at least present in all conditions. Total 3088 Proteins were filtered out from 4860 Proteins. These values were then Z-score standardized. Categorical grouping was also done for both the conditions: Control and Treatment- Control (Control1:F2, Control2:F4), Treatment (Treatment1:F1, Treatment2: F3, Treatment3: F5), as detailed above. Student t-test was used as the number of groups needed to be compared were 2 and statistical significance was considered for P value < = 0.05 and fold change > = 2. Correlation Plot: The correlation plot shows the spearman correlation coefficient value that lies between -1 (negative correlation) to +1 (positive correlation). The colour code follows the indicated values of correlation coefficient. PCA: PCA is a widely used mathematical technique designed to extract, display and rank the variance within a

 doi:10.20944/preprints202006.0206.v1

data set. The overall goal of PCA is to reduce the dimensionality of a data set, simultaneously retaining the information present in the data. The PCA- biplot contains a lot of information and can be helpful in interpreting relationships between experimental samples. In this biplot, we can see that runs from each sample as representing different experimental conditions are far from each other. Screeplot: The contribution of all ten principal components to the profiling classification in plot of percentage explained variance of PC.

Figure S3. The tabulated proteins represent all the proteins searched with key word “ubiquitin” (A), “phosphatase” (B), “Transporter/ SLC” (C), and “chaperon” (D) in the total data set, and are presented as relative fold changes in T1, T2, T3 over Caco-2 cells grown in serum (control 2). The red color in table denotes all proteins with log2 fold change of 0.5 (~1.4 fold) and above

Figure S4. The tabulated proteins represent all the proteins searched with key word “histone” in the total data set, and are presented as relative fold changes in T1, T2, T3 over Caco-2 cells grown in serum (control 2). The red color in table denotes all proteins with log2 fold change of 0.5 (~1.4 fold) and above.

Supplementary files: available at
https://drive.google.com/drive/folders/137nwE0yCaPR4gUETVCbp4G8_0aP1M94H?usp=sharing

ACKNOWLEDGEMENTS
We thank PGIMER for the intramural funding for the current study PGIMER Intramural grant: No.71/2-Edu-16/1098 and SERB for the extramural funding SERB-CRG/2019/006745. Thanks to Dr Manni-L-Guptasarma for permitting her lab space for conducting the experiments and Center for Sophisticated Instrumentation Cell, PGIMER for using the LCMS proteomics facility. VProteomics, New Delhi team members Dr Gagan, Ms. Kanika, and specially Mr. Shubham for the data analyses. Ms Kavita and Ms. Vanya for technical help during manuscript preparation.

AUTHOR CONTRIBUTIONS
M.S. conceived the project, designed, performed, and analyzed the experiments. N.K.P provided intellectual inputs. M.S wrote the manuscript.

CONFLICT OF INTEREST: We declare no conflict of interest.

References

Antoniak S. The coagulation system in host defense. Res Pract Thromb Haemost. 2018;2(3):549–57.

Aulas A, Fay MM, Lyons SM, Achorn CA, Kedersha N, Anderson P, Ivanov P. Stress-specific differences in assembly and composition of stress granules and related foci. Journal of cell science. 2017 Mar 1;130(5):927-37.

Azouz NP, Klingler AM, Rothenberg ME. Alpha 1 Antitrypsin is an Inhibitor of the SARS-CoV2-Priming Protease TMPRSS2. bioRxiv. 2020 Jan 1.

Balkrishna A, Thakur P, Singh S, Dev SN, Jain V, Varshney A, Sharma RK. Glucose antimetabolite 2-Deoxy-D-Glucose and its derivative as promising candidates for tackling COVID-19: Insights derived from in silico docking and molecular simulations.

Barbosa da Cruz D, Helms J, Aquino LR, Stiel L, Cougourdan L, Broussard C, Chafey P, Riès-Kautt M, Meziani F, Toti F, Gaussem P. DNA-bound elastase of neutrophil extracellular traps degrades plasminogen, reduces plasmin formation, and decreases fibrinolysis: proof of concept in septic shock plasma. The FASEB Journal. 2019 Dec;33(12):14270-80.

Barnes BJ, Adrover JM, Baxter-Stoltzfus A, Borczuk A, Cools-Lartigue J, Crawford JM, Daßler-Plenker J, Guerci P, Huynh C, Knight JS, Loda M. Targeting potential drivers of COVID-19: Neutrophil extracellular traps. Journal of Experimental Medicine. 2020 Jun 1;217(6).

Beck SJ, Guo L, Phensy A, Tian J, Wang L, Tandon N, et al. Deregulation of mitochondrial F1FO-ATP synthase via OSCP in Alzheimer's disease. Nat Commun. 2016;7(May).

Beigel JH, Tomashek KM, Dodd LE, Mehta AK, Zingman BS, Kalil AC, Hohmann E, Chu HY, Luetkemeyer A, Kline S, Lopez de Castilla D. Remdesivir for the treatment of Covid-19—preliminary report. New England Journal of Medicine. 2020 May 22.

Blanco-Melo D, Nilsson-Payant BE, Liu WC, Uhl S, Hoagland D, Møller R, et al. Imbalanced Host Response to SARS-CoV-2 Drives Development of COVID-19. Cell [Internet]. 2020;1–10. Available from: https://doi.org/10.1016/j.cell.2020.04.026

Bojkova D, McGreig JE, McLaughlin KM, Masterson SG, Widera M, Kraehling V, Ciesek S, Wass MN, Michaelis M, Cinatl JN. SARS-CoV-2 and SARS-CoV differ in their cell tropism and drug sensitivity profiles. bioRxiv. 2020 Jan 1..

Bonow RO, Fonarow GC, O'Gara PT, Yancy CW. Association of coronavirus disease 2019 (COVID-19) with myocardial injury and mortality. JAMA cardiology. 2020 Mar 27.

Boudreault S, Roy P, Lemay G, Bisaillon M. Viral modulation of cellular RNA alternative splicing: A new key player in virus–host interactions?. Wiley Interdisciplinary Reviews: RNA. 2019 Sep;10(5):e1543.

Brandt J, Wendt L, Bodmer BS, Mettenleiter TC, Hoenen T. The Cellular Protein CAD is Recruited into Ebola Virus Inclusion Bodies by the Nucleoprotein NP to Facilitate Genome Replication and Transcription. Cells. 2020 May;9(5):1126.

Brusletto BS, Løberg EM, Hellerud BC, Goverud IL, Berg JP, Olstad OK, Gopinathan U, Brandtzaeg P, Øvstebø R. Extensive Changes in Transcriptomic "Fingerprints" and Immunological Cells in the Large Organs of Patients Dying of Acute Septic Shock and Multiple Organ Failure Caused by Neisseria meningitidis. Frontiers in Cellular and Infection Microbiology. 2020 Feb 19;10:42.

Bryzek D, Ciaston I, Dobosz E, Gasiorek A, Makarska A, Sarna M, Eick S, Puklo M, Lech M, Potempa B, Potempa J. Triggering NETosis via protease-activated receptor (PAR)-2 signaling as a mechanism of hijacking neutrophils function for pathogen benefits. PLoS pathogens. 2019 May 20;15(5):e1007773.

Burke JM, Moon SL, Matheny T, Parker R. RNase L reprograms translation by widespread mRNA turnover escaped by antiviral mRNAs. Molecular cell. 2019 Sep 19;75(6):1203-17.

Camerer E, Huang W, Coughlin SR. Tissue factor-and factor X-dependent activation of protease-activated receptor 2 by factor VIIa. Proceedings of the National Academy of Sciences. 2000 May 9;97(10):5255-60.

Cao B, Wang Y, Wen D, Liu W, Wang J, Fan G, Ruan L, Song B, Cai Y, Wei M, Li X. A trial of lopinavir–ritonavir in adults hospitalized with severe Covid-19. New England Journal of Medicine. 2020 Mar 18.

Carroll KD, Khadim F, Spadavecchia S, Palmeri D, Lukac DM. Direct Interactions of Kaposi's Sarcoma-Associated Herpesvirus/Human Herpesvirus 8 ORF50/Rta Protein with the Cellular Protein Octamer-1 and DNA Are Critical for Specifying Transactivation of a Delayed-Early Promoter and Stimulating Viral Reactivation. J Virol. 2007;81(16):8451–67.
Cazzola M, Stolz D, Rogliani P, Matera MG. α1-Antitrypsin deficiency and chronic respiratory disorders. European Respiratory Review. 2020 Mar 31;29(155).
Chang R, Zen Sun W, Bun Ng T. Lactoferrin as potential preventative and treatment for COVID-19.
Chauhan K, Kalam H, Dutt R, Kumar D. RNA splicing: A new paradigm in host-pathogen interactions. Journal of molecular biology. 2019 Mar 8.
Chen G, Wu D, Guo W, Cao Y, Huang D, Wang H, Wang T, Zhang X, Chen H, Yu H, Zhang X. Clinical and immunological features of severe and moderate coronavirus disease 2019. The Journal of clinical investigation. 2020 Apr 13;130(5).
Cheng SC, Joosten LA, Netea MG. The interplay between central metabolism and innate immune responses. Cytokine & growth factor reviews. 2014 Dec 1;25(6):707-13.
Cheung PH, Lee TW, Chan CP, Jin DY. Influenza A virus PB1-F2 protein: An ambivalent innate immune modulator and virulence factor. Journal of Leukocyte Biology. 2020 May;107(5):763-71.
Coggins SA, Mahboubi B, Schinazi RF, Kim B. SAMHD1 functions and human diseases. Viruses. 2020;12(4):1–28
Connors JM, Levy JH. COVID-19 and its implications for thrombosis and anticoagulation. Blood, The Journal of the American Society of Hematology. 2020 Jun 4;135(23):2033-40.
Corsini NS, Peer AM, Moeseneder P, Roiuk M, Burkard TR, Theussl HC, Moll I, Knoblich JA. Coordinated control of mRNA and rRNA processing controls embryonic stem cell pluripotency and differentiation. Cell stem cell. 2018 Apr 5;22(4):543-58.
Crocetti L, Quinn MT, Schepetkin IA, Giovannoni MP. A patenting perspective on human neutrophil elastase (HNE) inhibitors (2014-2018) and their therapeutic applications. Expert opinion on therapeutic patents. 2019 Jul 3;29(7):555-78.
Cross ST, Michalski D, Miller MR, Wilusz J. RNA regulatory processes in RNA virus biology. Wiley Interdisciplinary Reviews: RNA. 2019 Sep;10(5):e1536.
Dalet A, Argüello RJ, Combes A, Spinelli L, Jaeger S, Fallet M, Manh TP, Mendes A, Perego J, Reverendo M, Camosseto V. Protein synthesis inhibition and GADD34 control IFN-β heterogeneous expression in response to dsRNA. The EMBO journal. 2017 Mar 15;36(6):761-82.
Danielsen ET, Olsen AK, Coskun M, Nonboe AW, Larsen S, Dahlgaard K, et al. Intestinal regulation of suppression of tumorigenicity 14 (ST14) and serine peptidase inhibitor, Kunitz type -1 (SPINT1) by transcription factor CDX2. Sci Rep. 2018;8(1):1–14.
Das A, Dinh PX, Panda D, Pattnaik AK. Interferon-Inducible Protein IFI35 Negatively Regulates RIG-I Antiviral Signaling and Supports Vesicular Stomatitis Virus Replication. J Virol. 2014;88(6):3103–13.
Das A, Dinh PX, Pattnaik AK. Trim21 regulates Nmi-IFI35 complex-mediated inhibition of innate antiviral response. Virology. 2015 Nov 1;485:383-92.
De Maat S, Sanrattana W, Mailer RK, Parr NMJ, Hessing M, Koetsier RM, et al. Design and characterization of a1-antitrypsin variants for treatment of contact system-driven thromboinflammation. Blood. 2019;134(19):1658–69.
Deniz AA. Networking and Dynamic Switches in Biological Condensates. Cell. 2020 Apr 16;181(2):228-30.
Dho SH, Lim JC, Kim LK. Beyond the role of CD55 as a complement component. Immune Netw. 2018;18(1):1–13.
Dong Y, Mo X, Hu Y, Qi X, Jiang F, Jiang Z, Tong S. Epidemiological characteristics of 2143 pediatric patients with 2019 coronavirus disease in China. Pediatrics. 2020 Mar 1.
Du S, Tian J, Xiao Z, Luo Z, Lin T, Zheng S, Ai J. Serum alpha 1-antitrypsin predicts severe acute kidney injury after cardiac surgery. Journal of Thoracic Disease. 2019 Dec 1;11(12).

Ducroux C, Di Meglio L, Loyau S, Delbosc S, Boisseau W, Deschildre C, Ben Maacha M, Blanc R, Redjem H, Ciccio G, Smajda S. Thrombus neutrophil extracellular traps content impair tPA-induced thrombolysis in acute ischemic stroke. Stroke. 2018 Mar;49(3):754-7.
Dummer J, Dobler CC, Holmes M, Chambers D, Yang IA, Parkin L, Smith S, Wark P, Dev A, Hodge S, Dabscheck E. Diagnosis and treatment of lung disease associated with alpha one-antitrypsin deficiency: A position statement from the Thoracic Society of Australia and New Zealand. Respirology. 2020 Mar;25(3):321-35.
Elnara Marcia Negri , Bruna Mamprim Piloto , Luciana Kato Morinaga1 , Carlos Viana Poyares Jardim, Shari Anne El- Dash Lamy, D. D. (2020) 'Heparin therapy improving hypoxia in COVID-19 patients - a case series', 2(11).
Emmerich J. A1-Antitrypsin and the Maintenance of Hemostatic Balance. Haematologica. 2009;94(6):762–3.
Encinar JA, Menendez JA. Potential Drugs Targeting Early Innate Immune Evasion of SARS-Coronavirus 2 via 2'-O-Methylation of Viral RNA. Viruses. 2020 May;12(5):525.
Estrabaud E, Appourchaux K, Bièche I, Carrat F, Lapalus M, Lada O, et al. IFI35, mir-99a and HCV Genotype to predict sustained virological response to pegylated-interferon plus ribavirin in chronic hepatitis C. PLoS One. 2015;10(4).
Fahmi, M., Kubota, Y. and Ito, M. (2020) 'Nonstructural proteins NS7b and NS8 are likely to be phylogenetically associated with evolution of 2019-nCoV', *Infection, Genetics and Evolution*. Elsevier B.V, 81, p. 104272. doi: 10.1016/j.meegid.2020.104272.
Fan JB, Miyauchi S, Xu HZ, Liu D, Kim LJY, Burkart C, et al. Type I interferon regulates a coordinated gene network to enhance cytotoxic T cell–mediated tumor killing. Cancer Discov. 2020;10(3):382–93.
Fay MM, Anderson PJ. The role of RNA in biological phase separations. Journal of molecular biology. 2018 Nov 2;430(23):4685-701.
Fox SE, Akmatbekov A, Harbert JL, Li G, Brown JQ, Vander Heide RS. Pulmonary and cardiac pathology in Covid-19: the first autopsy series from New Orleans. MedRxiv. 2020 Jan 1.
Fu XD. RNA helicases regulate RNA condensates. Cell Research. 2020 Apr;30(4):281-2.
Fung SY, Yuen KS, Ye ZW, Chan CP, Jin DY. A tug-of-war between severe acute respiratory syndrome coronavirus 2 and host antiviral defence: lessons from other pathogenic viruses. Emerging microbes & infections. 2020 Jan 1;9(1):558-70.
Gaete-Argel A, Márquez CL, Barriga GP, Soto-Rifo R, Valiente-Echeverría F. Strategies for Success. Viral infections and membraneless organelles. Frontiers in cellular and infection microbiology. 2019;9.
Gautret P, Lagier JC, Parola P, Meddeb L, Mailhe M, Doudier B, Courjon J, Giordanengo V, Vieira VE, Dupont HT, Honoré S. Hydroxychloroquine and azithromycin as a treatment of COVID-19: results of an open-label non-randomized clinical trial. International journal of antimicrobial agents. 2020 Mar 20:105949.
Gómez-Mariano G, Matamala N, Martínez S, Justo I, Marcacuzco A, Jimenez C, Monzón S, Cuesta I, Garfia C, Martínez MT, Huch M. Liver organoids reproduce alpha-1 antitrypsin deficiency-related liver disease. Hepatology international. 2020 Jan;14(1):127-37.
Gong J, Dong H, Xia SQ, Huang YZ, Wang D, Zhao Y, Liu W, Tu S, Zhang M, Wang Q, Lu F. Correlation analysis between disease severity and inflammation-related parameters in patients with COVID-19 pneumonia. MedRxiv. 2020 Jan 1.
Gong T, Liu L, Jiang W, Zhou R. DAMP-sensing receptors in sterile inflammation and inflammatory diseases. Nature Reviews Immunology. 2019 Sep 26:1-8.
Gordy JT, Mazumdar K, Dutta NK. Accelerating drug development through repurposed FDA approved drugs for COVID-19: speed is important, not haste. Antimicrob Agents Chemother. 2020;2019(May).
Gounder AP, Yokoyama CC, Jarjour NN, Bricker TL, Edelson BT, Boon ACM. Interferon induced protein 35 exacerbates H5N1 influenza disease through the expression of IL-12p40 homodimer. PLoS Pathog. 2018;14(4):1–25.
Grifoni A, Sidney J, Zhang Y, Scheuermann RH, Peters B, Sette A. A sequence homology and bioinformatic approach can predict candidate targets for immune responses to SARS-CoV-2. Cell host & microbe. 2020 Mar 16.

Gris JC, Perez-Martin A, Quéré I, Sotto A. COVID-19 associated coagulopathy: the crowning glory of thrombo-inflammation concept. Anaesthesia, Critical Care & Pain Medicine. 2020 May 4.

Guillén-Boixet J, Kopach A, Holehouse AS, Wittmann S, Jahnel M, Schlüßler R, Kim K, Trussina IR, Wang J, Mateju D, Poser I. RNA-induced conformational switching and clustering of G3BP drive stress granule assembly by condensation. Cell. 2020 Apr 16;181(2):346-61.

Gupta S, Ylä-Anttila P, Sandalova T, Achour A, Masucci MG. Interaction With 14-3-3 Correlates With Inactivation of the RIG-I Signalosome by Herpesvirus Ubiquitin Deconjugases. Front Immunol. 2020;11(March):1–10.

Guzzi N, Cieśla M, Ngoc PC, Lang S, Arora S, Dimitriou M, Pimková K, Sommarin MN, Munita R, Lubas M, Lim Y. Pseudouridylation of tRNA-derived fragments steers translational control in stem cells. Cell. 2018 May 17;173(5):1204-16.

Hadjadj J, Yatim N, Barnabei L, Corneau A, Boussier J, Pere H, Charbit B, Bondet V, Chenevier-Gobeaux C, Breillat P, Carlier N. Impaired type I interferon activity and exacerbated inflammatory responses in severe Covid-19 patients. MedRxiv. 2020 Jan 1.

Hartner JC, Walkley CR, Lu J, Orkin SH. ADAR1 is essential for the maintenance of hematopoiesis and suppression of interferon signaling. Nature immunology. 2009 Jan;10(1):109.

Hoffmann M, Kleine-Weber H, Schroeder S, Krüger N, Herrler T, Erichsen S, Schiergens TS, Herrler G, Wu NH, Nitsche A, Müller MA. SARS-CoV-2 cell entry depends on ACE2 and TMPRSS2 and is blocked by a clinically proven protease inhibitor. Cell. 2020 Mar 5.

Hou J, Wang T, Xie Q, Deng W, Yang JY, Zhang SQ, et al. N-Myc-interacting protein (NMI) negatively regulates epithelial-mesenchymal transition by inhibiting the acetylation of NF-κB/p65. Cancer Lett [Internet]. 2016;376(1):22–33. Available from: http://dx.doi.org/10.1016/j.canlet.2016.02.015

Hrecka K, Hao C, Gierszewska M, Swanson SK, Kesik-Brodacka M, Srivastava S, et al. Vpx relieves inhibition of HIV-1 infection of macrophages mediated by the SAMHD1 protein. Nature [Internet]. 2011;474(7353):658–61. Available from: http://dx.doi.org/10.1038/nature10195

Hu A, Li J, Tang W, Liu G, Zhang H, Liu C, et al. Anthralin Suppresses the Proliferation of Influenza Virus by Inhibiting the Cap-Binding and Endonuclease Activity of Viral RNA Polymerase. Front Microbiol. 2020;11(February):1–14.

Hung IF, Lung KC, Tso EY, Liu R, Chung TW, Chu MY, Ng YY, Lo J, Chan J, Tam AR, Shum HP. Triple combination of interferon beta-1b, lopinavir–ritonavir, and ribavirin in the treatment of patients admitted to hospital with COVID-19: an open-label, randomised, phase 2 trial. The Lancet. 2020 May 30;395(10238):1695-704.

Indalao IL, Agustiningsih A, Pratiwi E, Puspa KD, Ikawati HD, Ramadhany R. The Utilization of Alpha-1 Anti-trypsin (A1AT) in Infectious Disease Monitoring and Treatment. Journal of Microbiology and Infectious Diseases. 2019 Jan 1;9(01):51-8.

Indalao IL, Agustiningsih A, Pratiwi E, Puspa KD, Ikawati HD, Ramadhany R. The Utilization of Alpha-1 Anti-trypsin (A1AT) in Infectious Disease Monitoring and Treatment. Journal of Microbiology and Infectious Diseases. 2019 Jan 1;9(01):51-8.

Ishizuka JJ, Manguso RT, Cheruiyot CK, Bi K, Panda A, Iracheta-Vellve A, Miller BC, Du PP, Yates KB, Dubrot J, Buchumenski I. Loss of ADAR1 in tumours overcomes resistance to immune checkpoint blockade. Nature. 2019 Jan;565(7737):43-8.

Ivanov P, Kedersha N, Anderson P. Stress granules and processing bodies in translational control. Cold Spring Harbor perspectives in biology. 2019 May 1;11(5):a032813.

Jie Hu, Qingzhu Gao, Yang Yang, Jie Xia, Wanjun Zhang, Yao Chen, Zhi Zhou, Lei Chang, Yuan Hu, Hui Zhou, Li Liang1, Xiaosong Li, Quanxin Long1, Kai Wang, Ailong Huang NT. O-GlcNAcylation of SAMHD1 Indicating a Link between Metabolic Reprogramming 2 and Anti-HBV Immunity. 2020;(February 2019):1–13.

José Antonio Encinar and JAM, Z. Potential Drugs Targeting Early Innate Immune Evasion of SARS-Coronavirus 2 via 2'-O-Methylation of Viral RNA. 2020;

Kadkhoda K. COVID-19: an Immunopathological View. Msphere. 2020 Apr 29;5(2).
Kanehisa M, Goto S. KEGG: kyoto encyclopedia of genes and genomes. Nucleic acids research. 2000 Jan 1;28(1):27-30.
Kanehisa M, Sato Y, Furumichi M, Morishima K, Tanabe M. New approach for understanding genome variations in KEGG. Nucleic acids research. 2019 Jan 8;47(D1):D590-5.
Karatas E, Di-Tommaso S, Dugot-Senant N, Lachaux A, Bouchecareilh M. Overview of Alpha-1 Antitrypsin Deficiency-Mediated Liver Disease.
Karatas E, Di-Tommaso S, Dugot-Senant N, Lachaux A, Bouchecareilh M. Overview of Alpha-1 Antitrypsin Deficiency-Mediated Liver Disease.
Kasthuri RS, Taubman MB, Mackman N. Role of tissue factor in cancer. Journal of Clinical Oncology. 2009 Oct 10;27(29):4834.
Kawaguchi M, Yamamoto K, Kataoka H, Izumi A, Yamashita F, Kiwaki T, et al. Protease-activated receptor-2 accelerates intestinal tumor formation through activation of nuclear factor-κB signaling and tumor angiogenesis in ApcMin/+ mice. Cancer Sci. 2020;111(4):1193–202.
Kawaguchi M, Yamamoto K, Takeda N, Fukushima T, Yamashita F, Sato K, et al. Hepatocyte growth factor activator inhibitor-2 stabilizes Epcam and maintains epithelial organization in the mouse intestine. Commun Biol [Internet]. 2019;2(1):1–14. Available from: http://dx.doi.org/10.1038/s42003-018-0255-8
Kerr CH, Skinnider MA, Madero AM, Andrews DD, Stacey RG, Chan QW, Stoynov N, Jan E, Foster LJ. Dynamic rewiring of the human interactome by interferon signalling. bioRxiv. 2019 Jan 1:766808.
Kerr CH, Skinnider MA, Madero AM, Andrews DD, Stacey RG, Chan QW, et al. Dynamic rewiring of the human interactome by interferon signalling. bioRxiv. 2019;766808
Khalili JS, Zhu H, Mak NS, Yan Y, Zhu Y. Novel coronavirus treatment with ribavirin: Groundwork for an evaluation concerning COVID-19. Journal of medical virology. 2020 Mar 30.
Kikkert M. Innate Immune Evasion by Human Respiratory RNA Viruses. Journal of innate immunity. 2020;12(1):4-20.
Kim SS, Sze L, Lam KP. The stress granule protein G3BP1 binds viral dsRNA and RIG-I to enhance interferon-β response. Journal of Biological Chemistry. 2019 Apr 19;294(16):6430-8.
Kim SSY, Sze L, Lam KP. The stress granule protein G3BP1 binds viral dsRNA and RIG-I to enhance interferon-β response. J Biol Chem. 2019;294(16):6430–8.
Kmietowicz, Z. (2020) 'Covid-19: Selected NHS patients will be treated with remdesivir.', *BMJ (Clinical research ed.)*, 369(May), p. m2097. doi: 10.1136/bmj.m2097.
Kowalik MM, Trzonkowski P, Łasińska-Kowara M, Mital A, Smiatacz T, Jaguszewski M. COVID-19—Toward a comprehensive understanding of the disease. Cardiology journal. 2020 May 7.
Kowalik MM, Trzonkowski P, Łasińska-Kowara M, Mital A, Smiatacz T, Jaguszewski M. COVID-19—Toward a comprehensive understanding of the disease. Cardiology journal. 2020 May 7.
Kumari G. Lokugamage, Adam Hage1, Craig Schindewolf, Ricardo Rajsbaum, V. D. M. (2020) 'SARS-CoV-2 is sensitive to type I interferon pretreatment.', (February 2019), pp. 1–13.
Laguette N, Sobhian B, Casartelli N, Ringeard M, Chable-Bessia C, Ségéral E, et al. SAMHD1 is the dendritic- and myeloid-cell-specific HIV-1 restriction factor counteracted by Vpx. Nature. 2011;474(7353):654–7.
Lai CC, Shih TP, Ko WC, Tang HJ, Hsueh PR. Severe acute respiratory syndrome coronavirus 2 (SARS-CoV-2) and coronavirus disease-2019 (COVID-19): The epidemic and the challenges. Int J Antimicrob Agents [Internet]. 2020;55(3):105924. Available from: https://doi.org/10.1016/j.ijantimicag.2020.105924
Lamers MM, Beumer J, van der Vaart J, Knoops K, Puschhof J, Breugem TI, et al. SARS-CoV-2 productively infects human gut enterocytes. Science (80-). 2020;2:eabc1669.
Lan J, Ge J, Yu J, Shan S, Zhou H, Fan S, Zhang Q, Shi X, Wang Q, Zhang L, Wang X. Structure of the SARS-CoV-2 spike receptor-binding domain bound to the ACE2 receptor.

Nature. 2020 May;581(7807):215-20.
Lee, J. Y., Bae, S. and Myoung, J. (2019) 'Middle East respiratory syndrome coronavirus-encoded ORF8b strongly antagonizes IFN-β promoter activation: its implication for vaccine design', *Journal of Microbiology*, 57(9), pp. 803–811. doi: 10.1007/s12275-019-9272-7.
Lega S, Naviglio S, Volpi S, Tommasini A. Recent Insight into SARS-CoV2 Immunopathology and Rationale for Potential Treatment and Preventive Strategies in COVID-19. Vaccines. 2020 Jun;8(2):224.
Lemke G, Silverman GJ. Blood clots and TAM receptor signalling in COVID-19 pathogenesis. Nature Reviews Immunology. 2020 Jun 2:1-2.
Letko M, Marzi A, Munster V. Functional assessment of cell entry and receptor usage for SARS-CoV-2 and other lineage B betacoronaviruses. Nat Microbiol 2020; 5: 562-9.
Levi M, Thachil J, Iba T, Levy JH. Coagulation abnormalities and thrombosis in patients with COVID-19. The Lancet Haematology. 2020 May 11.
Li X, Song Y, Wong G, Cui J. Bat origin of a new human coronavirus: there and back again. Science China Life Sciences. 2020 Mar;63(3):461-2.
Li Y, Parks GD. Relative contribution of cellular complement inhibitors CD59, CD46, and CD55 to parainfluenza virus 5 inhibition of complement-mediated neutralization. Viruses. 2018;10(5).
Liu Y, Du X, Chen J, Jin Y, Peng L, Wang HH, Luo M, Chen L, Zhao Y. Neutrophil-to-lymphocyte ratio as an independent risk factor for mortality in hospitalized patients with COVID-19. Journal of Infection. 2020 Apr 10.
Lu S, Zhao Y, Yu W, Yang Y, Gao J, Wang J, Kuang D, Yang M, Yang J, Ma C, Xu J. Comparison of SARS-CoV-2 infections among 3 species of non-human primates. bioRxiv. 2020 Jan 1
Ma-Lauer Y, Carbajo-Lozoya J, Hein MY, Müller MA, Deng W, Lei J, Meyer B, Kusov Y, von Brunn B, Bairad DR, Hünten S. p53 down-regulates SARS coronavirus replication and is targeted by the SARS-unique domain and PLpro via E3 ubiquitin ligase RCHY1. Proceedings of the National Academy of Sciences. 2016 Aug 30;113(35):E5192-201.
Matsuyama S, Nao N, Shirato K, Kawase M, Saito S, Takayama I, Nagata N, Sekizuka T, Katoh H, Kato F, Sakata M. Enhanced isolation of SARS-CoV-2 by TMPRSS2-expressing cells. Proceedings of the National Academy of Sciences. 2020 Mar 31;117(13):7001-3.
Mehta P, McAuley DF, Brown M, Sanchez E, Tattersall RS, Manson JJ, HLH Across Speciality Collaboration. COVID-19: consider cytokine storm syndromes and immunosuppression. Lancet (London, England). 2020 Mar 28;395(10229):1033.
Menachery VD, Dinnon KH, Yount BL, McAnarney ET, Gralinski LE, Hale A, Graham RL, Scobey T, Anthony SJ, Wang L, Graham B. Trypsin treatment unlocks barrier for zoonotic bat coronavirus infection. Journal of virology. 2020 Feb 14;94(5).
Merad M, Martin JC. Pathological inflammation in patients with COVID-19: a key role for monocytes and macrophages. Nature Reviews Immunology. 2020 May 6:1-8.
Mercurio I, Tragni V, Busto F, De Grassi A, Pierri CL. Protein structure analysis of the interactions between SARS-CoV-2 spike protein and the human ACE2 receptor: from conformational changes to novel neutralizing antibodies. bioRxiv. 2020 Jan 1.
Mesplède T, Island M-L, Christeff N, Petek F, Doly J, Navarro S. The POU Transcription Factor Oct-1 Represses Virus-Induced Interferon A Gene Expression. Mol Cell Biol. 2005;25(19):8717–31
Mielech AM, Kilianski A, Baez-Santos YM, Mesecar AD, Baker SC. MERS-CoV papain-like protease has delSGylating and deubiquitinating activities. Virology. 2014 Feb 1;450:64-70.
Mo P, Xing Y, Xiao Y, Deng L, Zhao Q, Wang H, Xiong Y, Cheng Z, Gao S, Liang K, Luo M. Clinical characteristics of refractory COVID-19 pneumonia in Wuhan, China. Clinical Infectious Diseases. 2020 Mar 16.
Mohta S, Agarwal A, Makharia GK. Exploring COVID-19 Therapies: An Extraordinary Global Challenge. Journal of Digestive Endoscopy. 2020 Mar;11(01):73-5.
Mozzini C, Girelli D. The role of Neutrophil Extracellular Traps in Covid-19: Only an hypothesis or a potential new field of research?. Thrombosis Research. 2020 Jul 1;191:26-7.

Mukai S, Yamasaki K, Fujii M, Nagai T, Terada N, Kataoka H, et al. Dysregulation of type II transmembrane serine proteases and ligand-dependent activation of MET in urological cancers. Int J Mol Sci. 2020;21(8).
Narayanan A, Ruyechan WT, Kristie TM. The coactivator host cell factor-1 mediates Set1 and MLL1 H3K4 trimethylation at herpesvirus immediate early promoters for initiation of infection. Proceedings of the National Academy of Sciences. 2007 Jun 26;104(26):10835-40.
Netzband R, Pager CT. Epitranscriptomic marks: Emerging modulators of RNA virus gene expression. Wiley Interdisciplinary Reviews: RNA. 2020 May;11(3):e1576.
Nguyen B. In silico pharmacophore study and structural optimization of Nafamostat yield potentially novel Transmembrane Protease Serine 2 (TMPRSS2) inhibitors which block the entry of SARS-CoV-2 virus into human cells.
Nguyen BX. In Silico Pharmacophore Study and Structural Optimization of Nafamostat Yield Potentially Novel Transmembrane Protease Serine 2 (TMPRSS2) Inhibitors Which Block the Entry of SARS-CoV-2 Virus into. 2020;2(2).
Nhu QM, Shirey K, Teijaro JR, Farber DL, Antalis TM, Fasano A, et al. Novel signaling interactions between proteinase-activated receptor 2 and Toll-like receptors in vitro and in vivo. Mucosal Immunol [Internet]. 2010;3(1):29–39. Available from: http://dx.doi.org/10.1038/mi.2009.120
Ortea I, Bock JO. Re-analysis of SARS-CoV-2 infected host cell proteomics time-course data by impact pathway analysis and network analysis. A potential link with inflammatory response. BioRxiv. 2020 Jan 1.
Oyarzún-Arrau A, Alonso-Palomares L, Valiente-Echeverría F, Osorio F, Soto-Rifo R. Crosstalk between RNA Metabolism and Cellular Stress Responses during Zika Virus Replication. Pathogens. 2020 Mar;9(3):158.
Paranjpe I, Fuster V, Lala A, Russak A, Glicksberg BS, Levin MA, Charney AW, Narula J, Fayad ZA, Bagiella E, Zhao S. Association of treatment dose anticoagulation with in-hospital survival among hospitalized patients with COVID-19. Journal of the American College of Cardiology. 2020 May 6.
Petrache I. Is More Better? Promising Biological Effects of Double-Dose Alpha 1-Antitrypsin Therapy.
Pinto D, Park YJ, Beltramello M, Walls AC, Tortorici MA, Bianchi S, Jaconi S, Culap K, Zatta F, De Marco A, Peter A. Cross-neutralization of SARS-CoV-2 by a human monoclonal SARS-CoV antibody. Nature. 2020 May 18:1-0.
Posma JJ, Grover SP, Hisada Y, Owens III AP, Antoniak S, Spronk HM, Mackman N. Roles of coagulation proteases and PARs (protease-activated receptors) in mouse models of inflammatory diseases. Arteriosclerosis, thrombosis, and vascular biology. 2019 Jan;39(1):13-24.
Purdy JG, Luftig MA. Reprogramming of cellular metabolic pathways by human oncogenic viruses. Current opinion in virology. 2019 Dec 1;39:60-9.
Qin C, Zhou L, Hu Z, Zhang S, Yang S, Tao Y, Xie C, Ma K, Shang K, Wang W, Tian DS. Dysregulation of immune response in patients with COVID-19 in Wuhan, China. Clinical Infectious Diseases. 2020 Mar 12..
Rabouw HH, Langereis MA, Knaap RCM, Dalebout TJ, Canton J, Sola I, et al. Middle East Respiratory Coronavirus Accessory Protein 4a Inhibits PKR-Mediated Antiviral Stress Responses. PLoS Pathog. 2016;12(10):1–26.
Rallabhandi P, Nhu QM, Toshchakov VY, Piao W, Medvedev AE, Hollenberg MD, et al. Analysis of proteinase-activated receptor 2 and TLR4 signal transduction: A novel paradigm for receptor cooperativity. J Biol Chem. 2008;283(36):24314–25.
Rangaswamy US, Cotter CR, Cheng X, Jin H, Chen Z. CD55 is a key complement regulatory protein that counteracts complement-mediated inactivation of Newcastle Disease Virus. J Gen Virol. 2016;97(8):1765–70.
Rehwinkel J, Gack MU. RIG-I-like receptors: their regulation and roles in RNA sensing. Nat Rev Immunol [Internet]. 2020; Available from: http://dx.doi.org/10.1038/s41577-020-0288-3
Rice GI, Kasher PR, Forte GM, Mannion NM, Greenwood SM, Szynkiewicz M, Dickerson JE,

Bhaskar SS, Zampini M, Briggs TA, Jenkinson EM. Mutations in ADAR1 cause Aicardi-Goutieres syndrome associated with a type I interferon signature. Nature genetics. 2012 Nov;44(11):1243.
Robinson AR, Kwek SS, Hagemeier SR, Wille CK, Kenney SC. Cellular Transcription Factor Oct-1 Interacts with the Epstein-Barr Virus BRLF1 Protein To Promote Disruption of Viral Latency. J Virol. 2011;85(17):8940–53.
Ruggiero E, Richter SN. Viral G-quadruplexes: New frontiers in virus pathogenesis and antiviral therapy. Annual Reports in Medicinal Chemistry. 2020 May 18.
Sanduzzi A, Ciasullo E, Capitelli L, Sanduzzi Zamparelli S, Bocchino M. Alpha-1-Antitrypsin Deficiency and Bronchiectasis: A Concomitance or a Real Association?. International Journal of Environmental Research and Public Health. 2020 Jan;17(7):2294.
Sanrattana W, Maas C, de Maat S. SERPINs-From trap to treatment. Front Med. 2019;6(FEB):1–8.
Schmaier AH. Serpin targets in hemostasis/ kinin formation. Blood. 2019;134(19):1565–6.
Schneider WM, Chevillotte MD, Rice CM. Interferon-Stimulated Genes: A Complex Web of Host Defenses. Annu Rev Immunol. 2014;32(1):513–45.
Shang J, Ye G, Shi K, Wan Y, Luo C, Aihara H, Geng Q, Auerbach A, Li F. Structural basis of receptor recognition by SARS-CoV-2. Nature. 2020 Mar 30:1-4.
Sharma M, Kumar R, Ram J, Luthra-Guptasarma M. Establishment and characterization of a novel Serine Protease Induced Reprograming (SPIR) method with applications in ocular tissue regeneration. Investigative Ophthalmology & Visual Science. 2017 Jun 23;58(8):1426-.
Sharma M, Kumar R, Sharma S, Thomas B, Kapatia G, Singh G, Bal A, Ram J, Bhasin M, Guptasarma P, Luthra-Guptasarma M. Sustained exposure to trypsin causes cells to transition into a state of reversible stemness that is amenable to transdifferentiation. bioRxiv. 2019 Jan 1:679928.
Sharma M, Lei H, Pennock S, Kazlauskas A. Epithelial cells promote fibroblast-mediated contraction of collagen gels by secreting bFGF. Investigative Ophthalmology & Visual Science. 2013 Jun 16;54(15):6258-.
Shen C, Wang Z, Zhao F, Yang Y, Li J, Yuan J, Wang F, Li D, Yang M, Xing L, Wei J. Treatment of 5 critically ill patients with COVID-19 with convalescent plasma. Jama. 2020 Apr 28;323(16):1582-9.
Shulla A, Heald-Sargent T, Subramanya G, Zhao J, Perlman S, Gallagher T. A Transmembrane Serine Protease Is Linked to the Severe Acute Respiratory Syndrome Coronavirus Receptor and Activates Virus Entry. J Virol. 2011;85(2):873–82
Signes A, Fernandez-Vizarra E. Assembly of mammalian oxidative phosphorylation complexes I–V and supercomplexes. Essays Biochem. 2018;62(3):255–70.
Sodhi CP, Nguyen J, Yamaguchi Y, Werts AD, Lu P, Ladd MR, Fulton WB, Kovler ML, Wang S, Prindle T, Zhang Y. A Dynamic Variation of Pulmonary ACE2 Is Required to Modulate Neutrophilic Inflammation in Response to Pseudomonas aeruginosa Lung Infection in Mice. The Journal of Immunology. 2019 Dec 1;203(11):3000-12.
Stakos D, Skendros P, Konstantinides S, Ritis K. Traps N'Clots: NET-Mediated Thrombosis and Related Diseases. Thrombosis and Haemostasis. 2020 Jan 15.
Stark GR, Darnell JE. The JAK-STAT Pathway at Twenty. Immunity [Internet]. 2012;36(4):503–14. Available from: http://dx.doi.org/10.1016/j.immuni.2012.03.013
Stefan Bittmann*, Elisabeth Luchter, Anne Weissenstein, G. V. and E. M.-A. (2020) 'TMPRSS2-Inhibitors Play a role in Cell Entry Mechanism of COVID-19: An Insight into Camostat and Nafamostat', 2(2), pp. 1–3.
Sugitani Y, Nishida A, Inatomi O, Ohno M, Imai T, Kawahara M, Kitamura K, Andoh A. Sodium absorption stimulator prostasin (PRSS8) has an anti-inflammatory effect via downregulation of TLR4 signaling in inflammatory bowel disease. Journal of Gastroenterology. 2020 Jan 8:1-0.
Sun P, Qie S, Liu Z, Ren J, Li K, Xi J. Clinical characteristics of hospitalized patients with SARS-CoV-2 infection: a single arm meta-analysis. Journal of medical virology. 2020 Jun;92(6):612-7.
Sun Y, Chen C, Zhang X, Weng X, Sheng A, Zhu Y, Chen S, Zheng X, Lu C. High neutrophil-

to-lymphocyte ratio is an early predictor of bronchopulmonary dysplasia. Frontiers in pediatrics. 2019;7:464.
Tan Q, Guo P, Zhou J, Zhang J, Zhang B, Lan C, Xian J, Ge M, Feng H, Chen Z. Targeting neutrophil extracellular traps enhanced tPA fibrinolysis for experimental intracerebral hemorrhage. Translational Research. 2019 Sep 1;211:139-46.
Tauber D, Tauber G, Khong A, Van Treeck B, Pelletier J, Parker R. Modulation of RNA condensation by the DEAD-box protein eIF4A. Cell. 2020 Jan 9.
Tauber D, Tauber G, Khong A, Van Treeck B, Pelletier J, Parker R. Modulation of RNA condensation by the DEAD-box protein eIF4A. Cell. 2020 Jan 9.
Tay MZ, Poh CM, Rénia L, MacAry PA, Ng LF. The trinity of COVID-19: immunity, inflammation and intervention. Nature Reviews Immunology. 2020 Apr 28:1-2.
te Velthuis AJ. Flu transcription captured in action. Nature structural & molecular biology. 2019 Jun;26(6):393-5.
Thierry A, Roch B. NETs By-Products and Extracellular DNA May Play a Key Role in COVID-19 Pathogenesis: Incidence on Patient Monitoring and Therapy. MEDICINE & PHARMACOLOGY. 2020 Apr 15.
Thomas R. O'Brien*, David L. Thomas, S. S. J. and Ludmila Prokunina-Olsson, Raymond P. Donnelly, R. H. (2020) 'Weak Induction of Interferon Expression by SARS-CoV-2 Supports Clinical Trials of Interferon Lambda to Treat Early COVID-19', 0813(April), pp. 1–30. doi: 10.1080/1059924X.2017.1319315.
Tortorici MA, Veesler D. Structural insights into coronavirus entry. Advances in virus research. 2019 Aug 22;105:93-116.
van der Heide, V. (2020) 'Innate T cells in COVID-19: friend or foe?', *Nature Reviews Immunology*, 20089300(2020), p. 20089300. doi: 10.1038/s41577-020-0349-7
Vardhana SA, Arnold PK, Rosen BP, Chen Y, Carey BW, Huangfu D, Carmona-Fontaine C, Thompson CB, Finley LW. Glutamine independence is a selectable feature of pluripotent stem cells. Nature metabolism. 2019 Jul;1(7):676-87.
Varjú I, Kolev K. Networks that stop the flow: A fresh look at fibrin and neutrophil extracellular traps. Thrombosis research. 2019 Aug 7.
Varjú I, Kolev K. Networks that stop the flow: A fresh look at fibrin and neutrophil extracellular traps. Thromb Res [Internet]. 2019;182(May):1–11. Available from: https://doi.org/10.1016/j.thromres.2019.08.003
Vatansever EC, Yang K, Kratch KC, Drelich A, Cho CC, Mellot DM, Xu S, Tseng CT, Liu WR. Targeting the SARS-CoV-2 Main Protease to Repurpose Drugs for COVID-19. bioRxiv. 2020 Jan 1.
Vatansever EC, Yang K, Kratch KC, Drelich A, Cho CC, Mellot DM, Xu S, Tseng CT, Liu WR. Targeting the SARS-CoV-2 Main Protease to Repurpose Drugs for COVID-19. bioRxiv. 2020 Jan 1.
Walls AC, Park YJ, Tortorici MA, Wall A, McGuire AT, Veesler D. Structure, function, and antigenicity of the SARS-CoV-2 spike glycoprotein. Cell. 2020 Mar 9.
Walls AC, Tortorici MA, Snijder J, Xiong X, Bosch BJ, Rey FA, Veesler D. Tectonic conformational changes of a coronavirus spike glycoprotein promote membrane fusion. Proceedings of the National Academy of Sciences. 2017 Oct 17;114(42):11157-62.
Wang D, Hu B, Hu C, Zhu F, Liu X, Zhang J, Wang B, Xiang H, Cheng Z, Xiong Y, Zhao Y. Clinical characteristics of 138 hospitalized patients with 2019 novel coronavirus–infected pneumonia in Wuhan, China. Jama. 2020 Mar 17;323(11):1061-9.
Wegener M, Müller-McNicoll M. Nuclear retention of mRNAs–quality control, gene regulation and human disease. InSeminars in cell & developmental biology 2018 Jul 1 (Vol. 79, pp. 131-142). Academic Press.
Weithauser A, Bobbert P, Antoniak S, Böhm A, Rauch BH, Klingel K, et al. Protease-activated receptor-2 regulates the innate immune response to viral infection in a coxsackievirus B3-induced myocarditis. J Am Coll Cardiol. 2013;62(19):1737–45.
Wendt L, Brandt J, Bodmer BS, Reiche S, Schmidt ML, Traeger S, Hoenen T. The Ebola Virus Nucleoprotein Recruits the Nuclear RNA Export Factor NXF1 into Inclusion Bodies to Facilitate Viral Protein Expression. Cells. 2020 Jan;9(1):187.

Wojtukiewicz MZ, Hempel D, Sierko E, Tucker SC, Honn K V. Protease-activated receptors (PARs)—biology and role in cancer invasion and metastasis. Cancer Metastasis Rev. 2015;34(4):775–96.
Wong HH, Fung TS, Fang S, Huang M, Le MT, Liu DX. Accessory proteins 8b and 8ab of severe acute respiratory syndrome coronavirus suppress the interferon signaling pathway by mediating ubiquitin-dependent rapid degradation of interferon regulatory factor 3. Virology. 2018 Feb 1;515:165-75.
Wong HH, Fung TS, Fang S, Huang M, Le MT, Liu DX. Accessory proteins 8b and 8ab of severe acute respiratory syndrome coronavirus suppress the interferon signaling pathway by mediating ubiquitin-dependent rapid degradation of interferon regulatory factor 3. Virology. 2018 Feb 1;515:165-75.
Wrapp D, Wang N, Corbett KS, Goldsmith JA, Hsieh CL, Abiona O, Graham BS, McLellan JS. Cryo-EM structure of the 2019-nCoV spike in the prefusion conformation. Science. 2020 Mar 13;367(6483):1260-3.
Wu D, Yang XO. TH17 responses in cytokine storm of COVID-19: An emerging target of JAK2 inhibitor Fedratinib. Journal of Microbiology, Immunology and Infection. 2020 Mar 11.
Xia S, Zhou C, Kalionis B, Shuang X, Ge H, Gao W. Combined Antioxidant, Anti-inflammaging and Mesenchymal Stem Cell Treatment: A Possible Therapeutic Direction in Elderly Patients with Chronic Obstructive Pulmonary Disease. Aging and disease. 2020 Feb:0.
Xiahou Z, Wang X, Shen J, Zhu X, Xu F, Hu R, et al. NMI and IFP35 serve as proinflammatory DAMPs during cellular infection and injury. Nat Commun [Internet]. 2017;8(1):1–11. Available from: http://dx.doi.org/10.1038/s41467-017-00930-9
Xu H, Su C, Pearson A, Mody CH, Zheng C. Herpes simplex virus 1 UL24 abrogates the DNA sensing signal pathway by inhibiting NF-κB activation. Journal of virology. 2017 Apr 1;91(7):e00025-17.
Xu X, Han M, Li T, Sun W, Wang D, Fu B, Zhou Y, Zheng X, Yang Y, Li X, Zhang X. Effective treatment of severe COVID-19 patients with tocilizumab. Proceedings of the National Academy of Sciences. 2020 May 19;117(20):10970-5.
Yan R, Zhang Y, Li Y, Xia L, Guo Y, Zhou Q. Structural basis for the recognition of SARS-CoV-2 by full-length human ACE2. Science. 2020 Mar 27;367(6485):1444-8.
Yang P, Mathieu C, Kolaitis RM, Zhang P, Messing J, Yurtsever U, Yang Z, Wu J, Li Y, Pan Q, Yu J. G3BP1 is a tunable switch that triggers phase separation to assemble stress granules. Cell. 2020 Apr 16;181(2):325-45.
Yang Y, Shen C, Li J, Yuan J, Yang M, Wang F, Li G, Li Y, Xing L, Peng L, Wei J. Exuberant elevation of IP-10, MCP-3 and IL-1ra during SARS-CoV-2 infection is associated with disease severity and fatal outcome. MedRxiv. 2020 Jan 1.
Yao X, Ye F, Zhang M, Cui C, Huang B, Niu P, Liu X, Zhao L, Dong E, Song C, Zhan S. In vitro antiviral activity and projection of optimized dosing design of hydroxychloroquine for the treatment of severe acute respiratory syndrome coronavirus 2 (SARS-CoV-2). Clinical Infectious Diseases. 2020 Mar 9.
Yin, S., Huang, M., Li, D., & Tang, N. (2020). Difference of coagulation features between severe pneumonia induced by SARS-CoV2 and non-SARS-CoV2. *Journal of Thrombosis and Thrombolysis*, 3–6. https://doi.org/10.1007/s11239-020-02105-8
Yuan L, Chen Z, Song S, Wang S, Tian C, Xing G, Chen X, Xiao ZX, He F, Zhang L. p53 degradation by a coronavirus papain-like protease suppresses type I interferon signaling. Journal of Biological Chemistry. 2015 Jan 30;290(5):3172-82.
Zang R, Castro MF, McCune BT, Zeng Q, Rothlauf PW, Sonnek NM, Liu Z, Brulois KF, Wang X, Greenberg HB, Diamond MS. TMPRSS2 and TMPRSS4 promote SARS-CoV-2 infection of human small intestinal enterocytes. Science Immunology. 2020 May 13;5(47).
Zhang H, Penninger JM, Li Y, Zhong N, Slutsky AS. Angiotensin-converting enzyme 2 (ACE2) as a SARS-CoV-2 receptor: molecular mechanisms and potential therapeutic target. Intensive care medicine. 2020 Mar 3:1-5.
Zhang S, Carriere J, Lin X, Xie N, Feng P. Interplay between cellular metabolism and cytokine responses during viral infection. Viruses. 2018 Oct;10(10):521.

Zhou Y, Hou Y, Shen J, Huang Y, Martin W, Cheng F. Network-based drug repurposing for novel coronavirus 2019-nCoV/SARS-CoV-2. Cell discovery. 2020 Mar 16;6(1):1-8.

Zhou, P., Yang, X., Wang, X., Hu, B., Zhang, L., Zhang, W., … Shi, Z. (2020). A pneumonia outbreak associated with a new coronavirus of probable bat origin. *Nature*, *579*(March). https://doi.org/10.1038/s41586-020-2012-7

Zhu Z, Li W, Zhang X, Wang C, Gao L, Yang F, Cao W, Li K, Tian H, Liu X, Zhang K. Foot-and-Mouth Disease Virus Capsid Protein VP1 Interacts with Host Ribosomal Protein SA To Maintain Activation of the MAPK Signal Pathway and Promote Virus Replication. Journal of virology. 2020 Jan 17;94(3).

Zuo Y, Yalavarthi S, Shi H, Gockman K, Zuo M, Madison JA, Blair CN, Weber A, Barnes BJ, Egeblad M, Woods RJ. Neutrophil extracellular traps in COVID-19. JCI insight. 2020 Apr 24:138999.

Zuo Y, Yalavarthi S, Shi H, Gockman K, Zuo M, Madison JA, Blair C, Weber A, Barnes BJ, Egeblad M, Woods RJ. Neutrophil extracellular traps (NETs) as markers of disease severity in COVID-19. medRxiv. 2020 Jan 1.

Preprints (www.preprints.org) | NOT PEER-REVIEWED | Posted: 17 June 2020 doi:10.20944/preprints202006.0206.v1

A

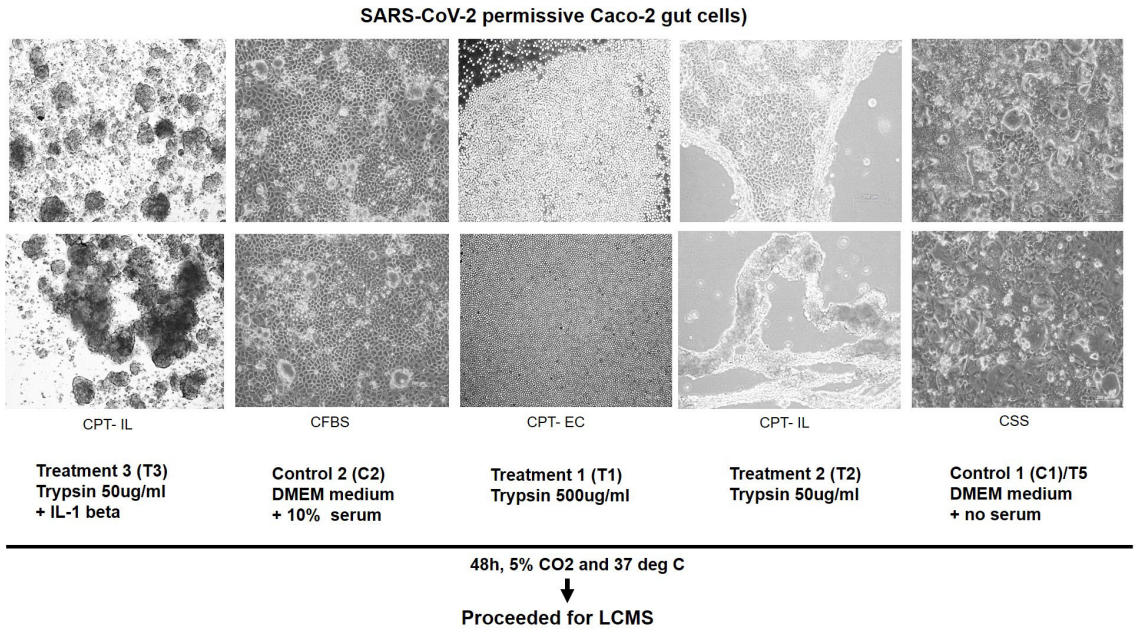

B

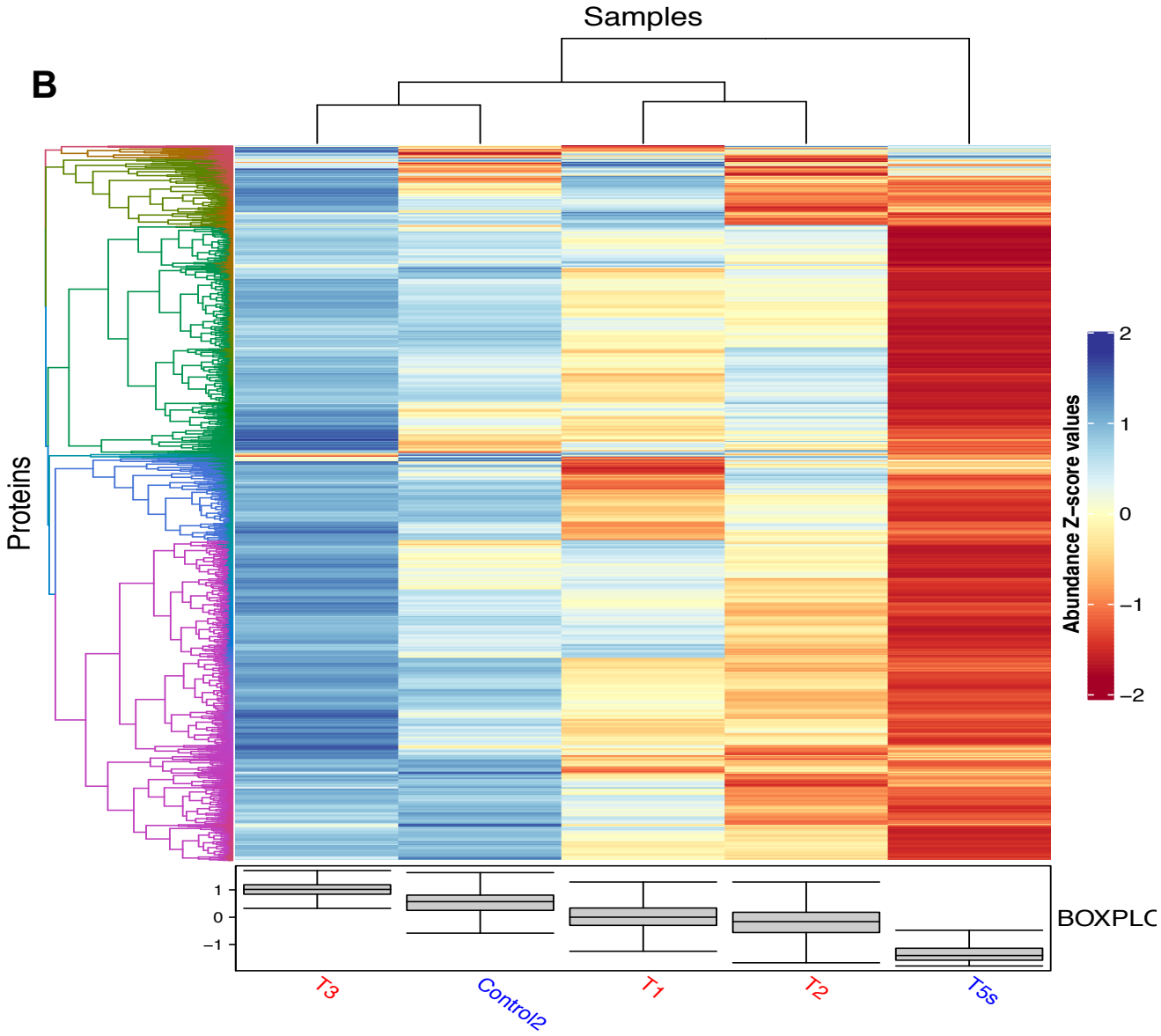

Preprints (www.preprints.org) | NOT PEER-REVIEWED | Posted: 17 June 2020 doi:10.20944/preprints202006.0206.v1

A

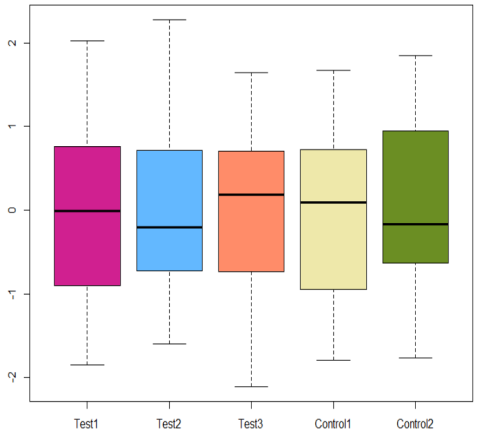

B

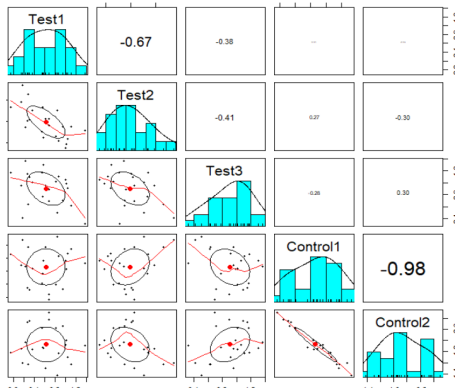

C

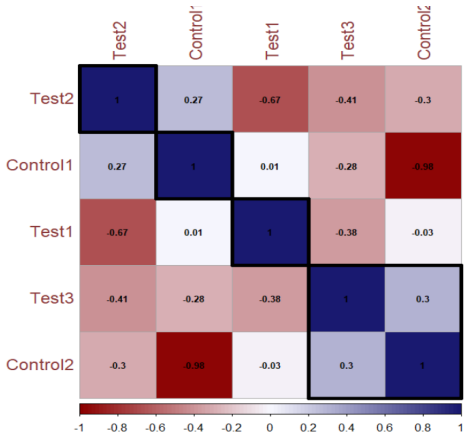

D

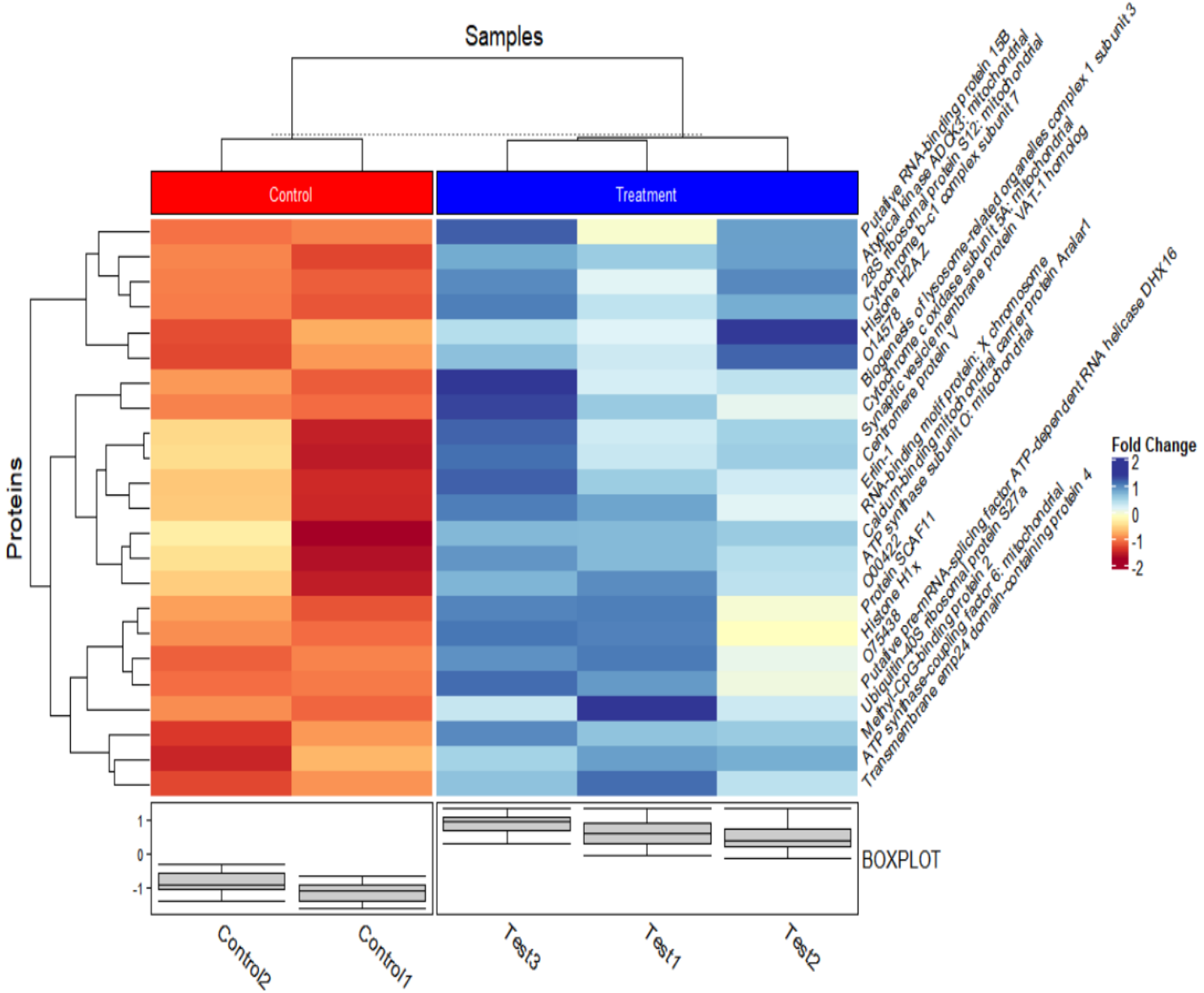

Preprints (www.preprints.org) | NOT PEER-REVIEWED | Posted: 17 June 2020 doi:10.20944/preprints202006.0206.v1

A

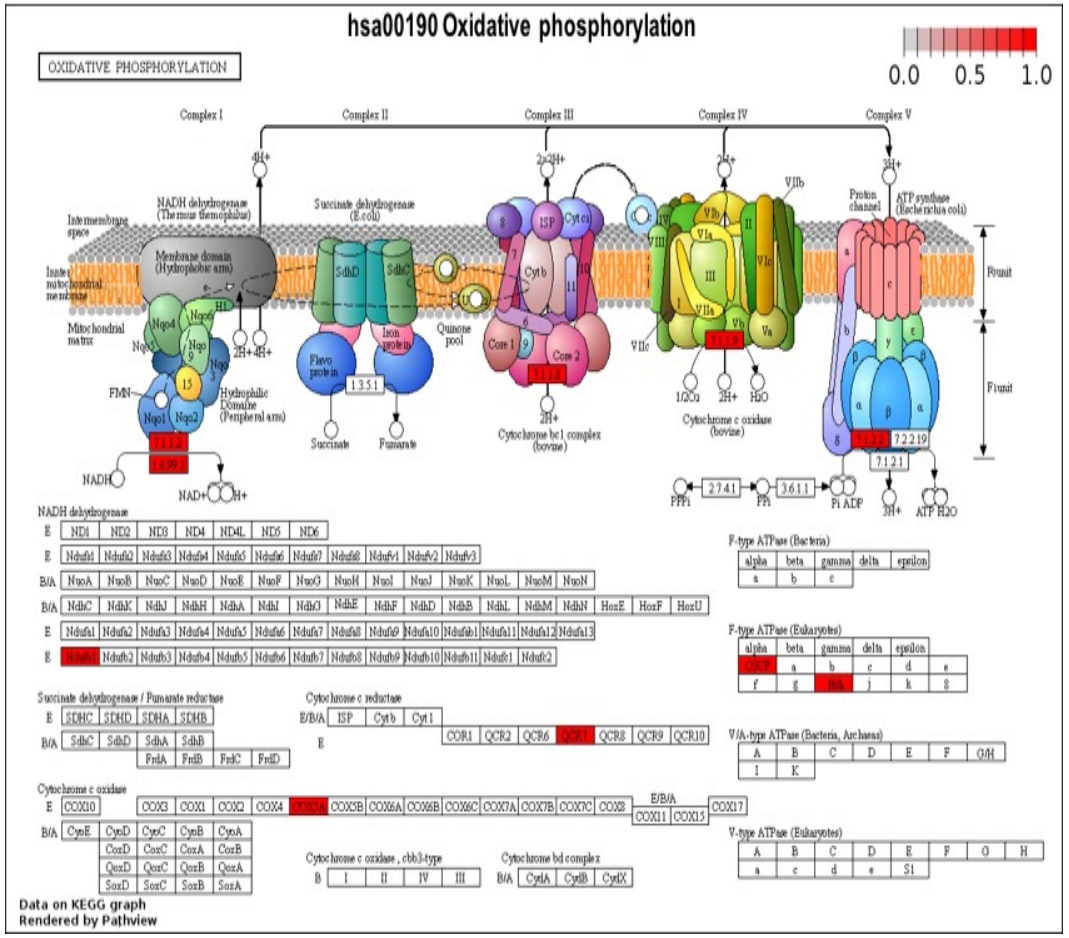

B

ACCESSION NUMBER		PROTEIN NAME	T1 log2FC	T2 log2FC	T3 log2FC
O95298	NDUFC2-KCTD14	NADH dehydrogenase [ubiquinone] 1 subunit C2 OS=Homo sapiens GN=NDUFC2 PE=1 SV=1	-0.99	0.99	1.90
O75438	Ndufb1	NADH dehydrogenase [ubiquinone] 1 beta subcomplex subunit 1 OS=Homo sapiens GN=NDUFB1 PE=1 SV=1	1.02	1.06	-0.05
P14927	QCR7/UQCRB	Cytochrome b-c1 complex subunit 7 OS=Homo sapiens GN=UQCRB PE=1 SV=2	1.12	1.72	0.48
P20674	COX5A	Cytochrome c oxidase subunit 5A, mitochondrial OS=Homo sapiens GN=COX5A PE=1 SV=2	1.25	1.32	0.65
P48047	OSCP/ ATP5O	ATP synthase subunit O, mitochondrial OS=Homo sapiens GN=ATP5O PE=1 SV=1	0.90	1.11	-0.02
P18859	F6/h ATP5J	ATP synthase-coupling factor 6, mitochondrial OS=Homo sapiens GN=ATP5J PE=1 SV=1	1.97	2.26	0.69

Preprints (www.preprints.org) | NOT PEER-REVIEWED | Posted: 17 June 2020 doi:10.20944/preprints202006.0206.v1

A **KEGG pathway analysis for 26 biological pathways implicated in viral pathogenesis**

00190 Oxidative phosphorylation

05168-Herpes simplex virus 1 infection
05203-Viral carcinogenesis
05416-Viral myocarditis
04061-Viral protein interaction with cytokine and cytokine receptor

04620-Toll-like receptor signaling pathway
04622-RIG-I-like receptor signaling pathway
04623-Cytosolic DNA-sensing pathway
04064-NF-kappa B signaling pathway

03010 Ribosome
03040 Spliceosome
03013 RNA transport
04141 Protein processing in endoplasmic reticulum
03050 Proteasome

04140-Autophagy - animal
04142-Lysosome
04144-Endocytosis
04130-SNARE interactions in vesicular transport

04062-Chemokine signaling pathway
04810-Regulation of actin cytoskeleton
04071-Sphingolipid signaling pathway
04024-cAMP signaling pathway
04151-PI3K-Akt signaling pathway
04520-Adherens junction
04530-Tight junction
04014-Ras signaling pathway

04610-Complement and coagulation cascades

B **Example of Expression Tags**

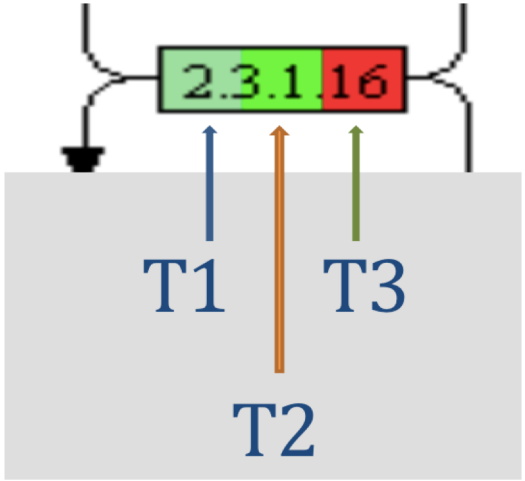

T1, T2, T3 over Control 2 (DMEM + 10%FBS)
T= Trypsin
Red= upregulated
Green=downregulated
The box is equally distributed in three parts, with T1 occupying the extreme left (as shown in light green here), T2 occupying the middle (fluorescent green) and T3 occupying the extreme right one-third (as shown in red here).
https://www.genome.jp/kegg-bin/show_organism?menu_type=pathway_maps&org=hsa
(KEGG PATHWAY LINK)

Preprints (www.preprints.org) | NOT PEER-REVIEWED | Posted: 17 June 2020 doi:10.20944/preprints202006.0206.v1

A

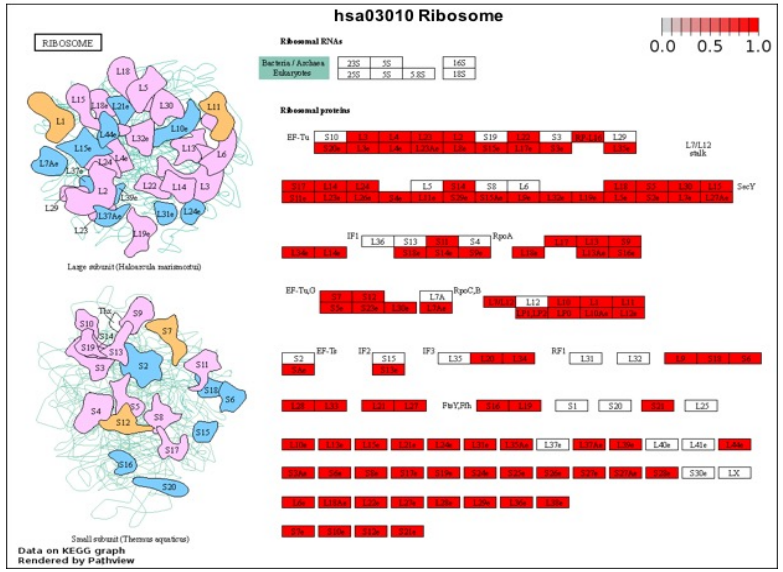

B

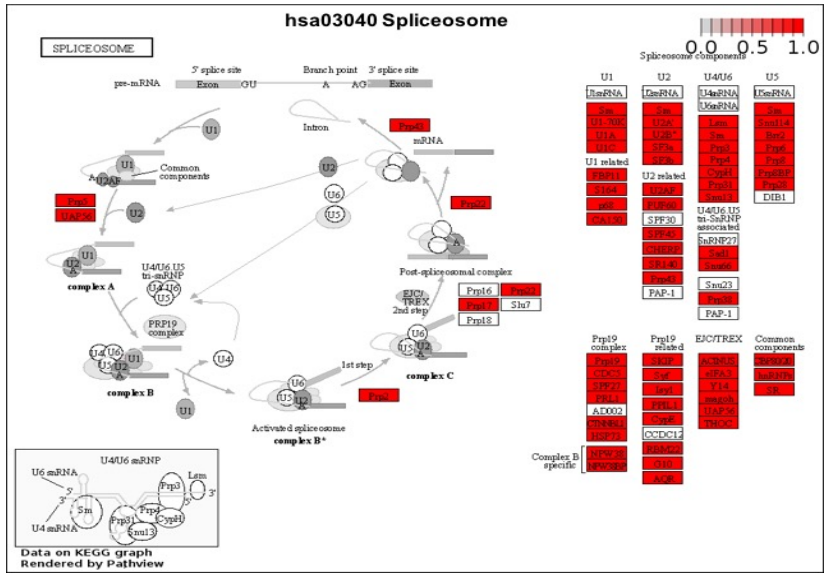

C

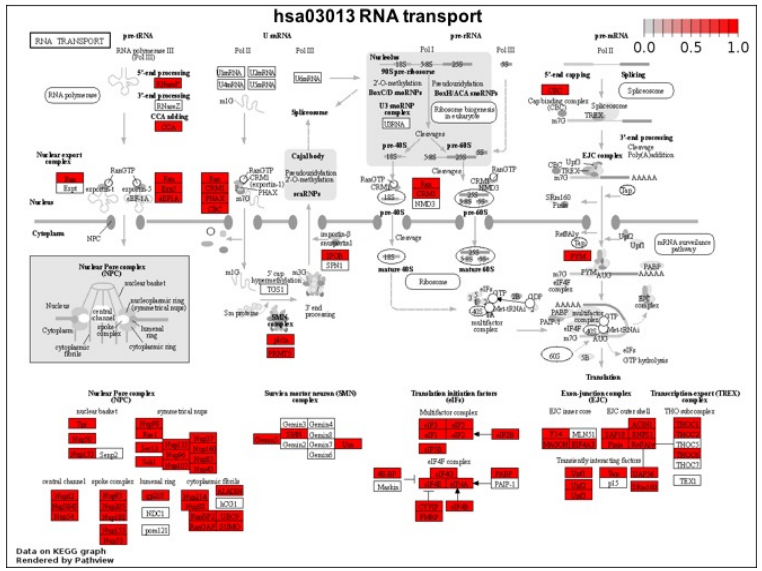

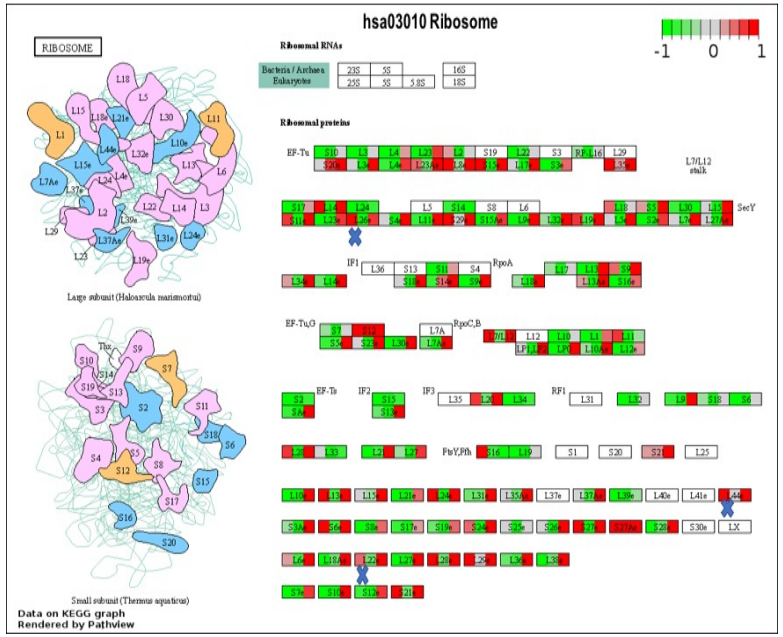

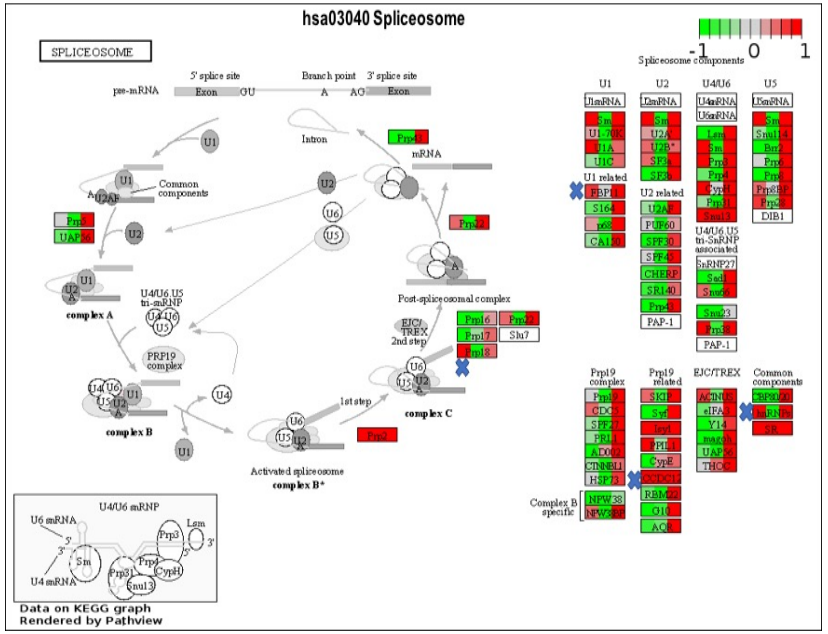

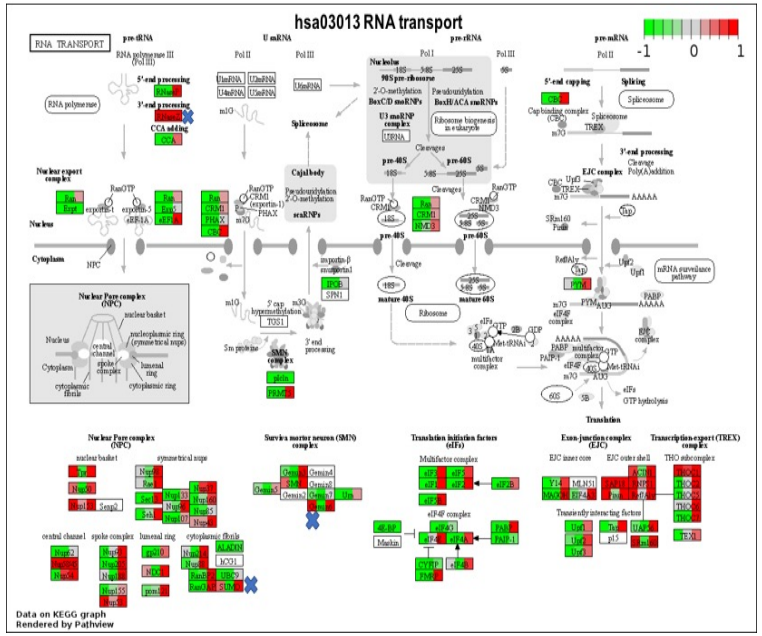

Preprints (www.preprints.org) | NOT PEER-REVIEWED | Posted: 17 June 2020 doi:10.20944/preprints202006.0206.v1

A

RPL23A 0.67 0.36 0.55	MRPL12 1.04 0.45 -0.17	RPS27A 1.27 1.16 -0.20	DHX16 4.95 3.28 4.51	SNRPB2 1.56 -2.81 0.49	ACIN1 0.86 0.31 0.52	Nup43 0.55 0.84 0.72
RPL8 1.87 0.21 1.35	MRPL11 0.75 -0.25 -0.83	RPL28 1.21 0.16 0.74	PRPF18 - -0.79 -0.04	SF3A1 0.33 -0.59 0.47	SNRNP40 0.74 0.68 0.95	SMN 0.63 0.07 0.29
RPL35 2.08 0.99 1.13	MRPL20 0.99 0.11 1.18	RPL29 2.87 0.62 2.04	DHX8 0.95 -0.45 1.29	SNW1 0.73 0.03 0.59	DDX23 1.01 0.15 1.05	SAP18 2.79 2.19 1.37
MRPL14 1.06 0.09 0.16	MRPL28 0.88 -0.28 0.00	RPS21 1.37 0.23 0.71	SNRPB 1.17 -0.76 -0.10	Isy1 1.72 2.19 2.28	SRSF10 0.87 0.93 0.85	Pinin 1.28 0.44 0.60
RPS11 0.96 -0.03 0.42	MRPS16 1.78 -0.19 -1.63	MRPL2 0.61 -1.01 -0.83	SNRNP70 0.68 -0.76 0.71	PPIL1 2.30 0.19 1.49	TPR 1.23 -0.02 0.69	ACIN1 0.86 0.31 0.52
MRPL18 0.68 -0.60 -0.70	RPL13 1.10 0.24 0.13	MRPS5 0.59 -0.71 0.04	SNRPA 1.00 -0.52 -0.30	PRPF3 1.47 0.04 0.88	Nup50 0.81 -1.05 0.00	RNPS1 1.92 0.89 0.99
RPS29 2.38 0.63 0.26	RSL24D1 2.44 1.19 1.52	RPL34 0.56 0.15 0.60	DDX5 0.48 -0.12 0.16	PPIH 1.55 0.76 1.66	Nup153 1.76 1.10 1.84	RefAly 1.38 0.59 1.06
RPL19 0.92 0.12 0.58	RPS6 0.76 0.25 0.09	MRPS9 0.74 -0.33 0.26	CDC5L 0.68 0.45 0.87	Snu13 0.97 1.29 0.97	Nup58/45 1.12 1.00 0.07	SRRM1 1.50 -0.18 1.31
RPL13A 0.68 -0.58 0.33	RPS24 0.61 -0.09 0.13	MRPS21 0.55 0.93 0.88	WBP11 0.78 -0.70 0.58	SART1 0.66 -0.11 0.30	Nup53 1.35 0.83 0.45	THOC1 3.11 1.75 3.06
MRPS12 0.69 1.31 -0.07	RPS27L 5.50 1.25 1.76	RPL6 0.59 0.03 0.67	SNRPA1 0.59 0.43 1.01	PRPF38B 1.46 - 0.14	NDC1 1.33 -2.33 2.61	

B

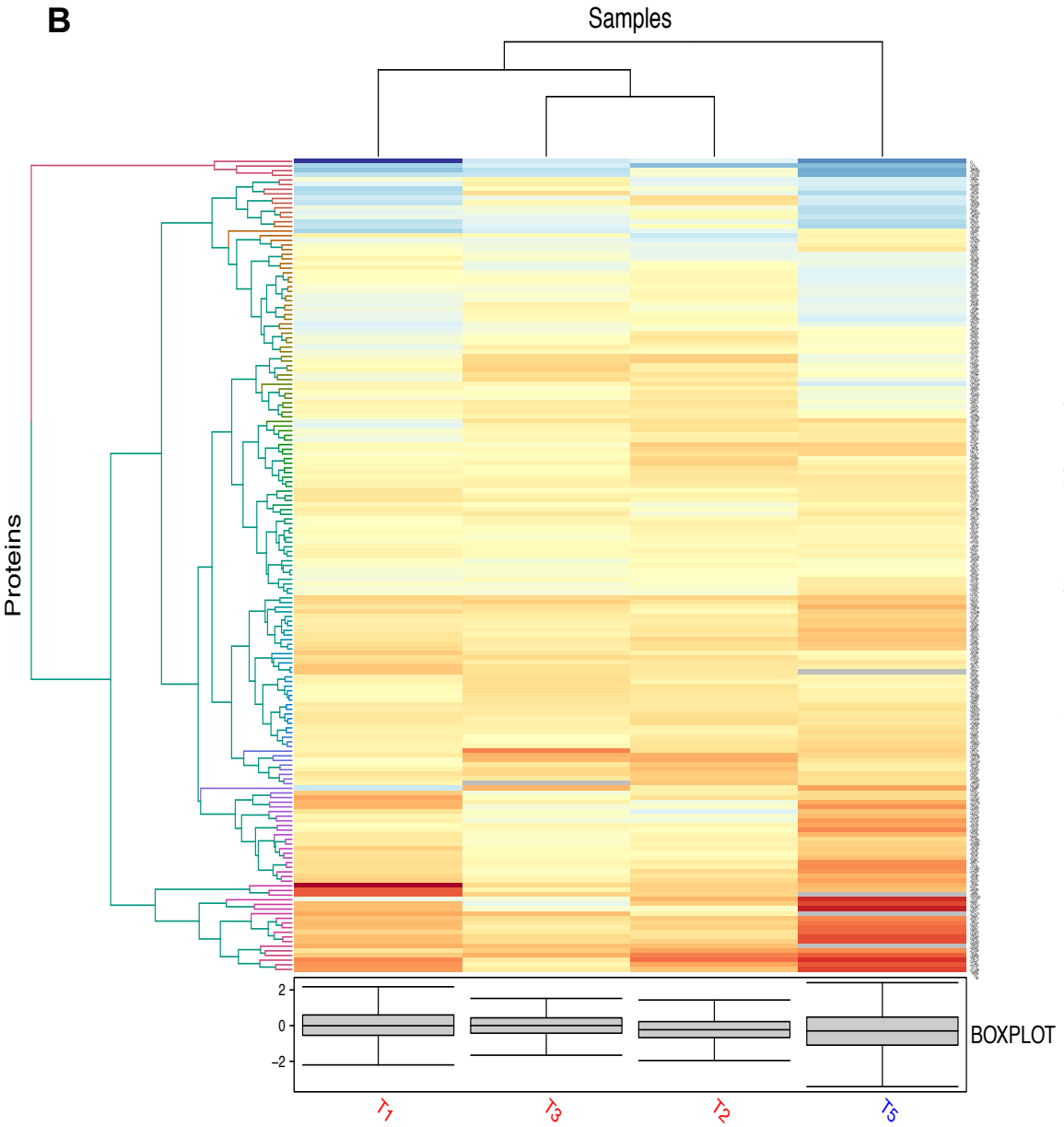

Preprints (www.preprints.org) | NOT PEER-REVIEWED | Posted: 17 June 2020 doi:10.20944/preprints202006.0206.v1

A

NOP10				HNRNPH2				SNRNP40				HNRNPF				SNRPN			
3.1	0.6	1.4	1.5	1.2	0.0	0.3	-0.4	0.7	0.7	0.9	-1.1	0.3	-0.0	0.8	-1.2	-0.4	1.5	0.6	-0.1
RRP9				SNRPB				UTP11				GAR1				RAVER1			
2.1	1.2	2.4	0.9	1.2	-0.7	-0.1	-1.2	0.7	1.1	-2.0	-	0.3	0.7	0.6	-1.2	-0.4	-1.6	0.6	-1.7
SARNP				HNRNPDL				NOC2L				NAF1				TROVE2			
1.7	-1.5	1.3	0.5	1.2	-0.1	0.5	0.5	0.7	1.0	0.8	-1.1	0.2	-1.5	-1.5	-	-0.4	-0.8	-0.0	-1.6
SNRPB2				SNRPE				SNRNP70				SNRPD3				IMP4			
1.6	-2.8	0.5	-1.3	1.0	-0.1	0.5	-1.7	0.7	-0.8	0.7	-0.5	0.2	-0.5	0.6	-1.6	-0.5	1.1	-0.2	-0.4
HNRNPM				HNRNPD				HNRNPH1				EFTUD2				SNRNP200			
1.5	0.7	0.5	-0.4	1.0	0.1	0.7	0.5	0.7	0.6	0.8	-0.7	0.1	-0.1	0.4	-2.2	-0.5	-0.3	0.1	-3.2
NOP16				HNRNPA3				HNRNPUL2				SNRPC				SYNCRIP			
1.5	1.1	1.2	0.7	1.0	0.2	0.7	-0.4	0.6	0.3	0.4	-1.1	0.0	-0.9	-0.4	-2.0	-0.5	-1.4	-0.2	-3.0
PRPF3				SNRPA				SNRPG				PRPF31				UTP14A			
1.5	0.0	0.9	0.6	1.0	-0.5	-0.3	-2.6	0.6	-0.2	-0.1	-0.4	0.0	-0.5	0.8	-1.7	-0.7	0.5	0.8	-1.6
NHP2				SNRPD2				SNRPA1				UTP15				HNRNPLL			
1.4	1.1	0.8	0.0	1.0	0.1	1.0	-0.0	0.6	0.4	1.0	-0.7	-0.1	1.1	0.6	0.1	-1.4	-0.7	0.3	-2.7
HNRNPU				DKC1				MPHOSPH10				PRPF4				IMP3			
1.3	0.0	0.8	-0.1	0.9	0.3	1.3	-0.9	0.6	0.7	1.2	-0.1	-0.1	-0.6	0.2	-2.1	-1.4	0.4	-0.2	-4.3
HNRNPAB				HNRNPA1				HNRNPR				SNRPD1				UTP18			
1.2	0.0	0.8	0.8	0.9	-0.1	1.1	-0.9	0.5	-0.2	0.4	-1.1	-0.2	-0.6	-0.1	-0.7	-1.7	-1.2	-0.7	-2.5
HNRNPL				HNRNPH3				HNRNPC				HNRNPK							
1.2	0.3	1.1	-0.3	0.8	0.5	0.9	-0.9	0.4	-0.2	0.4	-1.2	-0.2	-1.0	0.8	-2.0				
HNRNPUL1				HNRNPA2B1				HNRNPA0				SNRPF							
1.2	0.4	0.8	-0.6	0.7	0.2	0.9	-0.4	0.4	-0.6	0.1	-0.8	-0.3	-0.5	1.0	-1.6				

B

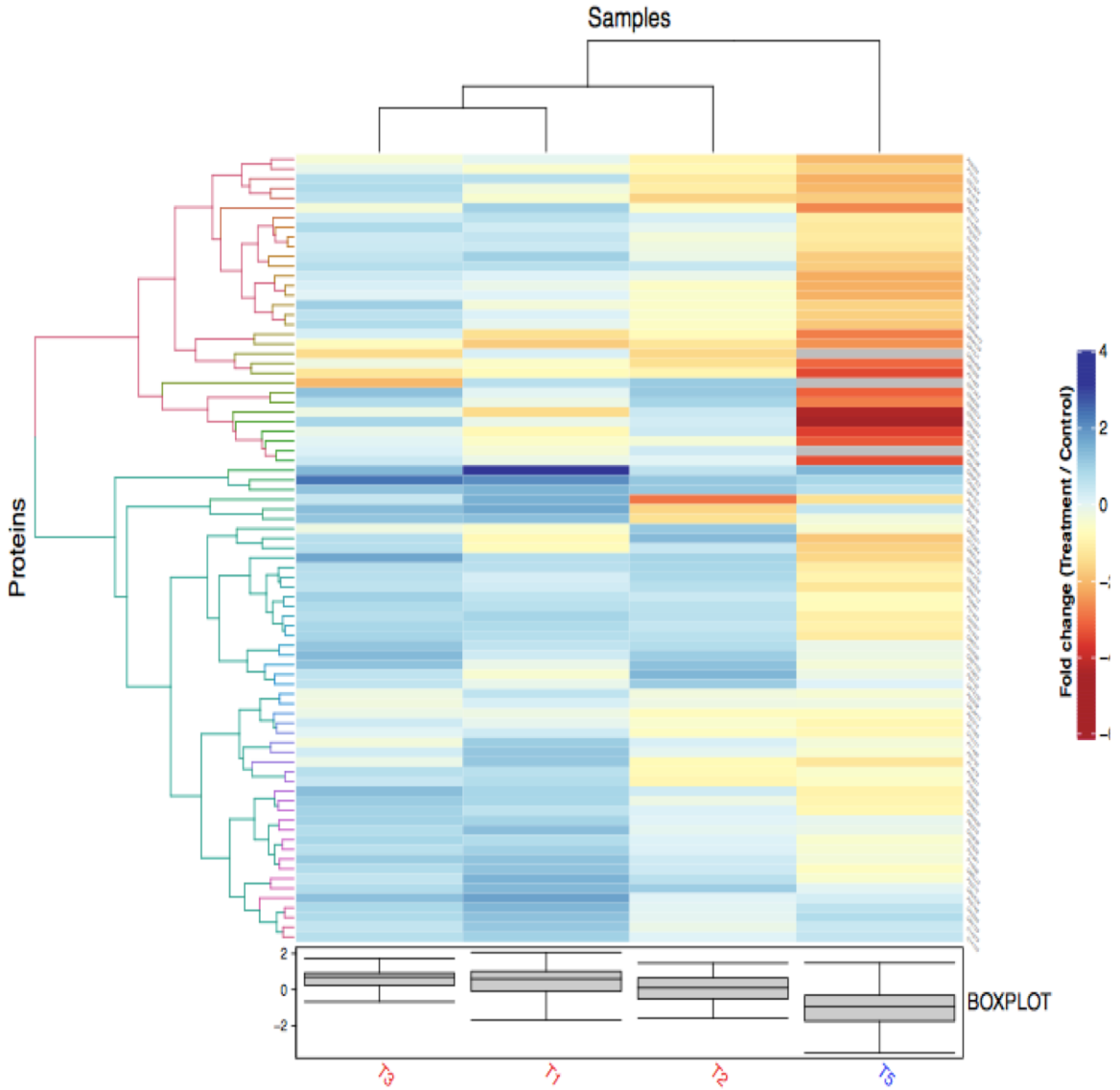

Preprints (www.preprints.org) | NOT PEER-REVIEWED | Posted: 17 June 2020 doi:10.20944/preprints202006.0206.v1

A

TAF15			HSPA9			NONO			QKI			DSP			DDX47			ZC3HAV1			UPF2			EIF4H		
2.8	0.8	1.6	1.1	0.1	0.4	0.9	0.1	0.6	0.8	-0.3	-0.3	0.6	0.6	1.0	0.3	0.4	0.8	-0.0	-1.2	-0.5	-0.3	-1.3	0.1	-0.5	-1.8	-0.7
SAFB2			RBM42			DKC1			SRSF1			DDX21			LSM3			TIAL1			PURA			GSPT1		
2.8	1.2	0.8	1.1	-0.0	-0.6	0.9	0.3	1.3	0.7	0.8	0.9	0.6	0.2	1.0	0.3	-1.5	-0.3	-0.0	-0.5	0.4	-0.3	0.1	0.0	-0.5	-0.5	0.2
H1F0			SRSF3			ZNF638			CCAR1			U2AF1			IGF2BP3			KHDRBS1			STAU1			NSUN2		
2.2	1.6	0.8	1.0	0.7	0.8	0.9	-1.8	0.3	0.7	-0.4	0.5	0.6	0.6	0.4	0.2	0.2	0.1	-0.0	-1.2	0.1	-0.3	-0.1	0.2	-0.6	0.0	0.4
CELF1			SRP14			HNRNPA1			CDC5L			HSPD1			SYNE2			MAP4			SRP9			STIP1		
1.8	-0.6	1.2	1.0	-1.6	0.0	0.9	-0.1	1.1	0.7	0.4	0.9	0.6	-1.0	-0.5	0.2	-0.8	-0.4	-0.0	-1.5	-0.9	-0.3	0.0	0.1	-0.6	-2.0	-0.1
FAM120A			LBR			SNTB2			RSL1D1			TUFM			HMGB3			RTCB			APEX1			UBA1		
1.6		1.6	1.0	0.5	0.2	0.9	0.0	-0.1	0.7	0.6	0.6	0.6	0.2	0.3	0.1	0.4	-0.6	-0.0	-0.1	0.6	-0.4	-0.7	0.2	-0.6	-1.6	-0.3
SFPQ			HNRNPD			FTSJ3			MK167			EPPK1			EIF4B			LARP1			PFN1			MAPRE1		
1.6	-0.4	1.1	1.0	0.1	0.7	0.9	1.3	1.5	0.7	-	-	0.5	0.2	0.2	0.1	-2.2	0.6	-0.1	-1.4	-0.2	-0.4	-0.9	-0.2	-0.6	-1.4	-0.1
H1FX			HNRNPA3			KHSRP			YBX3			DDX50			LUC7L			RPS19			RBM26			RCC2		
1.5	1.1	0.5	1.0	0.2	0.7	0.8	-1.3	0.3	0.6	-0.6	0.8	0.5	0.4	0.8	0.1	-0.0	-0.1	-0.1	-0.7	-0.4	-0.5	0.2	0.3	-0.7	-1.2	-0.2
HNRNPAB			IGF2BP1			MBNL			SRRT			PTBP3			RPS3A			PRRC2C			FLNB			FXR1		
1.2	0.0	0.8	1.0	0.3	0.2	0.8	-0.9	1.0	0.6	-0.5	0.7	0.5	0.4	0.9	0.1	-0.7	0.3	-0.2	-5.5	1.1	-0.5	-0.8	0.4	-0.7	0.6	0.2
HNRNPUL1			MFAP1			PRKRA			ATP5F1			CPSF7			ATXN2L			CAPRIN1			RPS2			TIA1		
1.2	0.4	0.8	0.9	0.4	-0.3	0.8	0.2	0.1	0.6	1.1	0.7	0.4	0.3	1.4	0.1	-1.0	0.3	-0.2	-1.2	-0.3	-0.5	-	-	-0.7	-0.9	-1.2
HNRNPH2			ADAR			DDX19A			SMN1			SPATS2L			CIRBP			HNRNPK			MAGOHB			MOV10		
1.2	0.0	0.3	0.9	-0.8	-0.2	0.8	-0.3	0.2	0.6	0.1	0.3	0.4	0.4	1.1	0.1	-0.6	-0.0	-0.2	-1.0	0.8	-0.5	-0.1	0.1	-0.7	0.0	-0.1
ELAVL1			FBL			HNRNPA2B1			ZC3H14			NUP98			CSTF1			EIF2S2			STAU2			DDX1		
1.2	-0.1	0.6	0.9	0.8	0.8	0.8	0.2	0.9	0.6	-1.3	0.1	0.4	0.4	0.3	0.0	-1.0	0.4	-0.3	-0.0	0.1	-0.5	0.2	-0.6	-0.7	-0.5	0.6
NUP58			AGO2			RPS6			SERBP1			PARP1			MYO6			G3BP2			DDX3X			RBMS1		
1.1	1.0	0.1	0.9	-1.5	0.4	0.8	0.2	0.1	0.6	-0.9	0.2	0.3	-0.4	0.0	0.0	0.4	0.3	0.3	-0.7	-0.2	-0.5	0.3	0.2	-0.7	-1.6	0.3

B

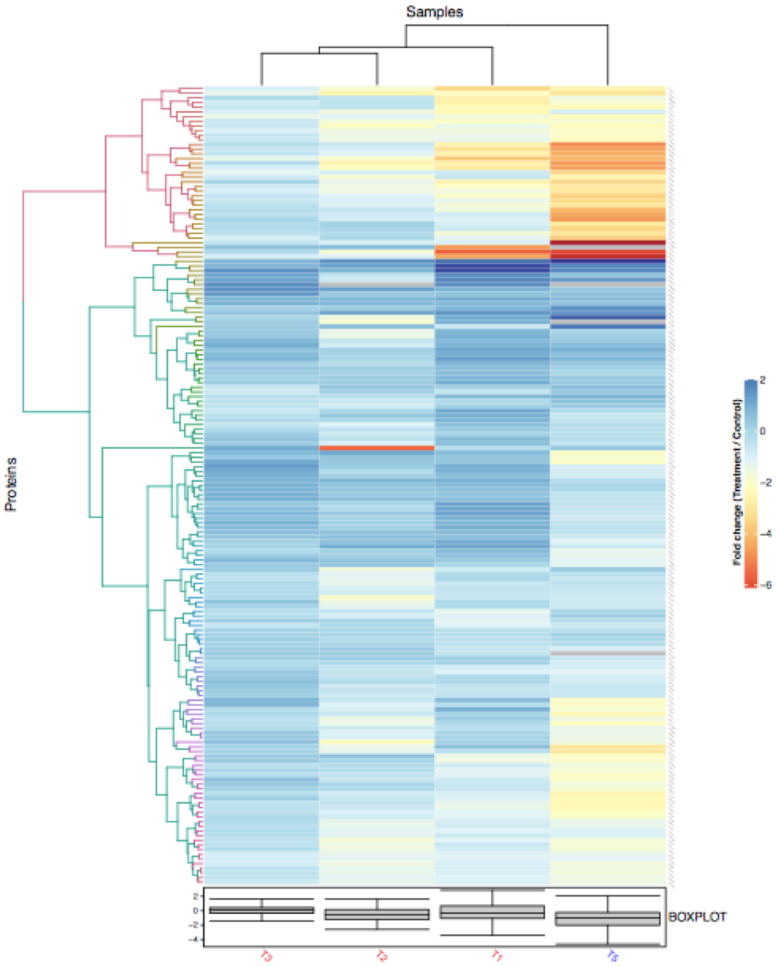

Preprints (www.preprints.org) | NOT PEER-REVIEWED | Posted: 17 June 2020 doi:10.20944/preprints202006.0206.v1

A

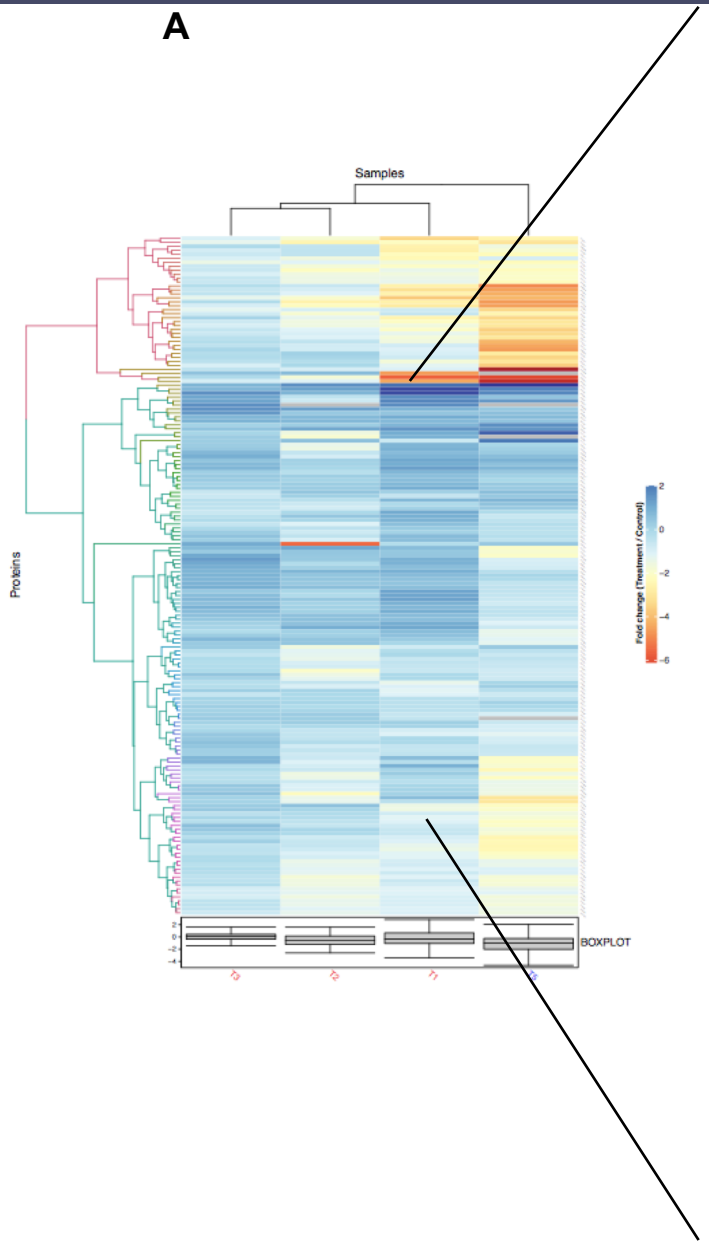

B

SAFB2				NUP58				ZNF638				RPS6				ZC3H14				G3BP2			
2.8	1.2	0.8	1.8	1.1	1.0	0.1	-0.7	0.9	-1.8	0.3	-	0.8	0.2	0.1	-1.1	0.6	-1.3	0.1	-3.0	0.3	-0.7	-0.2	-1.3
TAF15				RBM42				AGO2				CCAR1				TUFM				SYNE2			
2.8	0.8	1.6	1.8	1.1	-0.0	-0.6	-0.1	0.9	-1.5	0.4	0.2	0.7	-0.4	0.5	-0.2	0.6	0.2	0.3	0.2	0.2	-0.8	-0.4	0.4
H1F0				SRP14				FTSJ3				MKI67				YBX3				IGF2BP3			
2.2	1.6	0.8	3.2	1.0	-1.6	0.0	2.4	0.9	1.3	1.5	0.4	0.7	0.1	-0.1	-1.3	0.6	-0.6	0.8	-2.0	0.2	0.2	0.1	-0.6
CELF1				SRSF3				MFAP1				RSL1D1				DDX50				HMGB3			
1.8	-0.6	1.2	1.4	1.0	0.7	0.8	0.7	0.9	0.4	-0.3	-0.6	0.7	0.6	0.6	-0.4	0.5	0.4	0.8	-0.1	0.1	0.4	-0.6	0.6
SEPQ				IGF2BP1				SNTB2				CDC5L				PTBP3				RPS3A			
1.6	-0.4	1.1	-	1.0	0.3	0.2	0.3	0.9	0.0	-0.1	-0.4	0.7	0.4	0.9	0.0	0.5	0.4	0.9	-0.5	0.1	-0.7	0.3	-0.3
FAM120A				HNRNPD				NONO				DSP				EPPK1				ATXN2L			
1.6	-	1.6	-	1.0	0.1	0.7	0.5	0.9	0.1	0.6	-0.8	0.6	0.6	1.0	-0.4	0.5	0.2	0.2	-1.3	0.1	-1.0	0.3	-1.4
H1FX				HNRNPA3				ADAR				SMN1				CPSF7				EIF4B			
1.5	1.1	0.5	1.5	1.0	0.2	0.7	-0.4	0.9	-0.8	-0.2	-1.8	0.6	0.1	0.3	-0.0	0.4	0.3	1.4	0.6	0.1	-2.2	0.6	-1.5
HNRNPH2				LBR				PRKRA				ATP5F1				SRSF1				CIRBP			
1.2	0.0	0.3	-0.4	1.0	0.5	0.2	-1.0	0.8	0.2	0.1	1.6	0.6	1.1	0.7	-2.0	0.4	0.3	1.4	0.4	0.1	-0.6	-0.0	-2.4
ELAVL1				DKC1				MBNL				SERBP1				NUP98				LSM3			
1.2	-0.1	0.6	-0.5	0.9	0.3	1.3	-0.9	0.8	-0.9	1.0	0.6	0.6	-0.9	0.2	-0.4	0.4	0.4	0.3	-1.9	0.1	-0.6	-0.0	-1.5
HNRNPUL1				HNRNPA1				DDX19A				U2AF1				SPATS2L				LUC7L			
1.2	0.4	0.8	-0.6	0.9	-0.1	1.1	-0.9	0.8	-0.3	0.2	0.4	0.6	0.6	0.4	-0.7	0.4	0.4	1.1	-2.0	0.1	-0.0	-0.1	-0.9
HNRNPAB				DDX21				KHSRP				HSPD1				PARP1				MYO6			
1.2	0.0	0.8	0.8	0.6	0.2	1.0	-0.8	0.8	-1.3	0.3	0.0	0.6	-1.0	-0.5	-0.2	0.3	-0.4	0.0	-0.3	0.0	0.4	0.3	-1.2
HSPA9				FBL				HNRNPA2B1				SRRT				DDX47				CSTF1			
1.1	0.1	0.4	0.9	0.9	0.8	0.8	-0.2	0.8	0.2	0.9	-0.4	0.6	-0.5	0.7	0.3	0.3	0.4	0.8	-1.2	0.0	-1.0	0.4	-1.4

Preprints (www.preprints.org) | NOT PEER-REVIEWED | Posted: 17 June 2020 doi:10.20944/preprints202006.0206.v1

A

DHX16			
4.9	3.3	-	1.7

DDX21			
0.6	0.2	1.0	-0.8

PDHX			
-0.2	-0.2	-0.7	-0.0

DHX30			
-1.0	-1.3	-0.7	-1.5

DDX54			
1.2	1.1	1.6	-0.7

DDX50			
0.5	0.4	0.8	-0.1

DDX56			
-0.4	-0.2	0.1	-1.5

DHX38			
-1.0	-1.1	-0.3	-

DHX37			
1.0	0.1	0.2	-

DDX5			
0.5	-0.1	0.3	-1.1

DDX39B			
-0.3	-0.7	0.4	-2.0

DDX6			
-1.3	-0.9	-0.7	-3.3

DDX24			
1.1	0.5	1.2	-0.1

DDX47			
0.3	0.4	0.8	-1.2

DHX15			
-0.5	-0.5	0.1	-1.5

DDX41			
-1.3	-1.6	-1.6	-4.7

DDX23			
1.0	0.1	1.0	-0.9

DDX52			
0.3	-0.2	0.3	-2.2

DDX18			
-0.5	0.1	0.6	-3.0

DDX49			
-3.7	-1.5	-0.3	-

DHX8			
0.9	-0.4	1.3	-2.8

DDX17			
0.3	-0.2	0.4	-0.7

DDX3X			
-0.5	0.3	0.2	-0.9

DHX29			
-2.2	-2.3	0.3	-

DDX55			
0.8	1.2	3.2	-0.9

DDX42			
0.3	-1.3	0.0	-1.0

DDX10			
-0.7	-0.7	0.4	-1.6

DHX36			
-4.4	-1.1	-0.9	-6.9

DDX27			
0.8	0.5	0.8	-0.7

DDX46			
0.2	-0.3	0.8	-1.0

DDX1			
-0.7	-0.5	0.6	-2.0

DHX57			
-	0.3	-1.2	-

DDX19A			
0.8	-0.3	0.2	0.4

DHX9			
0.2	0.0	0.4	-2.0

DDX39A			
-1.0	-0.4	0.6	-1.7

B

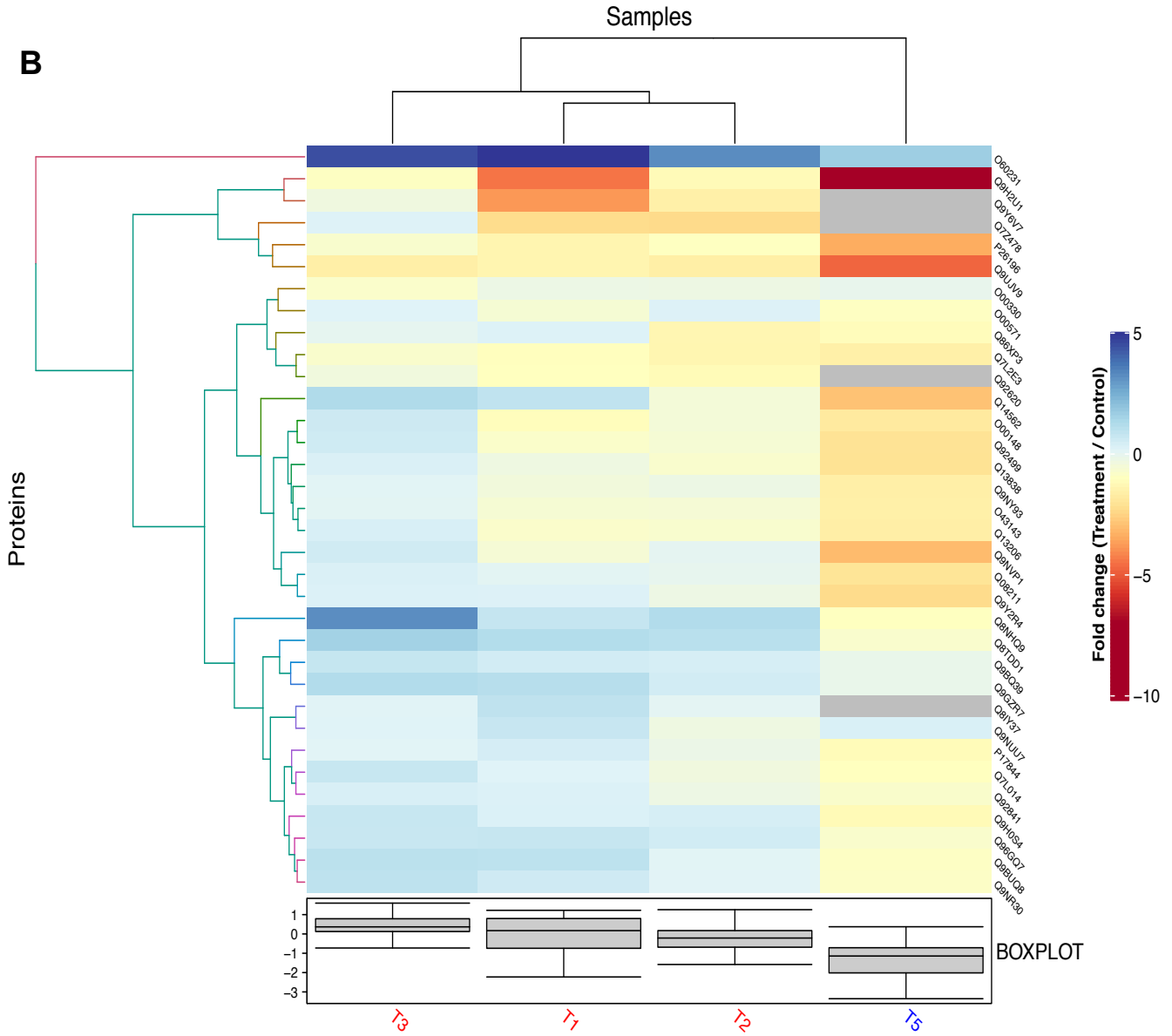

Preprints (www.preprints.org) | NOT PEER-REVIEWED | Posted: 17 June 2020 doi:10.20944/preprints202006.0206.v1

A

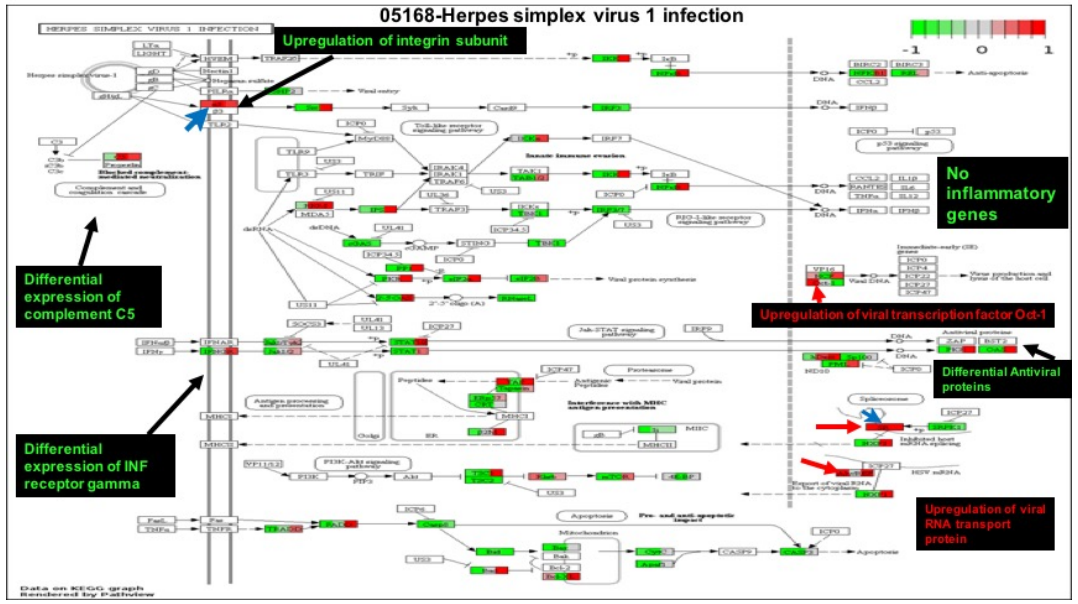

B

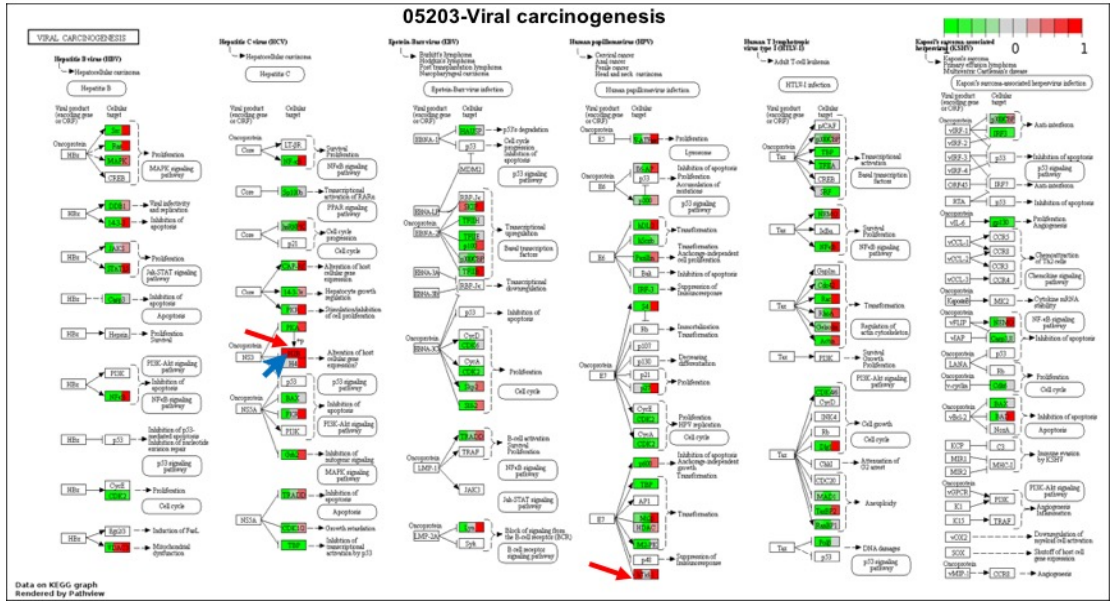

C

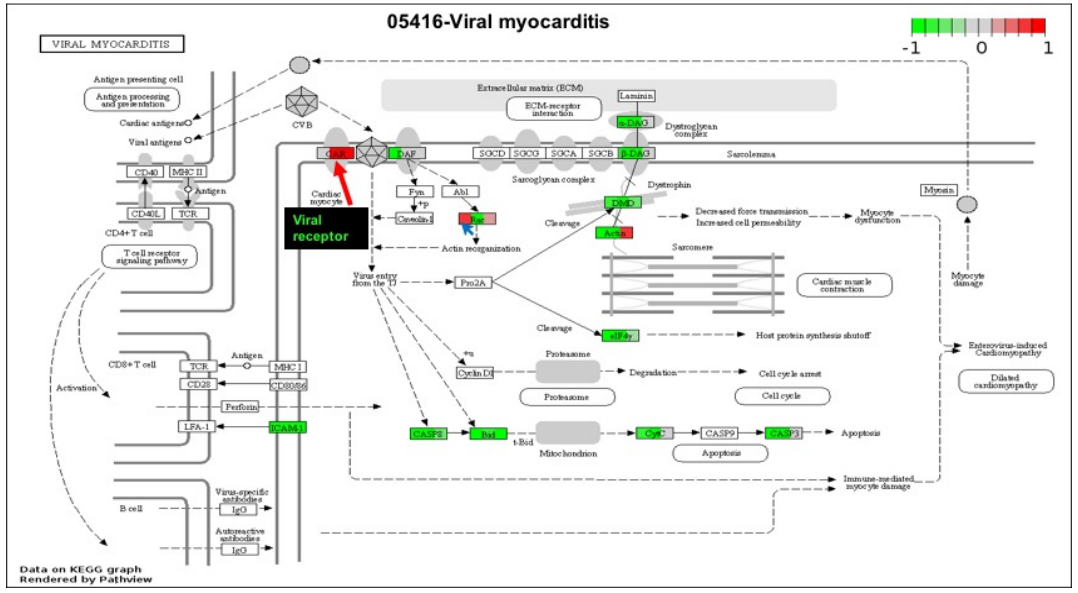

D

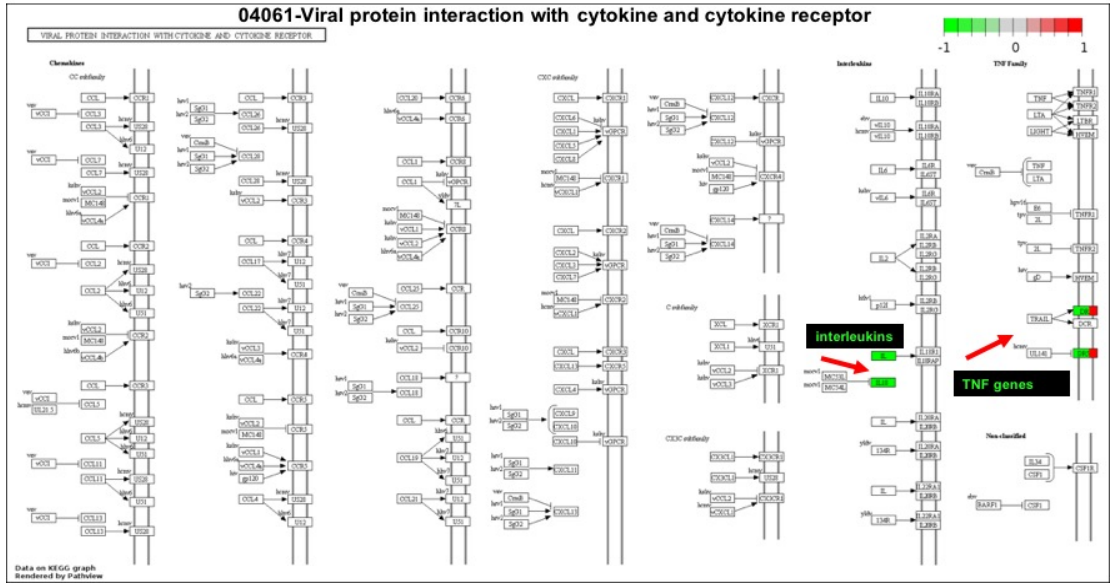

Preprints (www.preprints.org) | NOT PEER-REVIEWED | Posted: 17 June 2020 doi:10.20944/preprints202006.0206.v1

A

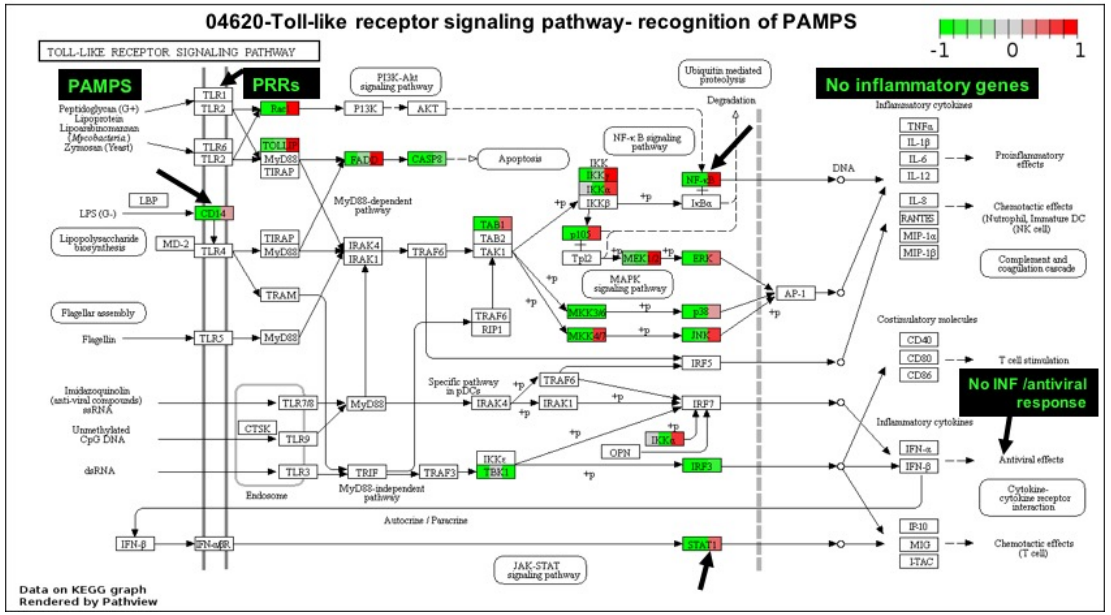

B

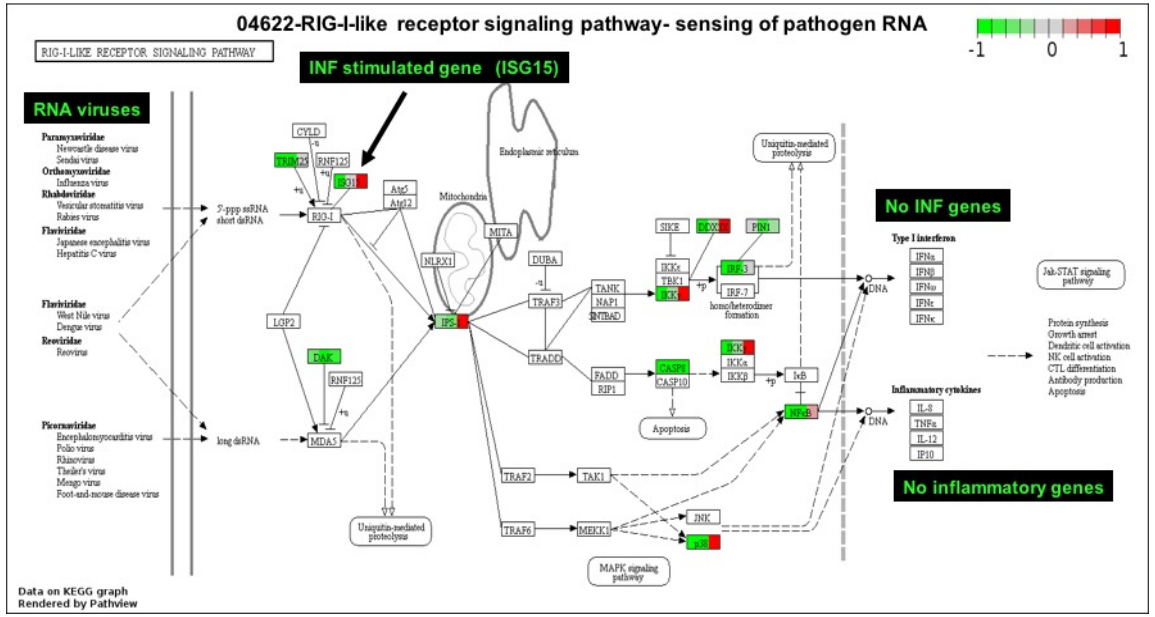

C

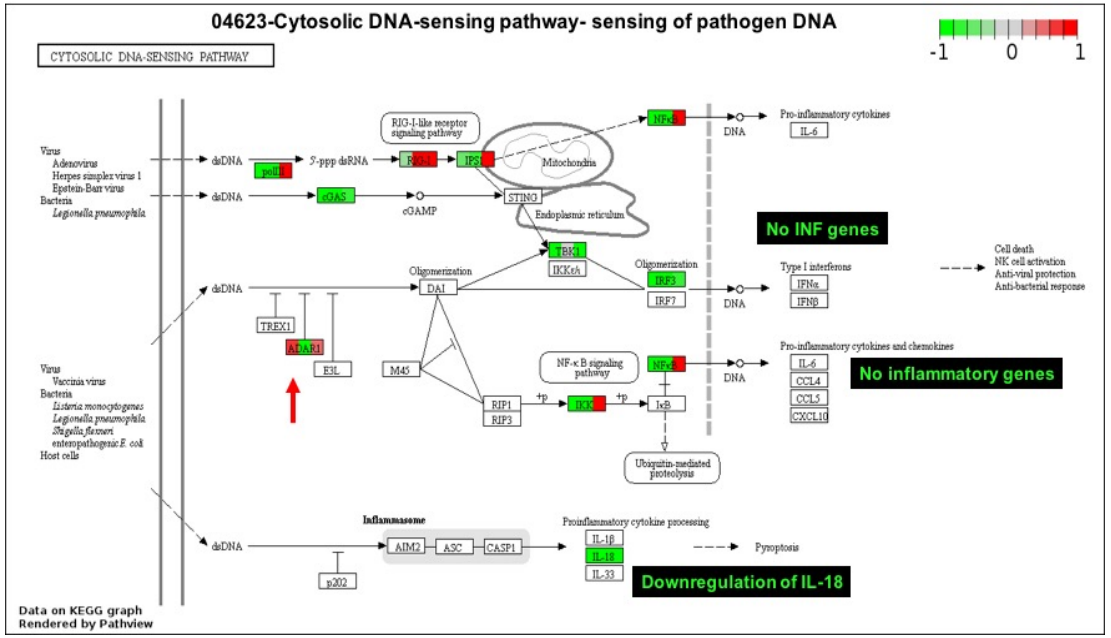

D

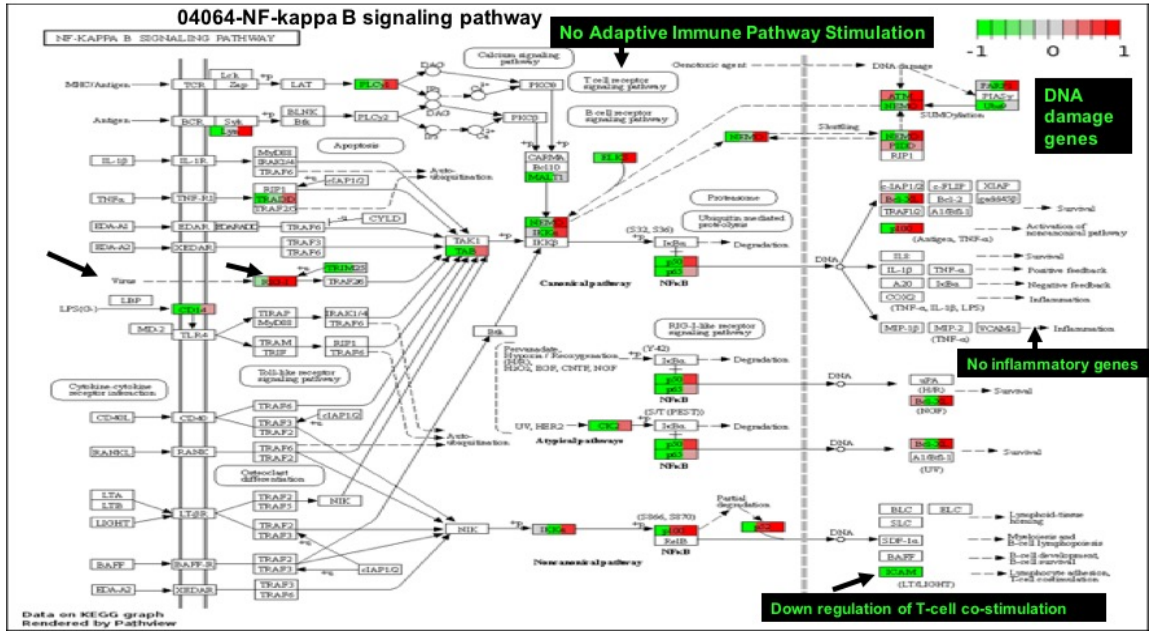

Preprints (www.preprints.org) | NOT PEER-REVIEWED | Posted: 17 June 2020 doi:10.20944/preprints202006.0206.v1

A

OASL		
0.64	0.13	-0.29

TOLLIP		
-0.06	0.41	0.09

STAT3		
-2.05	0.51	0.40

PIN1		
0.45	-0.07	-1.06

CNP		
-0.39	-0.16	0.06

TRIM25		
-2.69	-0.42	-0.82

OAS3		
0.34	-0.41	0.06

IRF3		
-0.88	-0.38	-

CASP8		
-2.96	-4.11	-1.90

IKBIP		
0.23	1.93	1.32

STAT1		
-0.91	-0.29	-0.27

STAT2		
-3.09	0.51	-0.05

MAVS		
-0.01	0.25	0.26

ISG15		
-1.80	0.48	1.06

cGAS		
-3.88	-2.45	-2.01

ZCEHAV1		
-0.01	-1.24	-0.50

OAS1		
-1.95	-0.36	-0.07

CD14		
-5.04	-1.97	0.42

B

PRKRA		
0.81	0.21	0.10

EIF2AK2		
-1.48	0.55	0.27

IFI30		
0.32	-4.30	-0.54

IFNGR1		
-2.88	0.70	0.78

IRF2BPL		
-0.23	-2.88	-1.28

IFI35		
-4.02	-1.98	-0.02

IRF2BP2		
-0.29	-1.57	-0.24

IFI6		
-	-1.49	-1.49

IRF2BP1		
-0.34	0.28	0.78

ISG20		
-	0.13	0.67

C

TRIM56		
-	-	0.73

STAT2		
-3.09	0.51	-0.05

OAS3		
0.34	-0.41	0.06

CNP		
-0.39	-0.16	0.06

TRIM25		
-2.69	-0.42	0.82

ADAR		
0.95	-0.84	-0.19

PNPT1		
0.12	-0.69	0.42

SP100		
-1.37	-0.76	-0.73

OGFR		
-2.41	0.32	0.12

LAP3		
0.08	-0.18	0.22

TRIM14		
-1.56	-0.60	-

SAMD9L		
3.23	0.03	1.20

TDRD7		
-	-1.86	0.11

EIF2AK2		
-1.48	0.55	0.27

TAP1		
0.99	0.33	0.02

OAS1		
-1.95	-0.36	-0.07

D

CD55		
-4.93	0.66	-0.35

PSMD1		
-1.90	-1.33	-1.04

ZC3HAV1		
-0.01	-1.24	-0.50

IFITM2		
-	-	-

PNPT1		
0.12	-0.69	0.42

SAMDH1		
-2.49	0.26	0.55

STAT1		
-0.91	-0.29	-0.27

MX1		
-	-	-

PSMC1		
-0.87	-0.68	0.43

ISG15		
-1.80	0.48	1.06

PSMD6		
-0.57	-0.47	0.20

RPL28		
1.21	0.16	0.74

E

HSPH1		
-1.1	-0.5	0.5

IFI35		
-4.0	-2.0	0.0

PARP14		
-	-2.4	0.0

NCEH1		
-1.3	0.5	0.5

RNF213		
-3.0	-1.0	-0.5

TRIM14		
-1.6	-0.6	-

NAMPT		
-1.8	0.3	-0.4

TRIM25		
-2.7	-0.4	-0.8

LGALS3BP		
-0.0	0.1	0.1

STAT2		
-3.1	0.5	-0.0

ISG15		
-1.8	0.5	1.0

MOV10		
-0.7	0.0	-0.1

STAT1		
-0.9	-0.3	-0.3

EIF2AK2		
-1.5	0.5	0.3

ISG20		
-	0.1	0.7

SLC25A22		
1.1	0.6	0.6

TDRD7		
-	-1.8	0.1

Preprints (www.preprints.org) | NOT PEER-REVIEWED | Posted: 17 June 2020 doi:10.20944/preprints202006.0206.v1

A

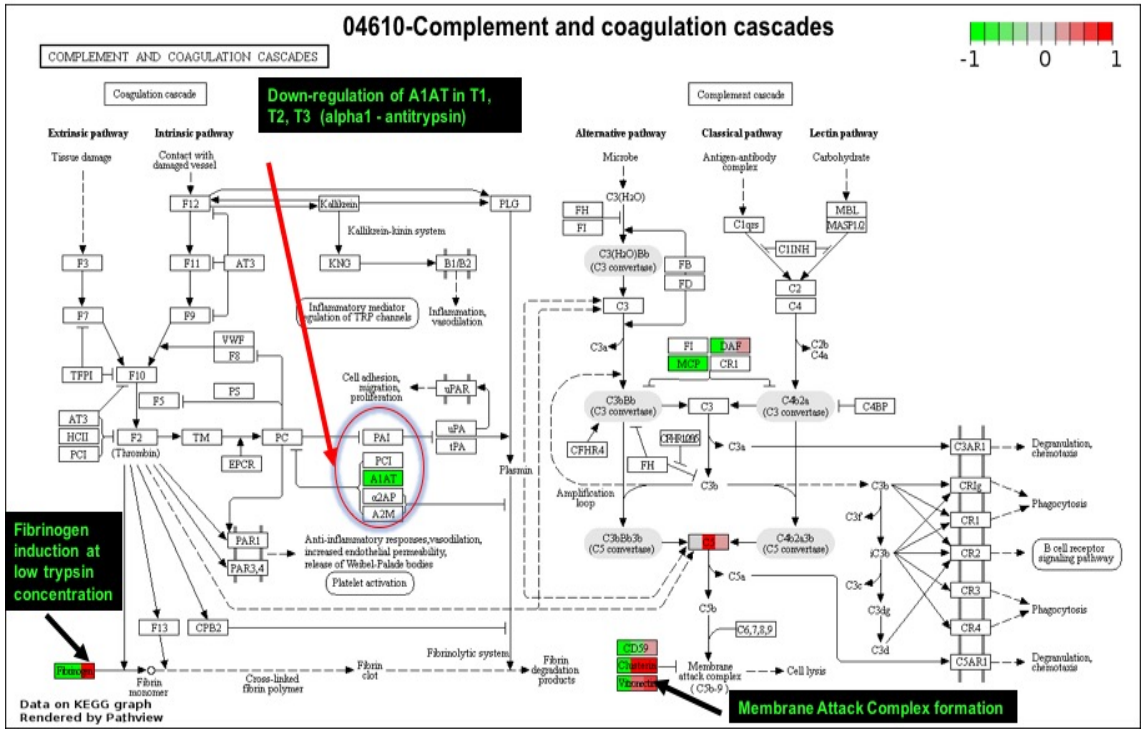

B

FGA		
4.7	-	1.3

FGG		
-4.9	-1.7	-1.1

FGB		
-	1.0	0.3

SERPINA1		
-2.0	-0.8	-2.7

CD46		
-	-2.9	-2.6

CD55		
-4.9	0.7	-0.3

C5		
0.1	1.6	-0.4

CD59		
-	0.2	-0.3

CLU		
-3.0	1.6	0.2

VTN		
-1.7	1.1	-0.0

C

SERPINS

SERPINB1		
-0.95	-2.08	-0.30

SERPINH1		
-1.06	-0.58	-1.21

SERPINA / A1AT		
-2.04	-0.81	-2.76

SERPINB6		
-2.99	-4.08	-1.55

SPINK1		
-0.58	-1.74	-1.02

SPINT2		
-1.34	0.78	0.71

SPINT1		
-4.03	-0.43	-1.20

SERINE PROTEASE

HTRA2		
1.46	1.17	0.55

ST14/MATRIPTASE		
-0.79	1.47	-0.38

PRSS8 / PROSTASIN		
-4.25	0.86	1.36